Structural Engineering Report No. 122

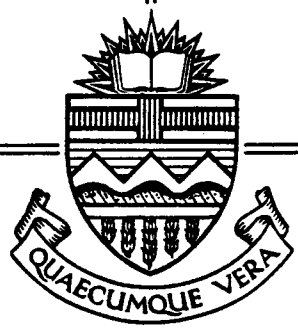

THE EFFECTS OF RESTRAINED SHRINKAGE ON CONCRETE SLABS

By

K. S. Stephen Tam

and

Andrew Scanlon

December, 1984

ABSTRACT

Two analyses are presented to study the effects of restrained shrinkage on reinforced concrete members. The first is a uniaxial shrinkage analysis of a symmetrically reinforced, completely restrained slab element. A procedure for calculating induced tensile stresses and spacing of cracks due to restraint of shrinkage is presented. The reduction of axial stiffness due to cracking is based on an assumption of linear steel stress distribution within the zone of influence of cracking. A parameter study was conducted to investigate various factors affecting the member's behaviour.

The second analysis involved the application of the finite element method in analyzing two-way continuous slab systems. Shrinkage cracks are assumed to exist in the slab prior to analyzing the slab for transverse loads. Methods for evaluating the reduced flexural stiffness due to shrinkage cracking and cracking due to transverse load are given. A brief investigation was performed to study the effects of number of shrinkage cracks and variation in effective tensile strength on slab deflections. It is proposed that shrinkage restraint be incorporated in a plate bending analysis by using a reduced effective modulus of rupture.

ACKNOWLEDGMENTS

Financial support for this study was provided by the Natural Science and Engineering Research Council of Canada through Operating Grant A5153.

TABLE OF CONTENTS

LIST OF TABLES

LIST OF FIGURES

LIST OF SYMBOLS

A_b	Area of a single reinforcing bar.
A_c	Area of concrete.
A_e	Equivalent transformed area when the steel area is replaced by an equivalent amount of concrete area.
A_g	Gross area of cross section.
A_s	Area of tension reinforcement.
b	Width of slab element.
c	Maximum concrete cover measured from the face of tension reinforcement to concrete surface.
C_t	Creep coefficient defined as ratio of creep strain to initial strain.
d	Diameter of Mohr's circle.

DL	Dead loads.
E_c	Modulus of elasticity for concrete.
E_{ct}	Reduced modulus of elasticity due to creep of concrete.
E_s	Modulus of elasticity of non-prestressed steel reinforcement.
E_x	Modulus of elasticity in x-direction.
E_y	Modulus of elasticity in y-direction.
$(EI)_{cr}$	Flexural stiffness within precracked region.
f_c	Induced concrete stress due to restrained shrinkage.
$f_c(t_k)$	concrete stress at time t_k.
f'_c	Specified compressive strength of concrete.

f_{c1}, f_{c2}, f_{cm}	Induced concrete stress due to restrained shrinkage after the formations of the first crack, the second crack and the m^{th} crack, respectively.
f_e	Effective modulus of rupture for computing deflections.
f_r	Modulus of rupture of concrete.
f_t	Tensile strength of concrete.
f_y	Specified yield strength of non-prestressed reinforcement.
FTOL	Acceptable tolerance in concrete stress.
G, G_{xy}	Shear modulus of elasticity.
h	Overall thickness of member.
I_{cr}	Moment of inertia of cracked section transformed to concrete.

I_{crx}	I_{cr} of a cross section perpendicular to x-axis.
I_{cry}	I_{cr} of a cross section perpendicular to y-axis.
I_{eff}	Effective moment of inertia for computing deflections.
I_{ex}	I_{eff} of a cross section perpendicular to x-axis.
I_{ey}	I_{eff} of a cross section perpendicular to y-axis.
I_g	Moment of inertia of gross concrete section about the centroidal axis, neglecting reinforcement.
I_{px}	Reduced moment of inertia of a precracked cross section perpendicular to x-axis.
I_{py}	Reduced moment of inertia of a precracked cross section perpendicular to y-axis.

k_1	Coefficient used to determine cracked length in the 'no-slip' approach.
k_2	Coefficient used to determine cracked length in the 'slip' approach.
k_r	Reduction factor to account for compressive steel and movement of neutral axis in computing long-time deflections.
K_1, K_2, K_m	Average axial stiffness of a slab element after formations of one crack, two cracks and m cracks, respectively.
K_c	Column stiffness.
K_{cr}	Axial stiffness in the cracked region of a slab element.
K_g	Axial stiffness of uncracked section of a slab element.
K_{sys}	Stiffness of a slab system with partial fixity.

L	Clear span length of a slab element.
L_c	Height of column.
L_{cr}	Cracked length within which the stiffness varies from the stiffness provided by reinforcement alone at the crack, to the full stiffness of the steel-concrete composite member at a distance $L_{cr}/2$ from the crack.
L_d	Development length.
L_{slip}	Slipping length.
LL	Live load.
m	Number of cracks formed in a slab element.
M	Moment.
M_{cr}	Cracking moment.
M_x	Moment in x-direction (reinforcement parallel to x-axis) shown in Figure 3.2.

M_{xy}, M_{yx}	Twisting moment shown in Figure 3.2.
M_y	Moment in y-direction (reinforcement parallel to y-axis) shown in Figure 3.2.
n	Modular ratio.
P	Tensile force applied to a slab element.
P_o	Compressive force in reinforcement.
P_c	Tensile force carried by concrete.
P_{net}	Net induced tensile force in a slab element due to restrained shrinkage.
P_s	Tensile force carried by steel.
q	Uniformly distributed load applied to slab shown in Figure 3.2.
S	Crack spacing.
$[t'_o, t''_o]$	Initial time interval used in the bisection method.

t_{cr}	Time at which cracking occurs.
t_k	Mid-point of the interval $[t'_k, t''_k]$.
$[t'_k, t''_k]$	Time interval obtained by the bisection method after k iterations.
$[t'_{k+1}, t''_{k+1}]$	Time interval obtained by the bisection method after k+1 iterations.
T	Maximum tensile load that can be carried by concrete.
TTOL	Acceptable tolerance in time.
y_t	Distance from centroidal axis of gross section, neglecting the reinforcement, to extreme top fibre of concrete member.
α	Axial stiffness reduction coefficient.
α_p	Flexural stiffness reduction coefficient for precracked element.
α_{px}	α_p in x-direction.

α_{py}	α_p in y-direction.
α_x	Flexural stiffness reduction coefficient in x-direction.
α_y	Flexural stiffness reduction coefficient in y-direction.
γ_{xy}	Shearing strain.
Δ	Displacement due to shrinkage of a released support slab element.
Δ_1, Δ_2	Displacement due to shrinkage of a released support slab element with one crack and two cracks respectively.
Δ_{cp}	Creep deflection for all sustained loads.
Δ_{cr}	Elongation of cracked region under load P.
Δ_g	Elongation of uncracked region under load P.
Δ_i	Immediate deflection.

$(\Delta_i)_D$	Immediate deflection due to all sustained load.
Δ_{slab}	Elongation of a released support slab element with partial fixity if restraint is reapplied.
Δt	Increment of time-step.
ϵ_1, ϵ_2, ϵ_m	Average unit strain in slab element after the formations of the first crack, the second crack and the m^{th} crack, respectively.
ϵ_{ave}	Average unit strain in reinforcement.
ϵ_c	Unit strain in concrete.
ϵ_s	Unit strain in steel.
ϵ_{sh}	Unrestrained shrinkage strain.
ϵ_{sh1}, ϵ_{sh2}, ϵ_{shm}	Unrestrained shrinkage shrain at which the first crack, the second crack and the m^{th} crack form in a slab element, respectively.

ϵ_{shu}	Ultimate shrinkage strain.
ϵ_x	Normal strain parallel to x-axis.
ϵ_y	Normal strain parallel to y-axis.
ν	Poisson's ratio.
ν_x	Poisson's ratio in x-direction.
ν_y	Poisson's ratio in y-direction.
ρ	Tension reinforcement ratio.
ρ'	Compressive reinforcement ratio.
$\sigma_{s,cr}$	Steel stress at a crack.
$\sigma_{s,g}$	Steel stress at uncracked section.
σ_x	Normal stress parallel to x-axis.
σ_y	Normal stress parallel to y-axis.
τ_b	Average bond stress.

τ_{xy}	Shearing stress.
τ_{ult}	Ultimate bond stress.
ϕ	Reinforcing bar diameter.
ϕ_{ave}	Average curvature within precracked region.
ϕ_{cr}	Curvature at cracked section.
ϕ_{g}	Curvature at uncracked section.
ϕ_{sh}	Shrinkage curvature.
ϕ_{x}	Curvature in x-direction.
ϕ_{xy}	Shearing curvature.
ϕ_{y}	Curvature in y-direction.

1. INTRODUCTION

1.1 Introductory Remarks and Literature Review

The current practice of ultimate strength design of reinforced concrete structures has resulted in more flexible and slender structures than in the past. The assessment of the performance of the structure at the working load levels thus becomes an extremely important consideration. Although strength requirements may be satisfied, cracking and deflections at the working loads may be excessive. Cracking may be excessive if the steel stresses are high or if the reinforcing bars are not properly distributed. Deflections may be critical when shallow sections, which are the case in ultimate strength design, are used and high stresses are present.

The concern for serviceability requirements is reflected in the current ACI Building Code, where methods are suggested to compute both short-term and long-term deflections. The Code however does not explicitly consider cracking of structures that often occurs at an early age of construction either due to construction loading or due to restraint of shrinkage. Failure to recognize these effects may lead to unconservative predictions of two-way slab deflections as revealed by some investigations (Heiman, 1974

and Rangan, 1976).

Observed cracking usually occurs for the following main reasons (Scanlon and Murray, 1982 and RILEM Committee 42-CEA, 1981):

1. Settlement of the newly placed concrete.
2. Early shrinkage and thermal variations.
3. Higher than design moments that occur adjacent to columns.
4. Excessive construction loading due to shoring procedure that results in overstressing of the slab before the concrete can reach its design strength.

A survey carried out by Mayer and Rusch (1967) has indicated that excessive slab deflection was the most common cause of damage to reinforced concrete structure. Insufficient consideration of creep and shrinkage on slab deflections was one of the causes cited for damage.

The ACI Building Code recognizes shrinkage effects on deflections in terms of shrinkage curvature due to warping that arises from nonuniform shrinkage. However, in continuous reinforced slab systems, tensile stresses are induced by shrinkage of the concrete when shrinkage strains are restrained. Stiff support elements provide the restraint and significant stresses can be developed. The

value of the induced tensile stresses may well exceed the tensile strength of the concrete, particularly at the early stages of hardening, resulting in additional cracking of the reinforced slab system. The overall stiffness of the slab system is thus reduced, causing an additional slab deflection. The current ACI Building Code calculation procedures may, therefore, underestimate slab deflections if the effects discussed above are not properly considered.

Cracking in certain regions reduces the slab stiffness and complicates the analysis of reinforced concrete slab systems. Classical plate-bending solutions cannot readily deal with slabs with varying stiffness. The introduction of the finite element method solves this problem by dividing the slab into finite regions allowing the stiffness to be varied from one element to another.

Successful modelling of cracking behaviour in slab systems has been made by Jofriet and McNeice (1971). A bilinear moment-curvature relationship formed the basis of the model of a cracked region. Cracks were assumed to initiate at a direction perpendicular to the major principal moment and unalter during any increase of load. Procedures were developed to give equivalent steel areas normal to the cracks for direct substitution in the calculation of the effective moment of inertia of a cracked region.

A much simplified method was developed by Scanlon and Murray (1982), who included the effects of cracking by reducing the values of the elastic constants. Moments in the x and y directions were checked. If the cracking moment in either direction was exceeded, reduction in stiffness was made using the ACI Building Code equation for effective moment of inertia. The procedure thus assumed that cracks were oriented parallel to and perpendicular to the direction of the reinforcement. The reinforcement was placed in the x and y directions of the global co-ordinate system so that transformation of steel areas was not necessary.

The additional shrinkage cracks that may occur in slab systems were not modelled in the two forementioned procedures. A finite element model that includes both cracking due to transverse loadings and due to shrinkage restraint is, therefore, required.

1.2 Objectives

The objectives of this investigation are:

1. To investigate the effects of shrinkage cracks on flexural stiffness of slabs,
2. to analyze reinforced concrete slabs that are subjected to shrinkage cracking using the finite element method, and

3. to assess a simplified procedure for calculating deflections which includes the effects of restraint stresses due to shrinkage of concrete.

1.3 Outline of Content

In Chapter 2, the analysis procedure of a member subjected to uniaxial shrinkage strain is described. The length and uniaxial stiffness of a cracked region is modelled. The induced tensile stresses in the concrete due to restraint of shrinkage are evaluated. Checking the value of the induced tensile stresses against the tensile strength of concrete, the number of cracks developed and the shrinkage strains at which cracks formed are also determined. A parameter study is then carried out to investigate the different effects of variations in several parameters.

The finite element procedure of the analysis of a slab system subjected to bending is described in Chapter 3. Cracking due to transverse loading and due to restraint of shrinkage is modelled. To complete the analysis, additional deflections due to shrinkage curvature and creep are approximated. The results of the analyses of three reinforced concrete slabs are used to assess a simplified method for evaluating slab deflections subjected to the

effects of early shrinkage cracking.

A brief summary and recommendations for further research are included in Chapter 4.

2. UNIAXIAL SHRINKAGE ANALYSIS

2.1 Introduction

Stresses are induced in concrete when volume change due to shrinkage is restrained. Restraint may be provided by support conditions and/or by reinforcing bars. Tensile stresses developed may exceed the tensile strength of the concrete, particularly at the early stages of hardening. When the tensile strength is exceeded, cracking occurs.

In this chapter a symmetrically reinforced slab element fixed at both ends and subjected to uniform, uniaxial shrinkage is analyzed. For a given shrinkage strain versus time history, the effect of progressive reduction in element stiffness as cracks form is taken into account in determining the spacing of cracks in the slab element due to restraint of shrinkage. Results obtained are used as a basis for specifying the extent of cracking resulting from restrained shrinkage in a slab prior to analyzing the slab for transverse loads.

2.2 Assumptions and Limitations of Analysis

The analysis has the following assumptions and limitations:

1. All concrete properties except shrinkage strain are

assumed to be constant with time. An example of a shrinkage strain versus time curve is shown in Figure 2.1.

2. A crack forms when the tensile stress in concrete exceeds the specified tensile strength.
3. Creep effects are not included explicitly in the analysis.
4. No yielding occurs in reinforcing bars.

2.3 Shrinkage Analysis

2.3.1 Outline of Analysis

In the following sections, the shrinkage analysis procedure of a symmetrically reinforced slab element with full fixity at ends will be presented. The slab element is first considered both at the uncracked state and at the first and second cracking states, then the analysis is generalized to consider the formation of any number of cracks.

2.3.1.1 Uncracked state

Consider the member in Figure 2.2a. Release one support and allow the concrete to shrink freely by an amount

$$\Delta = \epsilon_{sh} L$$

where ϵ_{sh} is the shrinkage strain that occurs in concrete. In order to force the steel bar to shorten by the same amount, a compressive force

$$P_o = -A_s E_s \epsilon_{sh}$$

must be applied to the bar as shown in Figure 2.2b. The concrete is now unstressed and the bar is under compression when one support is released.

For compatibility, a force P must be applied to bring the member back to its original length (Figure 2.2c). The applied load P is carried partly by the concrete (P_c) and partly by the steel bar (P_s) at any cross section.

Hence,
$$\begin{aligned} P &= P_c + P_s \\ &= A_c E_c \epsilon_c + A_s E_s \epsilon_s \end{aligned}$$

Before cracking occurs, there is no slipping between concrete and steel.

Hence, $\epsilon_{sh} = \epsilon_c = \epsilon_s$

Therefore,
$$\begin{aligned} P &= A_c E_c \epsilon_{sh} + A_s E_s \epsilon_{sh} \\ &= A_c E_c \epsilon_{sh} + (\rho A_c)(n E_c)\epsilon_{sh} \\ &= (1+n\rho) A_c E_c \epsilon_{sh} \\ &= A_e E_c \epsilon_{sh} \end{aligned}$$

where $A_e = (1+n\rho)A_c$

$n = E_s/E_c$

and $\rho = A_s/A_c$

A_e is the equivalent transformed area of the member if the steel area A_s is replaced by an equivalent amount of concrete area $n\rho A_c$.

The net force in the member is

$$\begin{aligned} P_{net} &= P + P_o \\ &= (A_c E_c \epsilon_{sh} + A_s E_s \epsilon_{sh}) + (-A_s E_s \epsilon_{sh}) \\ &= P_c \end{aligned}$$

Concrete stress in the member is

$$f_c = E_c \epsilon_{sh} = P/A_e = P_c/A_c \qquad (2.1)$$

Before cracking the net stress in the steel is zero. It may be noted that the same result is obtained if the bond between steel and concrete is released as well as the restraint at one of the fixed ends. In this case $P_o = 0$ and the net concrete and steel stresses are as indicated above when compatibility of deformations is applied.

2.3.1.2 Formation of the first crack

The concrete stress continues to increase as shrinkage continues until the concrete tensile strength f_t is reached, causing formation of the first crack. The shrinkage strain at which the first crack forms (i.e. when $f_c = f_t$, from Assumption 2) is

$$\epsilon_{sh1} = f_t/E_c \qquad (2.2)$$

If $\epsilon_{sh1} > \epsilon_{shu}$, then the first crack will not form.

Cracking causes a reduction in member stiffness with a resulting decrease in stress in the member. Figure 2.3 shows the variation in concrete tensile stress with increasing shrinkage strain. Initially, in the uncracked state, the tensile stress increases linearly with shrinkage strain along line OA. At point A the tensile strength is reached and the first crack forms. The reduction in stiffness causes a decrease in stress to f_{c_1} (point B). As shrinkage continues to take place, the concrete stress increases again along line BC up to point C where the tensile strength is again reached and a second crack is formed. This sequence continues until the shrinkage strain reaches its ultimate value.

The residual concrete stress f_{c_1} can be obtained using the following procedure.

Step 1. Figure 2.4a shows the member with one crack formed. As a result of the crack, the axial stiffness is reduced over a length L_{cr}. Within this length, the stiffness varies from the stiffness provided by steel alone at the crack, to the full stiffness of the steel-concrete composite member at a distance $L_{cr}/2$ from the crack.

If slipping between concrete and steel occurs within some distance L_{slip} due to bond failure around the first crack, then shrinkage within this slipping region will not induce

significant stresses. Hence, only shrinkage in the non-slip region ($L-L_{slip}$) is considered.

Consider again the released support member with one crack formed as shown in Figure 2.4b and allow the concrete to shorten freely by the amount

$$\Delta_1 = \epsilon_{sh_1}(L-L_{slip})$$

Define the average member strain to be

$$\epsilon_1 = \epsilon_{sh_1}(L-L_{slip})/L \qquad (2.3)$$

Therefore $\Delta_1 = \epsilon_1 L$

Then the compressive force P_o required to shorten the reinforcing bar by the same amount is

$$P_o = - A_s E_s \Delta_1 / L$$
$$= - A_s E_s \epsilon_1$$

Step 2. A force P is applied to bring the member length back to L. Because of the reduction in stiffness over L_{cr} the displacement Δ_1 is considered in two parts. The cracked region elongates by an amount

$$\Delta_{cr} = PL_{cr}/K_{cr}$$

where K_{cr} is the reduced stiffness over the length L_{cr}.

The gross section also elongates over a length of ($L - L_{cr}$) by an amount

$$\Delta_g = P(L-L_{cr})/K_g$$

where $K_g = A_e E_c$.

From compatibility,

$$\Delta_1 = \Delta_{cr} + \Delta_g$$

Therefore, $PL/K_1 = PL_{cr}/K_{cr} + P(L-L_{cr})/K_g$

in which K_1 is the overall member stiffness with one crack.

Rearranging the above expression,

$$K_1 = \frac{L}{(L-L_{cr})/K_g + L_{cr}/K_{cr}}$$

Similarly, for a member with m cracks,

$$K_m = \frac{L}{(L-mL_{cr})/K_g + mL_{cr}/K_{cr}} \quad (2.4)$$

where m = number of cracks in member

= 1, 2, 3...

Step 3. From Step 1, since $\Delta_1 = \epsilon_1 L$,

$$P = K_1 \Delta_1 / L$$
$$= K_1 \epsilon_1$$

Step 4. From Equation 2.1, concrete stress in gross section is

$$f_{c1} = P/A_e$$
$$= K_1 \epsilon_1 / A_e$$
$$= \frac{K_1 \epsilon_{sh1} (L - L_{slip})}{A_e L} \qquad (2.5)$$

Step 5. The net force in the member is

$$P_{net} = P + P_o$$
$$= K_1 \epsilon_1 - A_s E_s \epsilon_1$$
$$= (K_1 - A_s E_s) \epsilon_1 \qquad (2.6)$$

Step 6. After the first crack forms, the tensile stress in steel is no longer zero. At the crack the force P_{net} is carried entirely by the steel, producing a net tensile stress of

$$\sigma_{s,cr} = P_{net} / A_s \qquad (2.7)$$

Outside the cracked zone L_{cr}, the stress in the steel is compressive and is given by

$$\sigma_{s,g} = (P_{net} - P_c)/A_s$$
$$= \sigma_{s,cr} - f_c/\rho \qquad (2.8)$$

in which $f_c = f_{c1}$ in this case.

The variation of steel and concrete stresses along the length of the member after the first crack forms is shown in Figure 2.4c.

2.3.1.3 Formation of the second crack

Assume shrinkage continues to take place after the first crack forms. From Figure 2.3, when the shrinkage strain increases from ϵ_{sh1} to ϵ_{sh}, the concrete stress increases along line BC where the member has a stiffness of K_1. At point C, where $\epsilon_{sh} = \epsilon_{sh2}$, the concrete tensile strength is reached, i.e.

$$f_c = f_t$$

From Equation 2.5, substituting ϵ_{sh1} by ϵ_{sh2},

$$f_t = \frac{K_1 \epsilon_{sh2}(L-L_{slip})}{A_e L}$$

Rearranging, the shrinkage strain at which the second crack forms is

$$\epsilon_{sh2} = \frac{A_e f_t L}{K_1(L-L_{slip})} \qquad (2.9)$$

After the second crack is formed, the member has a stiffness of K_2 and a slipping length of $2L_{slip}$. Again release one support to allow the member to shrink by the amount

$$\Delta_2 = \epsilon_2 L$$

where $$\epsilon_2 = \epsilon_{sh_2}(L-2L_{slip})/L \qquad (2.10)$$

The force P applied to maintain compatibility is given by

$$P = K_2\Delta_2/L$$
$$= K_2\epsilon_2 \qquad (2.11)$$

where K_2 can be obtained from Equation 2.3 by letting m = 2.

The residual concrete stress at the uncracked section is

$$f_{c2} = P/A_e$$
$$= K_2\epsilon_2/A_e \qquad (2.12)$$

The net force in the member is

$$P_{net} = P + P_o$$

where P_o is the compressive force required to shorten the reinforcing by the amount Δ_2 when the restraint is released at one of the fixed ends and is given by

$$P_o = - A_s E_s \Delta_2 / L$$

$$= - A_s E_s \epsilon_2$$

Therefore $$P_{net} = K_2 \epsilon_2 - A_s E_s \epsilon_2$$

$$= (K_2 - A_s E_s) \epsilon_2 \qquad (2.13)$$

The steel stresses at the crack and at the gross section can be determined from Equations 2.7 and 2.8.

2.3.1.4 Formation of any number of crack

In general, the shrinkage strain ϵ_{shm} at which the m^{th} crack forms is given by the generalized form of Equations 2.2 and 2.9,

$$\epsilon_{shm} = \frac{A_e f_t}{K_{m-1}} \left[\frac{L}{L - (m-1)L_{slip}} \right] \qquad (2.14)$$

where K_{m-1} is obtained from Equation 2.4 by substituting m by (m-1).

Formation of the m^{th} crack is confirmed by checking that $\epsilon_{shm} < \epsilon_{shu}$.

The residual tensile concrete stress is given by the generalized form of Equations 2.5 and 2.12,

$$f_{cm} = K_m \epsilon_m / A_e \qquad (2.15)$$

where $$\epsilon_m = \epsilon_{shm}(L - mL_{slip})/L \qquad (2.16)$$

The net force in the member when the crack forms is derived from Equations 2.6 and 2.13,

$$P_{net} = (K_m - A_s E_s)\epsilon_m \qquad (2.17)$$

The steel stresses can be determined by substituting the appropriate values of concrete stress and P_{net} into Equations 2.7 and 2.8.

2.3.2 Shrinkage Crack Model

2.3.2.1 Reduced Stiffness of Cracked Region

In the above analysis procedure, the development of progressive cracking as shrinkage takes place depends on the effective stiffness K_{cr} over the region L_{cr}. If a force P is applied to the cracked member as indicated in Figure 2.5, the steel strain at the crack is given by

$$\begin{aligned}\epsilon_s &= P/(A_s E_s) \\ &= \frac{P}{(\rho A_c)(nE_c)} \\ &= \frac{P}{\left[\frac{\rho A_e}{(1+n\rho)}\right](nE_c)} \\ &= \frac{P(1+n\rho)}{n\rho A_e E_c}\end{aligned}$$

At a distance $L_{cr}/2$ from the crack, perfect bond is assumed between steel and concrete. The steel and concrete strains are therefore equal and given by

$$\epsilon_c = \frac{P}{A_e E_c}$$

Assuming a linear variation in steel strain within the cracked length L_{cr}, the average steel strain is given by

$$\begin{aligned}
\epsilon_{ave} &= (\epsilon_c + \epsilon_s)/2 \\
&= \frac{1}{2}\frac{P}{A_e E_c}\left[1 + \frac{(1+n\rho)}{n\rho}\right] \\
&= \frac{1}{2}\frac{P}{K_g}\left[2 + \frac{1}{n\rho}\right] \\
&= \frac{P}{K_g}\left[1 + \frac{1}{2n\rho}\right]
\end{aligned}$$

Therefore

$$\begin{aligned}
K_{cr} &= P/\epsilon_{ave} \\
&= K_g\left[\frac{1}{1 + \frac{1}{2n\rho}}\right] \\
&= \alpha K_g
\end{aligned} \tag{2.18}$$

where α = Stiffness reduction coefficient

$$= \frac{1}{1 + \frac{1}{2n\rho}} \tag{2.19}$$

Figure 2.6 from the CEB State-of-the-Art report (1982) shows the distribution of steel stress for a ribbed bar embedded in a concrete block for the working load and ultimate load levels. At the working load level, the stress distribution is close to linear and tends to become more linear at higher loads. The assumption of a linear steel strain distribution (or equivalently, steel stress distribution) is thus justified.

2.3.2.2 The Length of Cracked Region

The reduced stiffness of the member is affected by the length of the cracked region L_{cr} over which the steel stress is assumed to vary linearly as described above. Several approaches are considered for determination of the cracked length L_{cr}. It should be noted that all theories presented here deal with the cracking of hardened concrete and assume that the steel remains elastic after cracking has taken place (Beeby, 1979).

1. **'No-slip' Approach**

   The stress distribution in concrete within the cracked length can be approximated using the idea of stress diffusion. It is assumed that plane sections do not remain plane and that bond failure does not occur at the time the cracks developed (Beeby, 1979). Hence, there is no slip in the vicinity of the cracks, i.e. $L_{slip} = 0$.

   The tensile force in the steel bar at the cracked section is spread into the concrete by load. One may assume that the transfer force spreads into concrete roughly along a cone of slope $1/k_1$ as shown in Figure 2.7. The stress outside the cone is considered zero. From Figure 2.7, the cracked length is

$$L_{cr} = 2k_1c \qquad (2.20)$$

   where c is the maximum concrete cover measured from the

face of the bar to the concrete surface. The slope of the diffusion cone varies within a certain range and it can be calibrated according to test data. The diffusion concept was adopted by Bazant and Oh (1983), who took $k_1 = 1.4$, and Clark and Spiers(1978), who took $k_1 = 1$.

2. **'Slip' Approach**

To illustrate the concept, consider a segment of a cracked member subjected to pure tension as shown in Figure 2.8a. For simplicity, assume that the tension reinforcement consists of a single bar of diameter ϕ. When the bar segment AB is considered as a free body in Figure 2.8b, the tensile force T carried by the steel alone at B must be transferred to the concrete by bond stress τ_b over the development length L_d. The maximum force that can be transferred to the concrete is

$$T = A_c f_t$$

If τ_b is the average bond stress, then

$$T = \tau_b \pi \phi L_d = A_c f_t$$

Multiply the above expression by $\phi/4$,

$$\tau_b(\pi\phi^2/4)L_d = A_c f_t \phi/4$$

or $$\tau_b A_s L_d = A_c f_t \phi/4$$

or $$L_d = \frac{1}{4}\frac{\phi}{\rho}\frac{f_t}{\tau_b} \qquad (2.21)$$

where A_s = area of the steel bar

$= \pi\phi^2/4$

and $\rho = A_s/A_c$.

If the ultimate bond strength τ_{ult} is reached at the maximum load, then the bond stress τ_b may be substituted by τ_{ult}. And because τ_{ult} is proportional to f_t for a given bar type (Beeby, 1979 and Leonhardt, 1977), the above expression can be rewritten as:

$$L_d = k_2\phi/\rho \tag{2.22}$$

The above approach had been considered by Saliger (1936). It was assumed that plane sections remain plane within the concrete and that there will be slipping between the steel and the concrete. Bond failure is thus assumed to occur at each crack (Beeby, 1979).

Since the crack affects the stresses only within a distance $\pm L_d$ from the crack, the cracked length is

$$\begin{aligned} L_{cr} &= 2L_d \\ &= 2k_2\phi/\rho \end{aligned} \tag{2.23}$$

and because slipping occurs over the same distance,

$$L_{slip} = 2k_2\phi/\rho \tag{2.24}$$

The coefficient k_2 can be derived from the ultimate bond strength suggested in the 1963 ACI Code for the development length. The derivation is shown in Appendix A.

3. General approach

Beeby (1979) explained that the two forementioned approaches should be considered together to describe the actual cracking behaviour of axially reinforced tension members. A general formula for crack spacing is given by (Beeby, 1979; Ferry-Borges, 1966):

$$S = k_1 c + k_2 \phi/\rho$$

The cracked length can then be expressed as:

$$\begin{aligned} L_{cr} &= 2S \\ &= 2(k_1 c + k_2 \phi/\rho) \end{aligned} \tag{2.25}$$

and the slipping length is

$$L_{slip} = 2k_2 \phi/\rho \tag{2.26}$$

Note that Equations 2.20 and 2.23 are only special cases of Equation 2.25. Table 2.1 summarizes the different values of k_1 and k_2 used by others (Bazant and Oh, 1983; Clark and Spiers, 1978; Beeby, 1979 and Leonhardt, 1977).

2.4 Solution Algorithm

Step 1. Refering to Figure 2.2a, calculate the following constants for the member.

Total gross area, $A_g = hb$

Net concrete area, $A_c = A_g - A_s$

Steel ratio, $\rho = A_s/A_c$

Modular ratio, $n = E_s/E_c$

Equivalent transformed concrete area,

$$A_e = (1 + n\rho)A_c$$

Stiffness at uncracked section,

$$K_g = A_e E_c$$

Stiffness reduction coefficient,

$$\alpha = \frac{1}{1 + \frac{1}{2n\rho}}$$

Stiffness at cracked section,

$$K_{cr} = \alpha K_g$$

Step 2. Calculate the shrinkage strain at which first crack forms (m = 1) from Equation 2.14.

Step 3. Check if the shrinkage strain ϵ_{shm} is greater than the ultimate shrinkage strain ϵ_{shu}.

If $\epsilon_{shm} \geq \epsilon_{shu}$, the crack does not develop. The analysis is completed.

If $\epsilon_{shm} < \epsilon_{shu}$, the member cracks and member stiffness is reduced.

Step 4. Check if total cracked length is greater than the span length of the member.

If $mL_{cr} > L$, then no further cracks can form since the transfer length available will be insufficient to develop the concrete stress up to the concrete tensile strength and therefore no new cracks will form.

concrete stress in uncracked section after formation of crack.

Step 6. For the formation of subsequent shrinkage cracks, set m = 2, 3, ... and repeat steps (2) to (5).

A computer program as listed in Appendix B was written to perform the above analysis for given A_g, A_s, c, L, f_t, E_c, E_s, k_1, k_2, ϕ and ϵ_{shu}.

In the following section results are presented of a parametric study done to evaluate the effects of significant parameters on shrinkage crack spacing.

2.5 Parameter Study

The number of shrinkage cracks that would occurs in a member depends primarily on the ultimate shrinkage strain, span length, reinforcement ratio, reinforcing bar size and the tensile strength of concrete. ACI Committee 209 has recommended an average ultimate shrinkage strain value of 800 millionths for concrete with 100 mm or less slump, and minimum thickness of members 150 mm or less, and 40% or less ambient relative humidity. Since the basic analysis procedure assumes full fixity at ends and ignores creep effects, an ultimate shrinkage strain of 400 millionths in addition to the recommended value of 800 millionths was considered as an approximate allowance for partial fixity

considered as an approximate allowance for partial fixity and creep. Partial fixity results from both the effects of flexible supports and the fact that slab systems are normally cast in parts (Martin, 1971). Creep reduces stresses induced in concrete by restraint of shrinkage.

Thirteen members with the following basic properties were analysed.

A_g = 190mm²/mm

c = 154mm

E_c = 25900MPa

E_s = 200000MPa

The following parameters were varied:

(a) Member span length, L

(b) Steel area, A_s (mm²/mm)

(c) Reinforcing bar size, ϕ

(d) Tensile strength of concrete, f_t

To compare the results of using different approaches for estimating the cracked length, three analyses were carried out on each member with the following variations:

(a) $L_{cr} = 2k_1c$, $k_1 = 1.0$

(b) $L_{cr} = 2k_1c$, $k_1 = 1.4$

(c) $L_{cr} = 2k_2\phi/\rho$, k_2 derived from the development length in Appendix A.

Figure 2.9 shows a comparison of the cracked length estimated by different methods. Beeby's expression,

Leonhardt's expression and the development length give similar cracked length and should yield similar analytical results; therefore Beeby's expression and Leonhardt's expression are not considered in the present study.

Each of the parameters listed above will be considered in turn. A summary of members analyzed is given in Table 2.2. Details of parameters investigated are given in Table 2.3.

2.5.1 Span Length

Four members M1, M2, M3 and M4 of span lengths 2000mm, 4000mm, 6000mm and 8000mm respectively were considered in this study. For each span length, tensile stress induced in the slab member as a result of restraint of shrinkage is plotted in Figure 2.10 as a function of shrinkage strain. For this series, L_{cr} was taken as $2k_1c$, with $k_1 = 1.4$. As discussed previously in Section 2.3.1, a sudden drop in the induced force occurs at formation of a crack. The analysis was continued to an ultimate strain of 800 millionths. However it can be seen that the number of cracks formed for any value of ultimate shrinkage strain less than 800 millionths can also be determined from the plot. For example in the case of a span length of 4000mm and ultimate shrinkage strain of 800 millionths results in four cracks forming, whereas at 400 millionths ultimate shrinkage strain, only two cracks form.

The results show that the longer the length of the member, the greater the number of cracks. In effect the crack spacing becomes essentially the same for each span length as the ultimate shrinkage strain increases. This aspect of behaviour can be attributed to the fact that formation of a crack in a long member causes less reduction in stiffness than in a short member and consequently a higher residual stress in the uncracked region as can be seen from the plot.

2.5.2 Steel Area

Members M5, M3, M6 and M7 have steel areas 0.4mm²/mm, 0.6mm²/mm, 0.8mm²/mm and 1.0mm²/mm respectively. These steel areas correspond to the usual range of steel percentages used in concrete slab systems. Figure 2.11 shows the results of the analyses of these four members indicating that the number of cracks increases with area of reinforcement. Again, the number of cracks formed is related to the effective stiffness of the member after initial cracking takes place.

2.5.3 Reinforcing Bar Size

The effects of bar size on the number of cracks can only be revealed by using the 'slip' approach in estimating cracked length (length of reduced section stiffness). The

formula for the basic development length of tension reinforcement as stated in ACI Building Code is

$$L_d = 0.019 A_b f_y / \sqrt{f'_c}$$
$$\text{or} \quad 0.058 \phi f_y$$
$$\text{or} \quad 300\text{mm},$$

whichever is greater, for 35M or smaller bars. The expression shows that the development length increases with increased bar diameter.

As cracks form, the member with larger bars will have more reduction in stiffness because of longer cracked length, and thus the restraint stresses are lowered. Fewer cracks will therefore form in the member. This is shown in Figure 2.12 for members M7, M8, M9 and M10, each with the same steel area but with bar sizes 10M, 15M, 20M and 25M respectively. The use of a larger bar with longer development length has the effect of lowering the induced concrete tensile stress and reducing the number of cracks. However, a longer development length implies an increase in slip at the loaded end of the bar (i.e. at the face of a crack). Too high a slip may produce excessive crack width and thus fail to satisfy serviceability requirements for cracking.

The results show that for an ultimate shrinkage strain of 400 millionths, the use of smaller bars does not significantly increase the number of cracks but it has the advantage of limiting the crack width. In slab design,

using small bars such as 10M and/or 15M for reinforcement is good practice as far as controlling crack width is concerned.

2.5.4 Tensile Strength

To study the effects of variations in tensile strength, four members M3, M11, M12 and M13 were analyzed. Member M3 has the value of tensile strength based on the ACI expression for modulus of rupture,

$$f_r = 0.6\sqrt{f'_c} \text{ MPa}$$

Members M11, M12 and M13 have reduced tensile strength values of 0.50, 0.33 and $0.17\sqrt{f'_c}$ respectively. The results of the analyses are presented in Figure 2.13. As expected, the number of cracks increases with decrease in tensile strength.

2.5.5 Length of Reduced Member Stiffness

The general approach and the 'slip' approach to estimate the cracked length L_{cr}, which require knowledge of the reinforcement ratio and the bar size, is more difficult to use in analysis. In contrast, the 'no-slip' approach is very simple. An effort is therefore made to obtain a k_1 value in the expression $L_{cr} = 2k_1c$, such that the results will be in good agreement with those obtained from the

'slip' approach.

Table 2.4 is a summary of the total number of cracks formed in each member. Each member was analysed by the three different procedures for estimating L_{cr} mentioned earlier. From the table, it is found that results for $2k_1c$, $k_1 = 1.4$, and $2(L_d)$ agree well. A value of $k_1 = 1.4$ is therefore suggested for use in the analysis procedure. In most concrete slab systems, where span lengths range from 4000mm to 8000mm, reinforcing bar sizes 10M and 15M with tensile strength values $0.6\sqrt{f'_c}$, the total number of shrinkage cracks formed is only one or two, as can be seen from the results for members M2 to M8 based on ultimate shrinkage strain of 400 millionths. using the 'slip' approach. For a continuous slab system supported on columns, a single shrinkage crack would correspond to a crack along each column line while two cracks per span would correspond to cracks along the column lines and the mid-span lines.

2.6 Summary

A mathematical model to analyze the uniaxial shrinkage behaviour of a completely restrained reinforced concrete member has been developed. In the analysis, elastic characteristics are assumed in both concrete and steel and effects of creep are not explicitly included. The analytical procedure involves allowing shrinkage to occur

freely in the concrete, then applying the necessary forces required to maintain compatibility of deformations. These forces produce cracking as shrinkage strains increase. The member stiffness is reduced when cracks form, such that the internal force decreases by some extent and increases again as shrinkage continues. The reduction in stiffness is assumed over a cracked length within the vicinity of influence of a crack. The reduced stiffness in the cracked region is developed by assuming a linear steel strain distribution over the length concerned. Three approaches, 'no-slip' approach, 'slip' approach and a general approach, for estimating the cracked length are described.

A parametric study was performed to investigate the effects of several parameters on the total number of cracks forming in members subjected only to uniaxial shrinkage. The study illustrated the effects of variations in span length, reinforcing area, reinforcing bar size and tensile strength. The results show that the number of cracks formed is sensitive to the variations in concrete tensile strength but relatively insensitive to variations in other parameters. The results also indicate that for span lengths of 4000mm to 8000mm, one or two cracks per span length can be expected under normal circumstances. A value of $k_1 = 1.4$ used in the 'no-slip' approach was found to give results similar to the 'slip' or general approaches.

Method	k_1	k_2
Bazant and Oh	1.4	-
Clark and Spiers	1.0	-
Beeby	1.33	0.08
Leonhardt	1.2	0.1
Development Length	-	0.16 for $f_t = 0.62\sqrt{f'_c}$* 0.12 $0.50\sqrt{f'_c}$ 0.082 $0.33\sqrt{f'_c}$ 0.041 $0.17\sqrt{f'_c}$

* f'_c = 30MPa

Table 2.1 Summary of values of k_1 and k_2

Member	Span (mm)	Steel area (mm^2/mm)	Bar size	f_r (MPa)
M1	2000	0.6	10M	3.415
M2	4000	0.6	10M	3.415
M3	6000	0.6	10M	3.415
M4	8000	0.6	10M	3.415
M5	6000	0.4	10M	3.415
M6	6000	0.8	10M	3.415
M7	6000	1.0	10M	3.415
M8	6000	1.0	15M	3.415
M9	6000	1.0	20M	3.415
M10	6000	1.0	25M	3.415
M11	6000	0.6	10M	2.732
M12	6000	0.6	10M	1.821
M13	6000	0.6	10M	0.911

All members $A_g = 190mm^2/mm$

$E_c = 25900MPa$

$c = 154mm$

$n = 7.72$

Table 2.2 Summary of members analyzed

Parameter Study	Member	Variables	Constants
Span length	M1 M2 M3 M4	L = 2000 mm 4000 6000 8000	A_s = 0.6 mm^2/mm 10M Bar size f_r = 3.415 MPa
Steel area	M5 M3 M6 M7	A_s = 0.4 mm^2/mm 0.6 0.8 1.0	L = 6000 mm 10M Bar size f_r = 3.415 MPa
Bar size	M7 M8 M9 M10	Size 10M 15M 20M 25M	L = 6000 mm A_s = 1.0 mm^2/mm f_r = 3.415 MPa
Tensile strength	M3 M11 M12 M13	f_r = 3.415 MPa 2.732 1.821 0.911	L = 6000 mm 10M Bar size A_s = 0.6 mm^2/mm

Table 2.3 Summary of member properties in each parameter study

L_{cr}	M1	M2	M3	M4	M5	M6	M7	M8	M9	M10	M11	M12	M13
2(1.0)c	1	2	2	3	2	3	4	4	4	4	3	5	10
2(1.4)c	1	1	2	2	1	2	3	3	3	3	2	4	8
$2(L_d)$	1	1	1	1	1	1	2	1	1	1	1	2	7

Table 2.4 Summary of total number of cracks formed in members for $\epsilon_{shu} = 400 \times 10^{-6}$

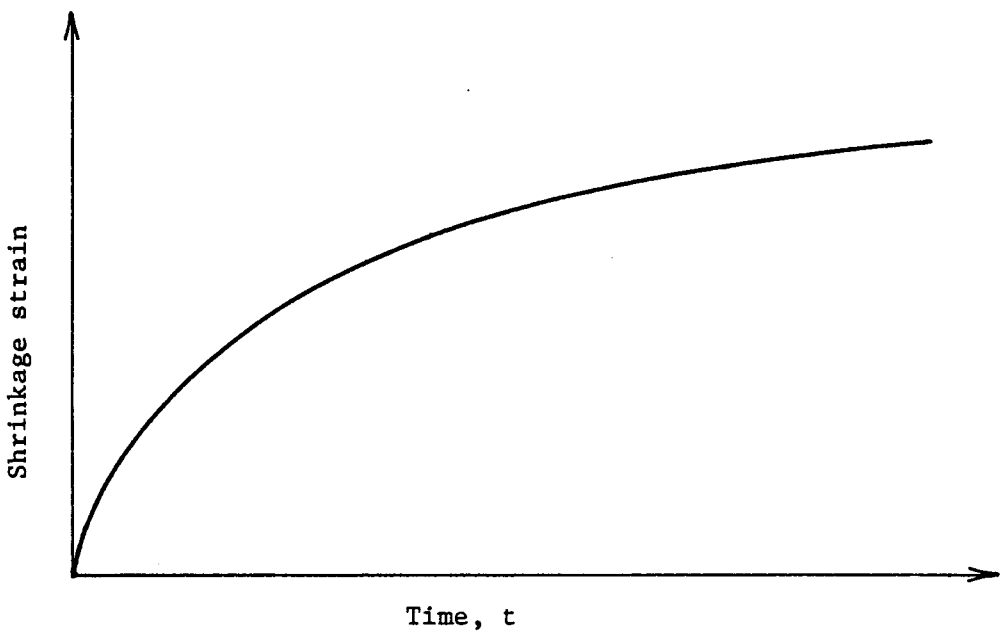

Figure 2.1 Shrinkage strain versus time curve

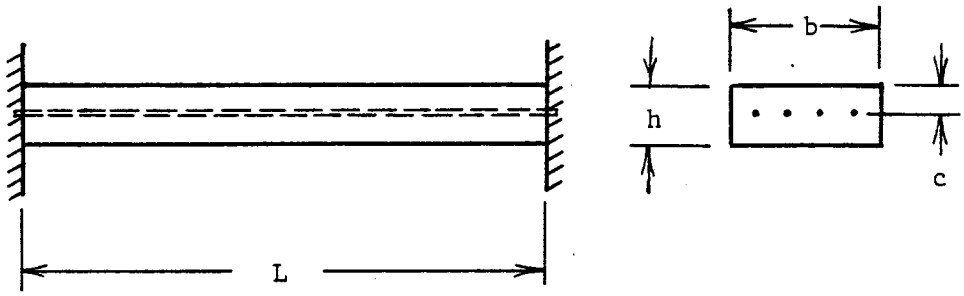

(a) Fixed support member

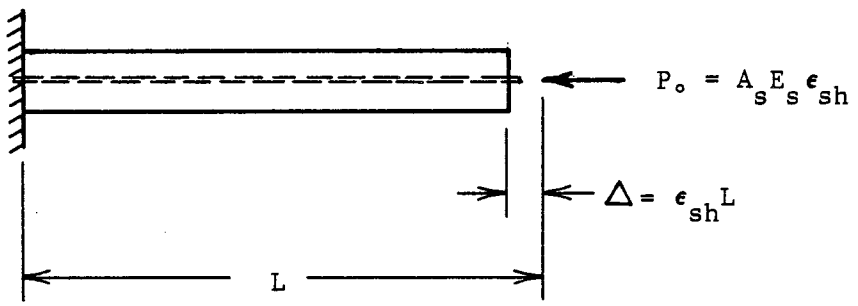

(b) Release one support

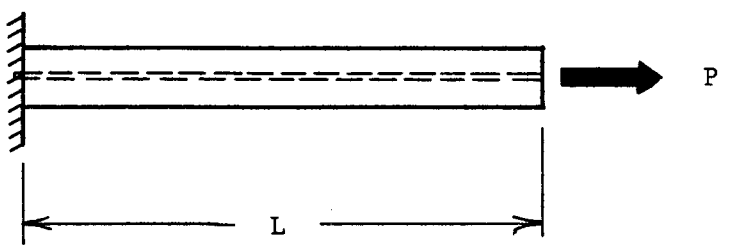

(c) Compatible member

Figure 2.2 Symmetrically reinforced slab element

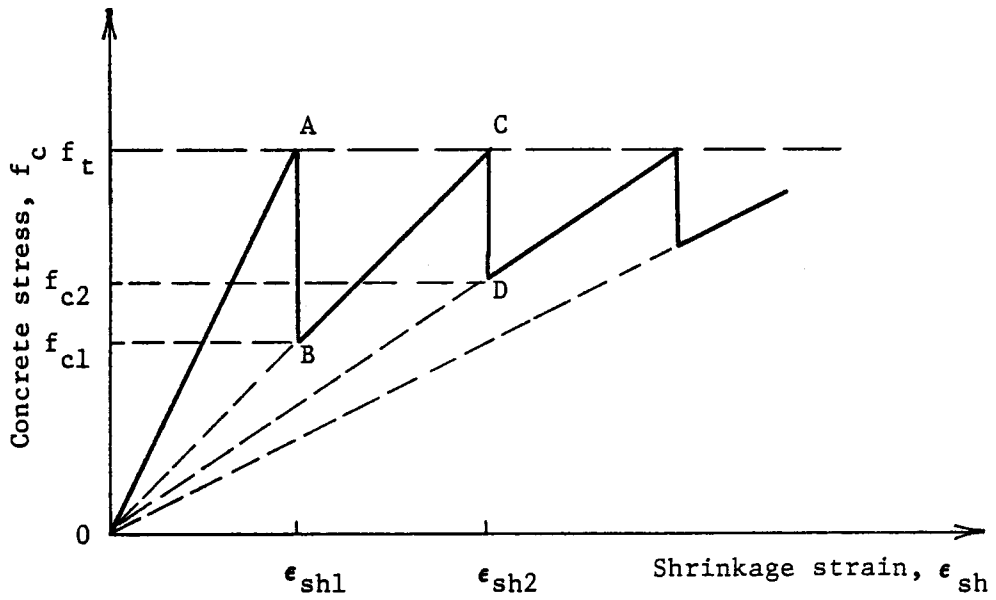

OA Uncracked member response

BC Member response after first crack forms

Figure 2.3 Member response curve

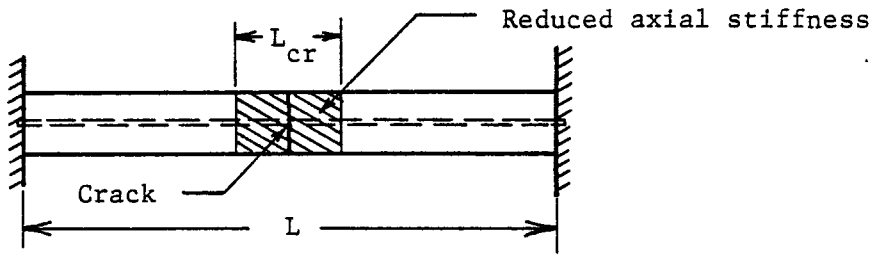

(a) Fixed support member with one crack

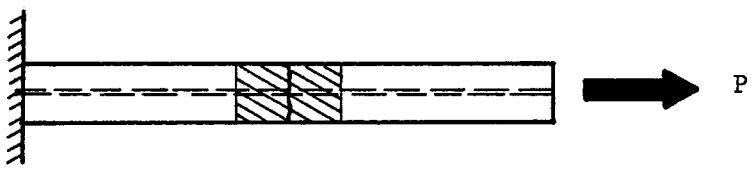

(b) Release one support

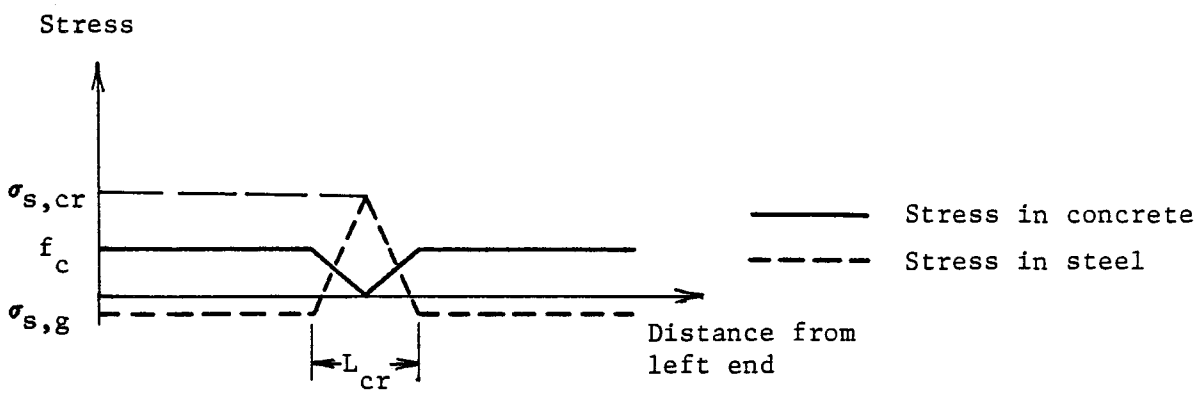

(c) Stress distribution after first crack forms

Figure 2.4 Cracked slab element

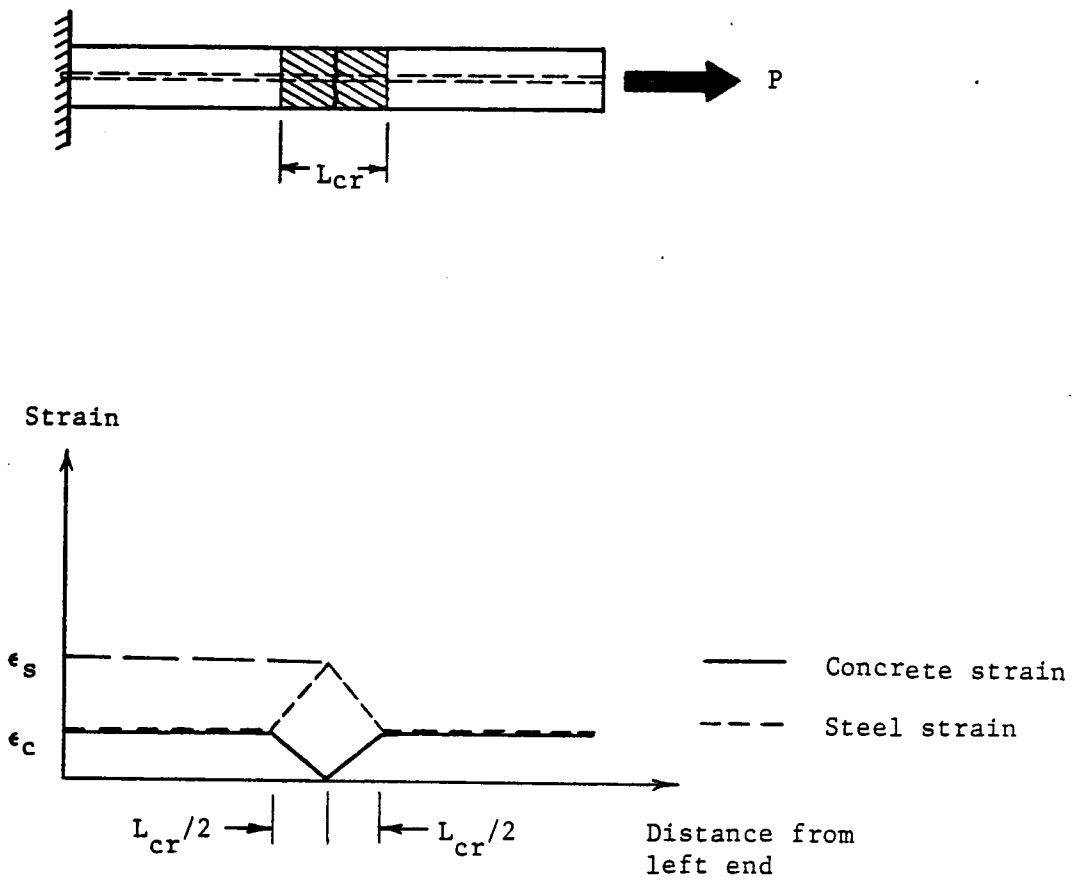

Figure 2.5 Strain distribution in a cracked member

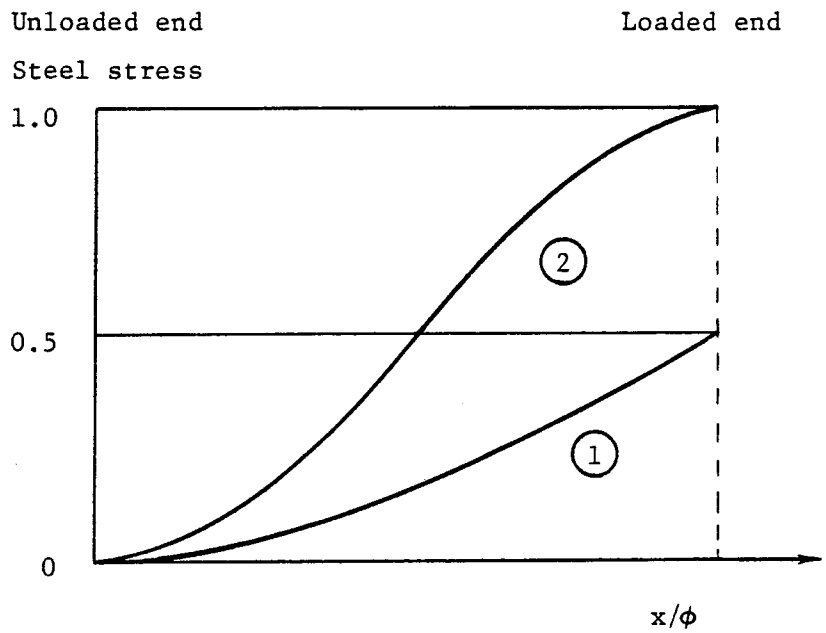

① Service load

② Ultimate load

Figure 2.6 Distribution of steel stress along the anchorage length
(CEB, 1982)

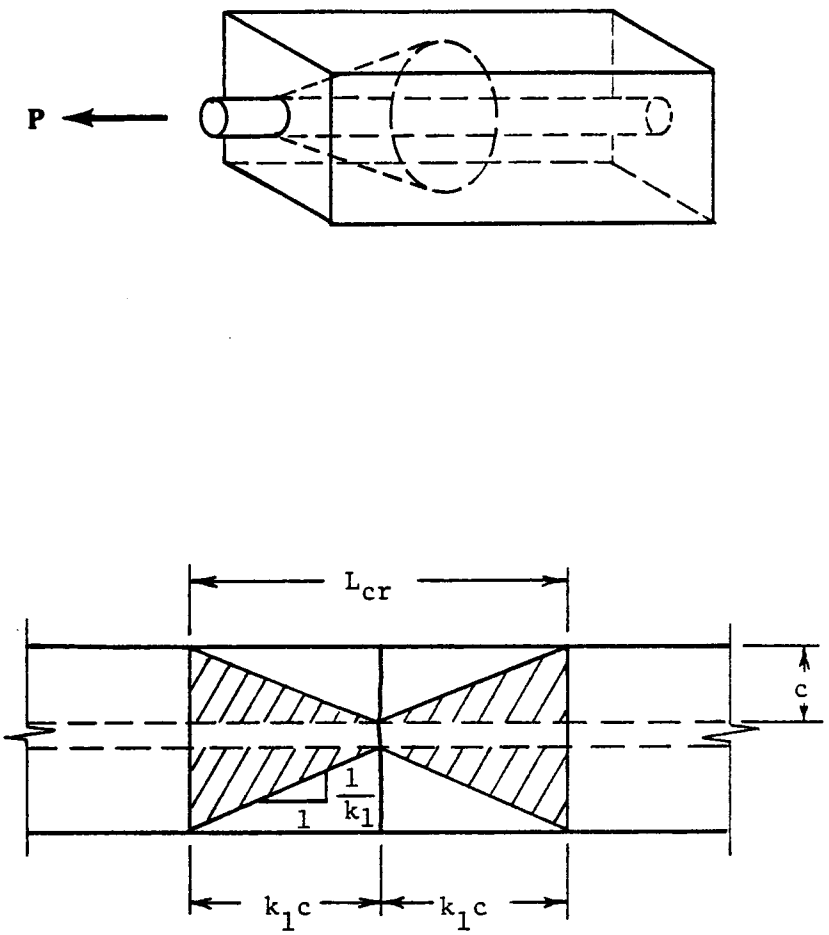

Figure 2.7 'No-slip' Approach

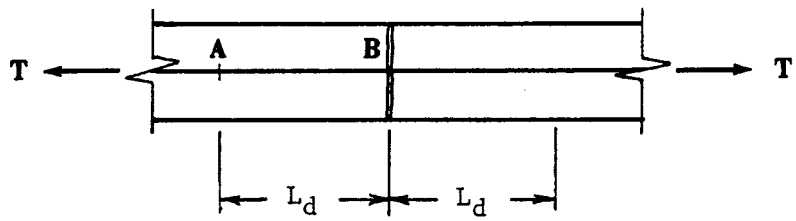

(a) Slab element subjected to pure tension

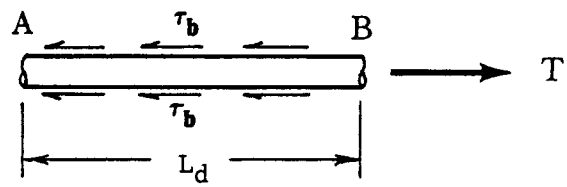

(b) Free body diagram of bar segment AB

Figure 2.8 'Slip' Approach

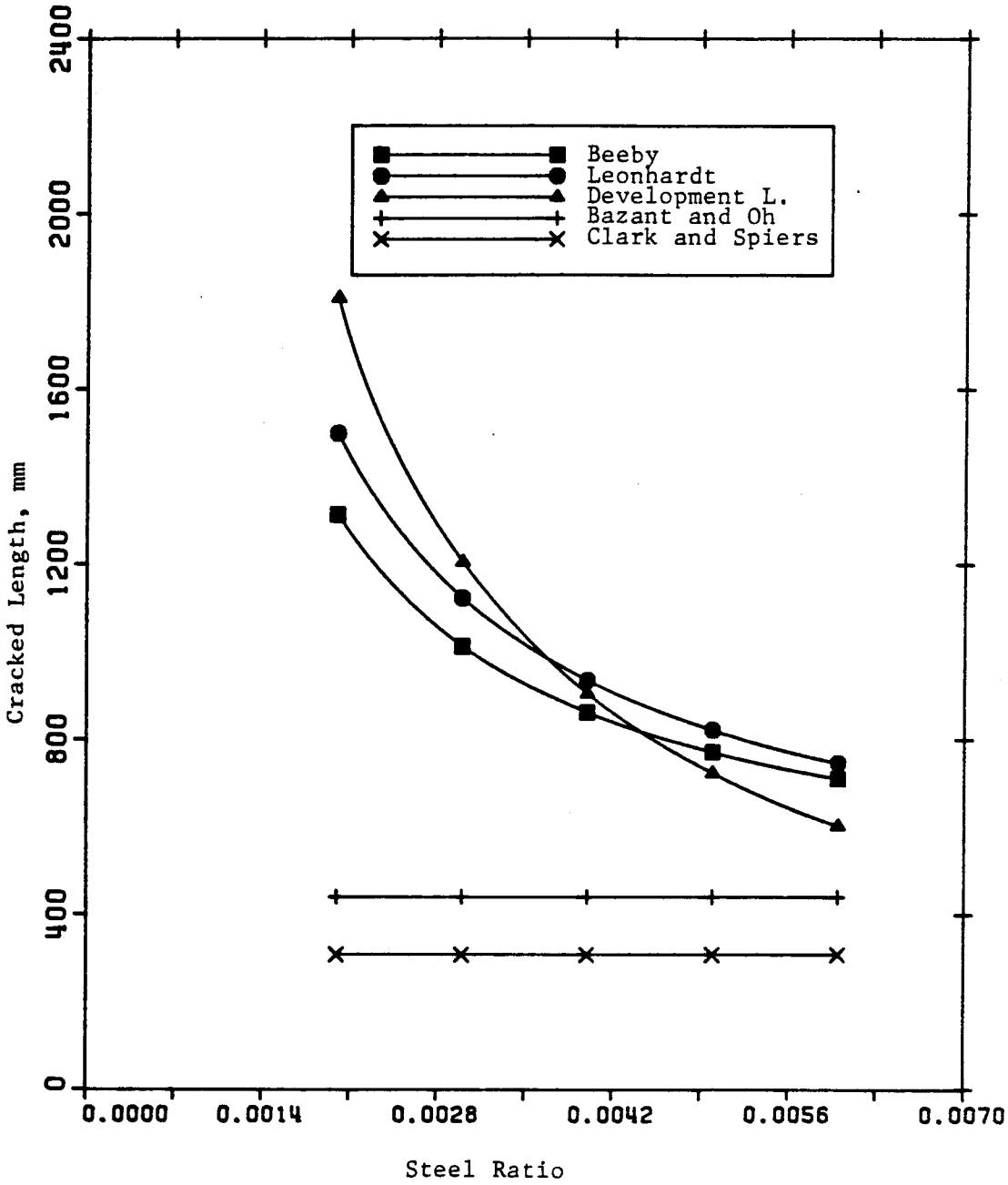

Figure 2.9 Comparison on cracked length using different expression

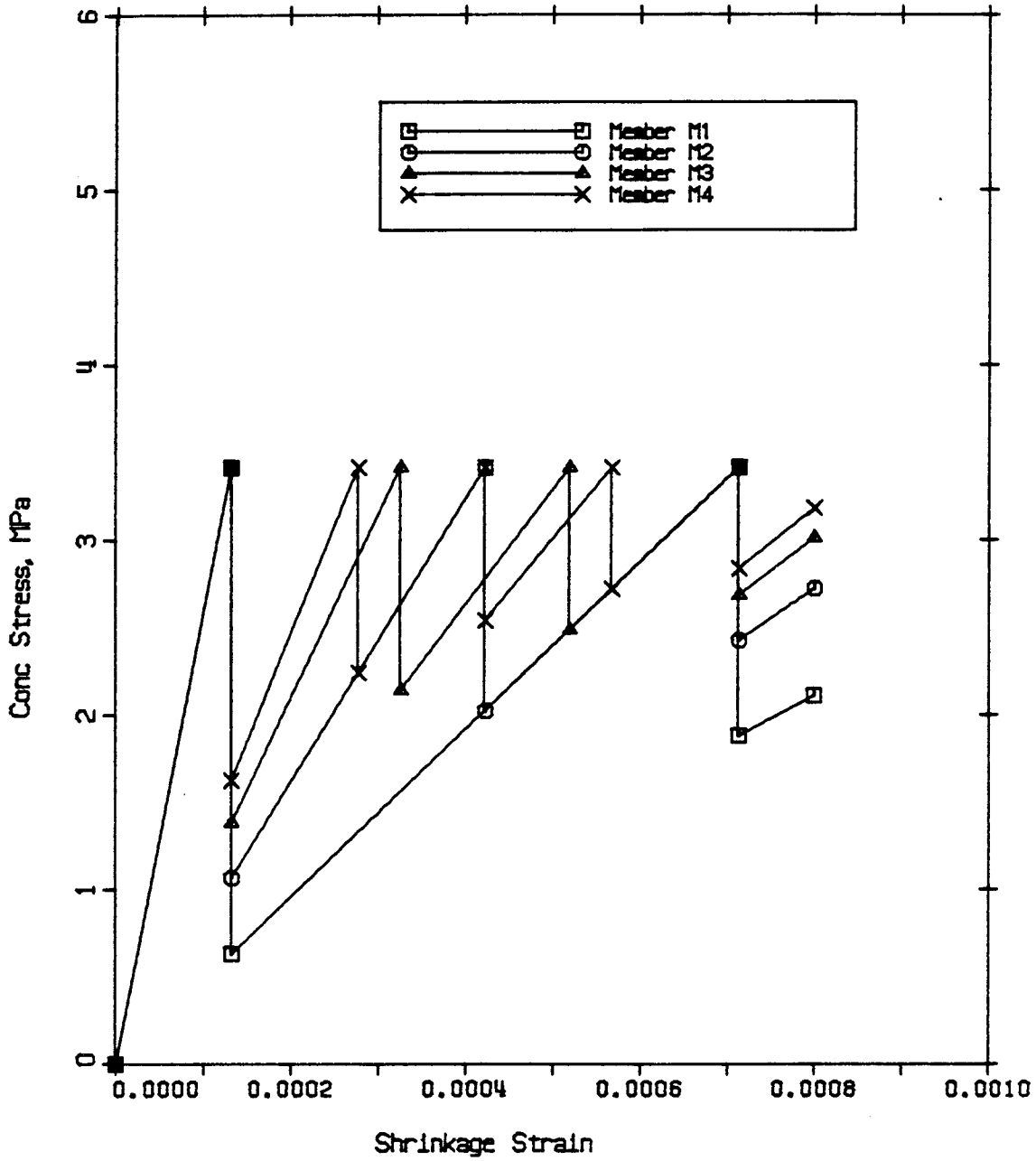

Figure 2.10 Effects of variations in span length

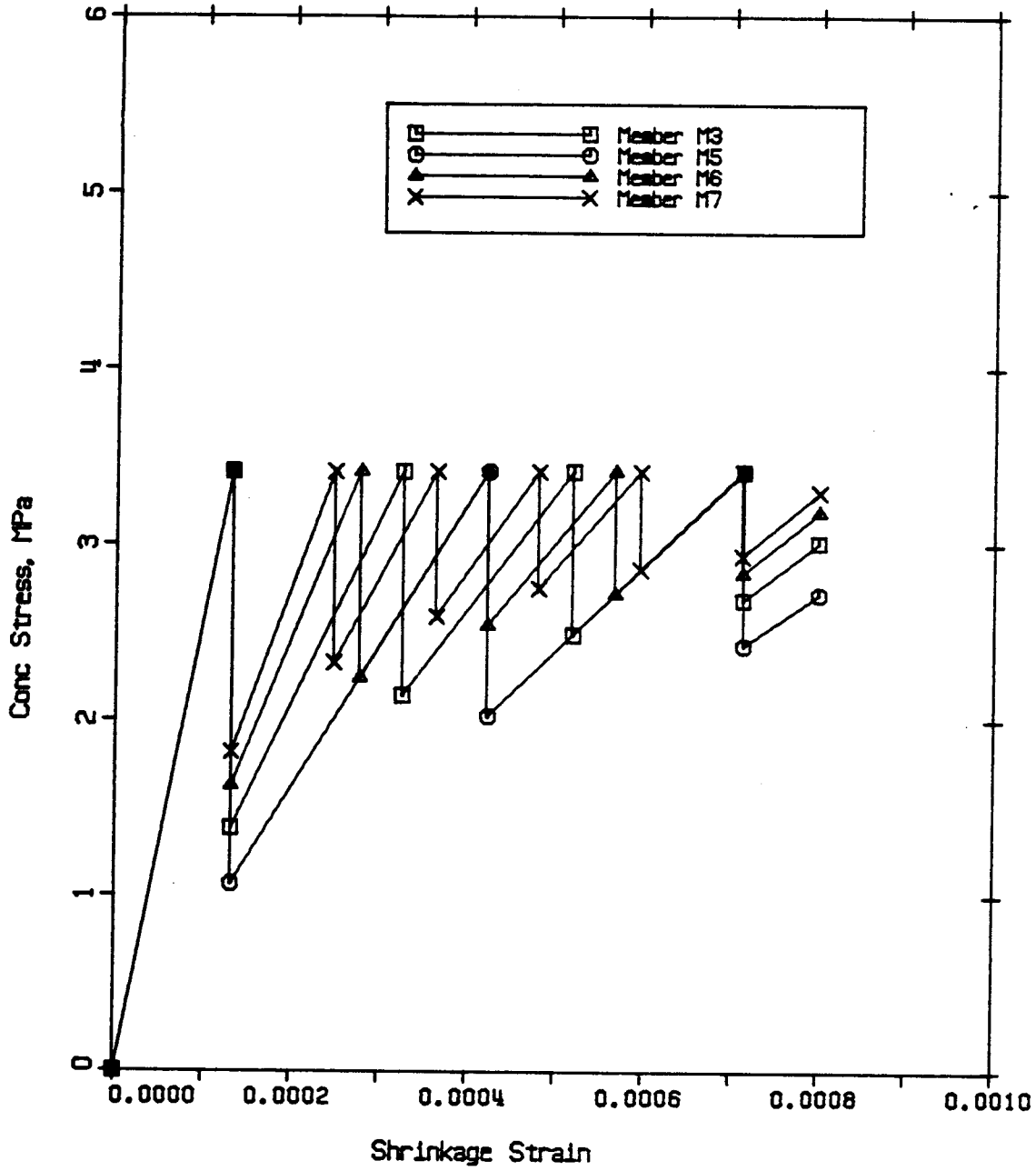

Figure 2.11 Effects of variations in steel area

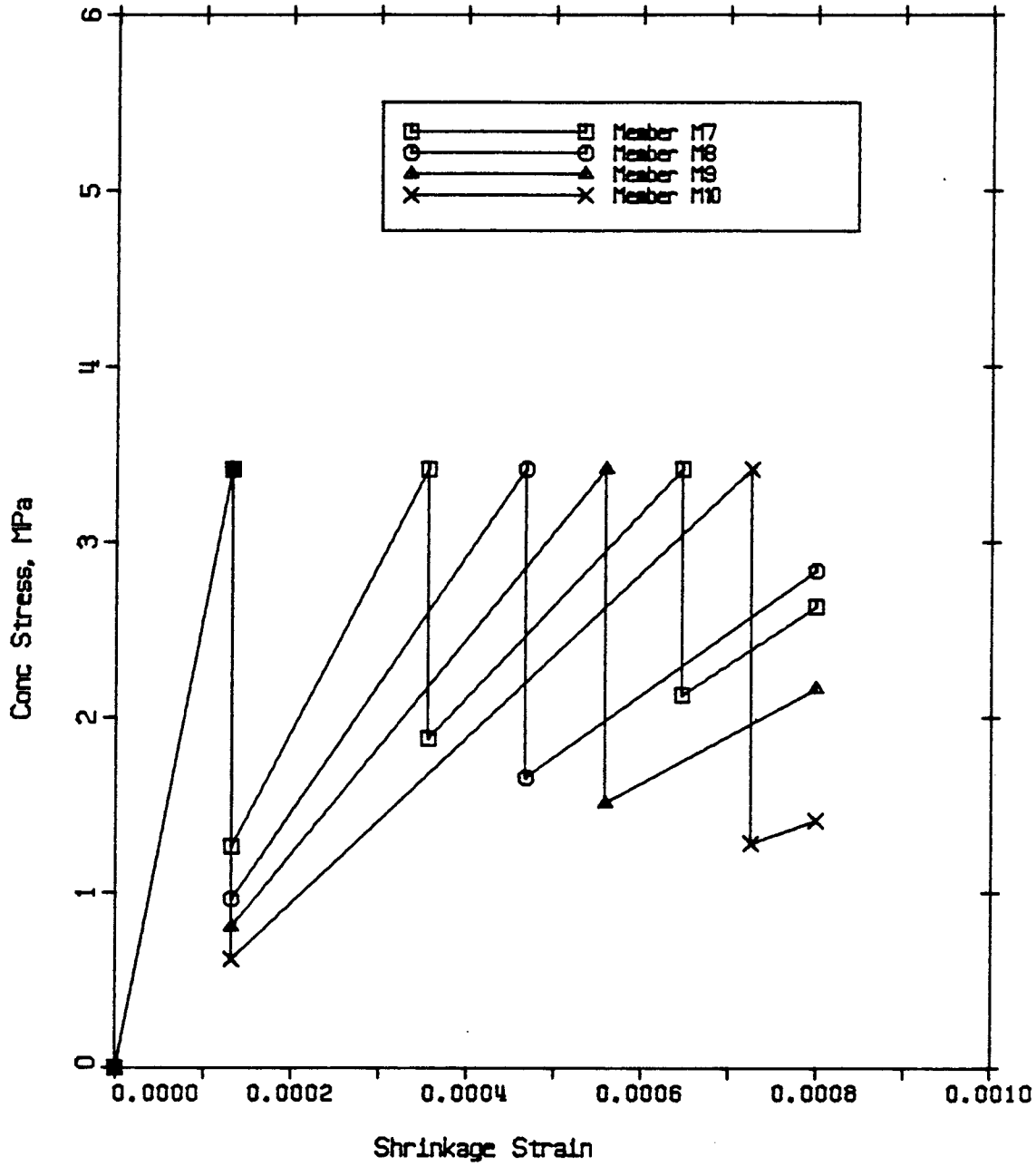

Figure 2.12 Effects of variations in bar size

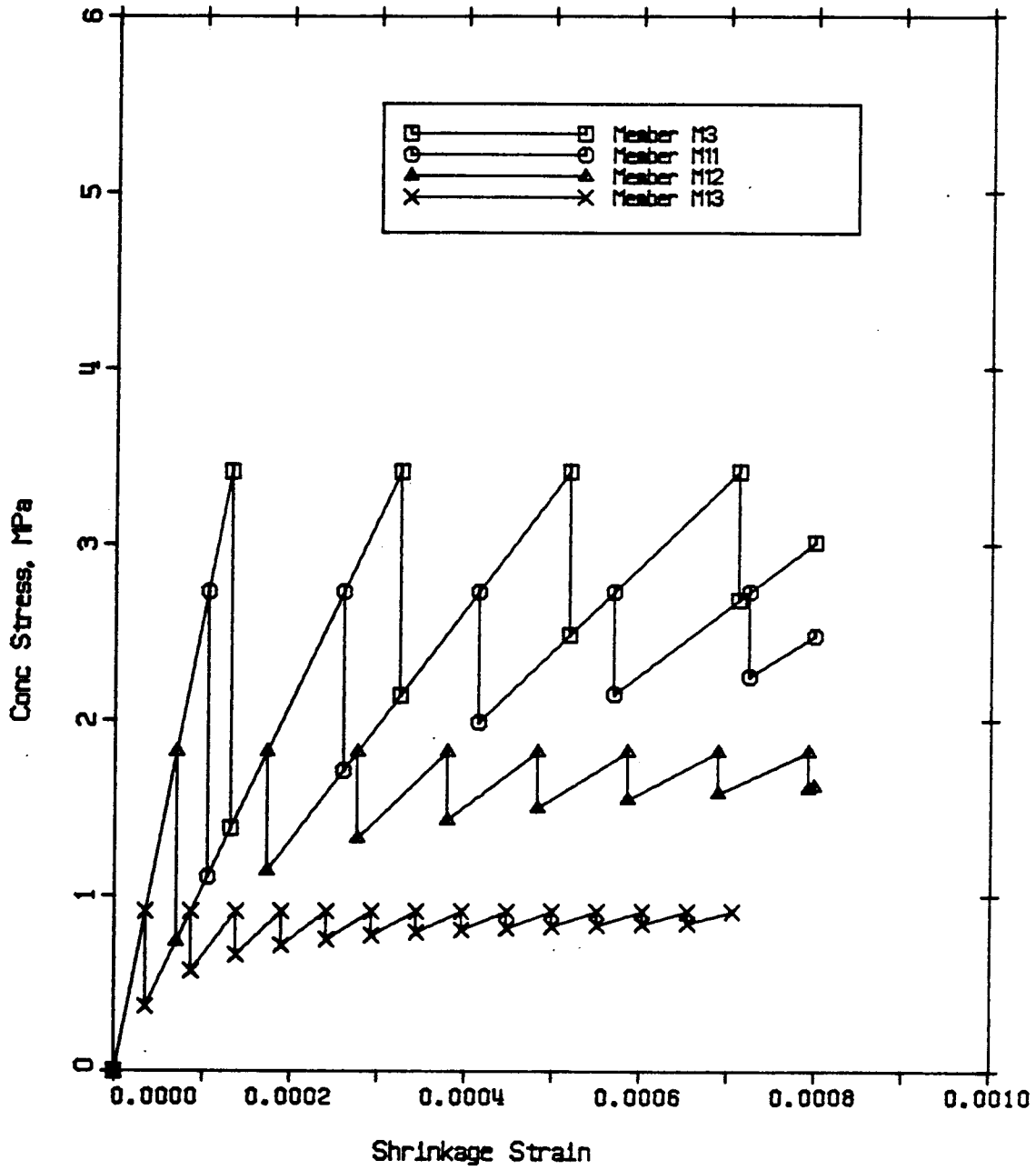

Figure 2.13 Effects of variations in tensile strength

3. ANALYSIS OF SLAB SYSTEMS INCLUDING EFFECTS OF CRACKING

3.1 Introduction

In the analysis of reinforced concrete slabs, effects of cracking due to both shrinkage restraint and transverse loads should be considered. Cracking reduces the overall flexural stiffness of slabs, resulting in increase in deflection and redistribution of moments. Serviceability may be adversely affected by excessive deflections and extensive cracking.

The finite element method provides a means to take account of different properties in each region of the slab, in particular, the reduced flexural stiffness due to cracking. In the finite element model described subsequently, cracking due to transverse loads and due to restraint of shrinkage is modelled. Long-term deflections due to shrinkage curvature and creep are also included in the model.

Analyses are carried out on three reinforced concrete slabs to study the effects of number of shrinkage cracks and variation in modulus of rupture. Results of the study are used to develop a simplified method to calculate slab deflections including shrinkage effects.

3.2 Finite Element Model

3.2.1 Assumptions and Limitations

The finite element computer program SAPIV (Bathe, Wilson and Peterson, 1974) was modified to account for reduced stiffness due to cracking, using a procedure proposed by Scanlon and Murray (1982). This procedure contains the following assumptions and limitations:

1. Linear elastic response is assumed for reinforcement and for concrete in compression. The analysis is therefore not valid for the post-yield range of behaviour.
2. Effects of cracking are included using the effective moment of inertia procedure proposed by Branson (1963). This procedure provides for a transition in flexural stiffness between the uncracked and fully cracked limits. Originally proposed for beam analysis, the procedure is generalized in this investigation to consider two-way (plate) action.
3. The tensile strength of concrete under biaxial stress is assumed to be equal to the uniaxial value of modulus of rupture. Figure 3.1 shows the biaxial failure envelope of concrete in terms of principal stresses. Combined tension and compression loadings reduce the tensile strength; however, in the service load range, the reduction is not significant and therefore the use of uniaxial value is reasonable in two-way slabs (Scanlon

and Murray, 1982).

4. It is assumed that cracking is initiated when M_x or M_y exceeds the cracking moments M_{cr}. M_x and M_y are defined for the local coordinates of the plate bending elements as shown in Figure 3.2. In general, for the finite element mesh layouts used in this study, the local coordinates coincide with the slab global coordinates defined by orthogonal reinforcement directions.
5. The shear modulus, G, for concrete, required for determination of the plate torsional rigidity is assumed to be unaffected by cracking. In another study (Hand, Pecknold and Schnobrich, 1973) it has been shown that plate bending analysis is not significantly affected by variations in the assumed value of G.

3.2.2 Flexural Stiffness of Cracked Region

The analysis of a reinforced concrete slab is treated as a problem of orthotropic plate bending. The plane stress constitutive relations for orthotropic material are given by:

$$\begin{Bmatrix} \sigma_x \\ \sigma_y \\ \tau_{xy} \end{Bmatrix} = \begin{bmatrix} \frac{E_x}{(1-\nu_x\nu_y)} & \frac{\nu_x E_y}{(1-\nu_x\nu_y)} & \bullet \\ \frac{\nu_y E_x}{(1-\nu_x\nu_y)} & \frac{E_y}{(1-\nu_x\nu_y)} & \bullet \\ \bullet & \bullet & G_{xy} \end{bmatrix} \begin{Bmatrix} \epsilon_x \\ \epsilon_y \\ \gamma_{xy} \end{Bmatrix} \quad (3.1)$$

The moments are related to the curvatures by

$$\begin{Bmatrix} M_x \\ M_y \\ M_{xy} \end{Bmatrix} = \begin{bmatrix} \frac{E_x h^3}{12(1-\nu_x\nu_y)} & \frac{\nu_x E_y h^3}{12(1-\nu_x\nu_y)} & \bullet \\ \frac{\nu_y E_x h^3}{12(1-\nu_x\nu_y)} & \frac{E_y h^3}{12(1-\nu_x\nu_y)} & \bullet \\ \bullet & \bullet & \frac{G_{xy} h^3}{12} \end{bmatrix} \begin{Bmatrix} \phi_x \\ \phi_y \\ \phi_{xy} \end{Bmatrix} \quad (3.2)$$

M_x and M_y can be obtained for each element from an analysis of the uncracked slab and then checked against M_{cr} for cracking. If cracking is detected, reduction in flexural stiffness in each direction can be accounted for using the Branson's expression (1963):

$$I_{ex} = (M_{cr}/M_x)^3 I_g + [\ 1 - (M_{cr}/M_x)^3\ ]\ I_{crx} \quad (3.3)$$

$$I_{ey} = (M_{cr}/M_y)^3 I_g + [\ 1 - (M_{cr}/M_y)^3\ ]\ I_{cry} \quad (3.4)$$

where $M_{cr} = f_r I_g / y_t$ (3.5)

The reduction in flexural stiffness due to cracking is implemented by modifying the plane stress constitutive properties as follows:

$$E_x = \alpha_x E_c \qquad \nu_x = \alpha_x \nu$$
$$E_y = \alpha_y E_c \qquad \nu_y = \alpha_y \nu \quad (3.6)$$

where, $\alpha_x = I_{ex}/I_g$ and $\alpha_y = I_{ey}/I_g$ (3.7)

The analysis is repeated using the reduced values until the results converge. Three iterations appear to be adequate for the slab systems considered in this study.

3.2.3 Finite Element Model of Shrinkage Cracks

To study the influence on load-deflection response of cracking due to shrinkage restraint, concrete slabs were assumed to be precracked as a result of shrinkage restraint, prior to applying transverse loads. The following procedure was used:

1. **Reduced flexural stiffness of precracked region**

   In the analysis of the symmetrically reinforced member subjected to shrinkage, described in Chapter 2, a linear variation of steel strain within the cracked region L_{cr} was assumed. For analysis of slabs in bending, a linear variation of curvature within the precracked region was assumed in deriving the reduced flexural stiffness.

   At the gross section

$$\phi_g = \frac{M}{E_c I_g}$$

   and at the cracked section

$$\phi_{cr} = \frac{M}{E_c I_{cr}}$$

   where I_{cr} is the moment of inertia of cracked

transformed section. It is implicitly assumed that the crack width is initially zero for precracked region so that an application of bending moment compressive stresses can immediately be transferred across the crack.

The average curvature within the precracked region is

$$\phi_{ave} = (\phi_g + \phi_{cr})/2$$

$$= \frac{1}{2}\left[\frac{M}{E_c I_g} + \frac{M}{E_c I_{crx}}\right]$$

If I_{px} is the reduced moment of inertia of the precracked region in x-direction, then

$$\phi_x = \frac{M_x}{E_c I_{px}} = \frac{1}{2}\left[\frac{M_x}{E_c I_g} + \frac{M_x}{E_c I_{crx}}\right]$$

$$\text{or} \quad I_{px} = \frac{2}{\frac{1}{I_g} + \frac{1}{I_{crx}}}$$

$$= \alpha_{px} I_g \tag{3.8}$$

$$\text{where} \quad \alpha_{px} = \frac{2}{1 + I_g/I_{crx}} \tag{3.9}$$

Similarly in the y-direction

$$I_{py} = \alpha_{py} I_g \tag{3.10}$$

$$\text{where} \quad \alpha_{py} = \frac{2}{1 + I_g/I_{cry}} \tag{3.11}$$

As for the cracking model, material properties in the constitutive relation are modified for precracked elements as follows:

$$E_x = \alpha_{px} E_c \qquad \nu_x = \alpha_{px} \nu$$
$$E_y = \alpha_{py} E_c \qquad \nu_y = \alpha_{py} \nu \qquad (3.12)$$

The analysis then proceeds as for an uncracked slab.

2. **Location and width of precracked region**

It is observed that elastic flexural tensile stresses due to transverse loading are highest along the interior column line and then along the mid-panel as indicated in Figure 3.3. When tensile stresses due to shrinkage restraint are superimposed with flexural tensile stresses, cracks are expected to form first along the interior column line when the resultant stresses exceed the tensile strength of concrete. When combined tensile stresses are high enough, cracks will form next along the mid-panel.

In the parametric study of the uniaxial member, the width of a cracked region of reduced stiffness was determined to be approximately

$$L_{cr} = 2(1.4)c \qquad (3.13)$$

This relationship was used to specify the width of zones of reduced stiffness due to pre-cracking and

formed the basis for specifying the width of precracked elements.

3.2.4 Long-term Effects due to Shrinkage Curvature and Creep

Deflections of reinforced concrete slabs increase with time. The additional deflections are caused by creep and shrinkage curvature. This additional inelastic deflection increases at a decreasing rate during the time loading. Procedures recommended by ACI Committee 209 (1971) and 435 (1966) were used to calculate long-term deflections in addition to immediate deflections.

1. **Shrinkage curvature**

Concrete shrinkage in unsymmetrically reinforced members, as in the case of slabs, causes a nonuniform strain distribution and results in curvature of the member. In flexural members, shrinkage is more restrained at the tension face where heavier reinforcement is placed. Therefore, shrinkage curvatures will have the same sign as the curvatures due to transverse loads and consequently increase the deflections.

Expressions for shrinkage curvature are provided by Branson (Branson, 1963; ACI Committee 435, 1966):

$$\phi_{sh} = \frac{0.7\ \epsilon_{sh}(\rho-\rho')^{1/3}}{h}\left[\frac{\rho-\rho'}{\rho}\right]^{1/2}$$

for $(\rho-\rho')$ ≤ 3%, which is generally the case for reinforced concrete slab systems. Note that ρ and ρ' are in percent.

In the modified SAPIV program, shrinkage curvatures were treated as equivalent temperature curvatures for each plate element. Deflections were then computed based on the equivalent temperature curvature.

2. **Creep**

ACI Committee 435 (1966) recommended a procedure for computing the deflection due to creep based on the work of Branson as given by

$$\Delta_{cp} = k_r C_t (\Delta_i)_D$$

where k_r = compression steel factor

$$= \frac{0.85}{1+50\rho'}$$

C_t = creep coefficient

and $(\Delta_i)_D$ = instantaneuous deflection due to all sustained load

This is equivalent to using a modified modulus of elasticity in the computation of elastic deflection,

$$E_{ct} = \frac{E_c}{(1+k_r C_t)}$$

In the finite element analysis, the values of k_r in x and y directions are obtained to compute the modified modulus of elasticity in the corresponding direction.

The reduced values are used in the constitutive relations to calculate deflections. In this study, k_r = 0.85 was used, since only small amounts of reinforcement are provided in compressed concrete zones.

3.3 Finite Element Analysis and Parameter Study

3.3.1 Slab descriptions

To study the effects of precracking due to shrinkage restraint analyses were carried out for no precracking, precracking along column lines only, and for precracking along both column lines and mid-panel lines. The slab for which no precracking was assumed, was analyzed for a range of modulus of rupture values. Details of the slabs analyzed are as follows:

1. A square two-way slab S1, designed by the direct design method, was used to study the effects of variations in modulus of rupture on the deflection of a slab with no pre-cracking. The slab has three 6m span in each direction, a thickness of 190mm and 550x550mm square columns. The slab is a flat plate with no edge beams or drop panels. The thickness selected satisfies minimum thickness requirements of the ACI Code. Column size and reinforcement were selected on the basis of strength requirements. The structure layout is shown in Figure 3.4 and a finite element mesh layout is shown in

Figure 3.5. Because of symmetry, only a quarter of the slab need be considered in the finite element analysis. Results of the analysis are presented in Figure 3.6 in the form of load-deflection curves for the center of the exterior panel. The deflection at this location was observed to be the maximum for all values of modulus of rupture. Figure 3.7 shows the additional deflections due to creep and shrinkage curvature.

2. The same slab system appears in Figure 3.8 as slab S2, except that the slab is precracked along the interior column line. The distance from extreme compression fiber to the face of tension reinforcement c is assumed to be 154mm for all sizes of reinforcing bars in both directions. The resulting width of precracked region is

$$L_{cr} = 2(1.4)154$$
$$\simeq 440\text{mm}$$

Figure 3.9 shows load-deflection curves for the center of the exterior panel.

3. Slab S3 is the same slab system but precracked both along the interior column lines and mid-panel, as shown in Figure 3.10. This slab represents the more severe case where tensile stresses induced by restraint to shrinkage are high enough to produce cracks at both locations. Figure 3.11 shows the load deflection curves for center of exterior panel.

3.3.2 Parameter Study

1. Effects of precracking

Moments along the interior column strip of precracked slabs S2 and S3 are compared to that of uncracked slab S1 in Figure 3.12. Slab S2 has the highest moment at the mid-span, which is a result of redistribution of moments when a shrinkage crack is formed along the column lines. The cracks at mid-panel of slab S3 reduce some mid-span moments and redistribute the moments to the columns. The significant effect of precracking on the redistribution of moments is illustrated here.

The effect of various degrees of precracking on deflections is shown in Figure 3.13. The excessive slab deflections of slab S3 would probably occur under extreme adverse condition and therefore represents a conservative deflection calculation. Slab S2 represents an average condition where the deflections do not deviate greatly from the uncracked slab S1.

2. Effects of variation in modulus of rupture

For slab S1, deflections were computed based on the effective moment of inertia using different values of modulus of rupture in Equation 3.5. The modulus of rupture f_r in Equation 3.5 may be replaced by the effective modulus of rupture f_e:

$$M_{cr} = f_e I_g / y_t \qquad (3.14)$$

The effective moment of inertia I_{eff} is then calculated using the reduced value of M_{cr} and subsequent deflection calculations are carried out in this simplified method to take account of restraint stresses (Scanlon and Murray, 1982).

Variation of deflection with effective modulus of rupture at different load levels is shown in Figure 3.14. It is observed that at lower load level, variations of modulus of rupture has little effect on slab deflections. Indicated in the plot is also the deflections of the two precracked slabs. The results show that effective modulus of rupture values of 0.3 to $0.4\sqrt{f'_c}$ MPa at service load level corresponds approximately to the case of precracking along column lines only. Effective modulus of rupture of 0.2 to $0.3\sqrt{f'_c}$ applied to an uncracked slab corresponds to the case of a slab precracked along both column and mid-panel lines.

3.4 Summary

This chapter describes a finite element analysis of slab systems that may be precracked in prescribed locations as a result of restraint of shrinkage. The analysis was applied to a slab system under no precracking, precracking

along column lines only and precracking along both column and mid-panel lines. These cases represent the range of conditions likely to occur under normal conditions. By means of a brief parameter study it was shown that the effects of precracking due to shrinkage restraint could be accounted for by applying a reduced effective modulus of rupture in the analysis of an initially uncracked slab.

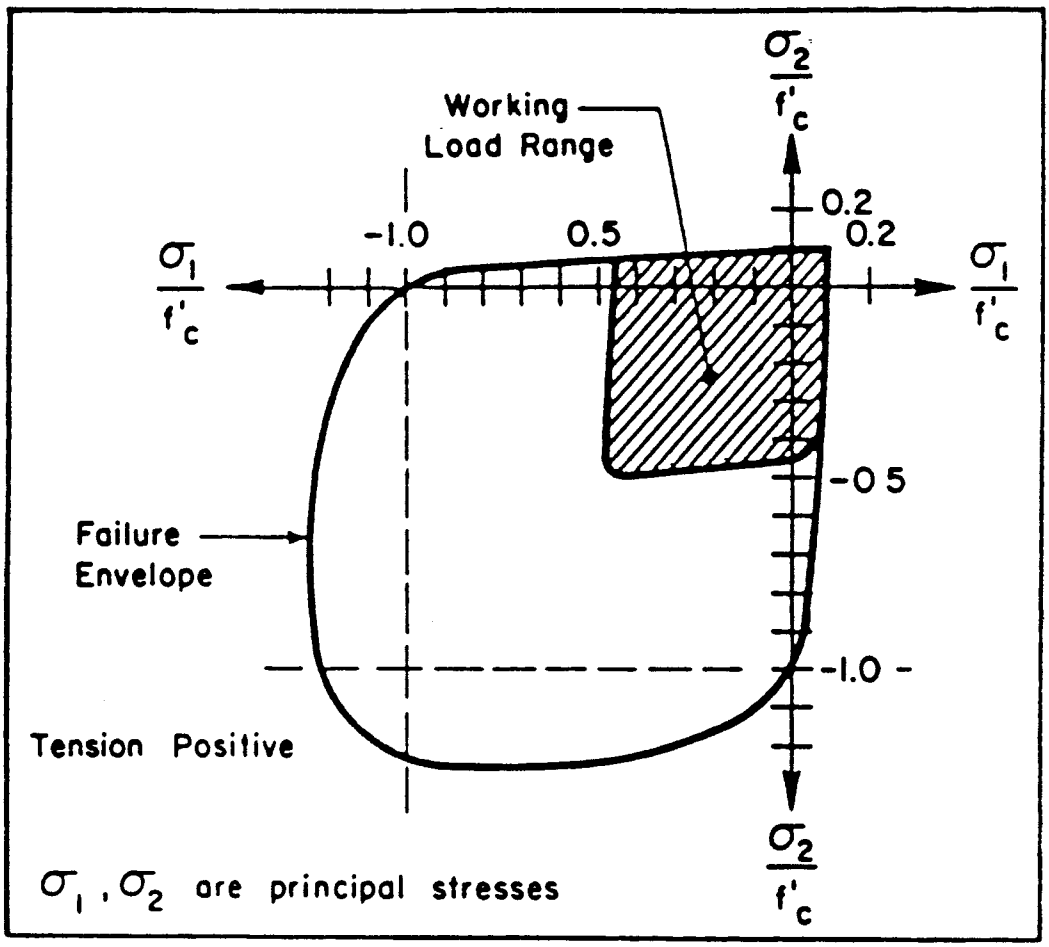

Figure 3.1 Biaxial strength of plain concrete
(Kupfer, Hilsdorf and Rusch, 1969)

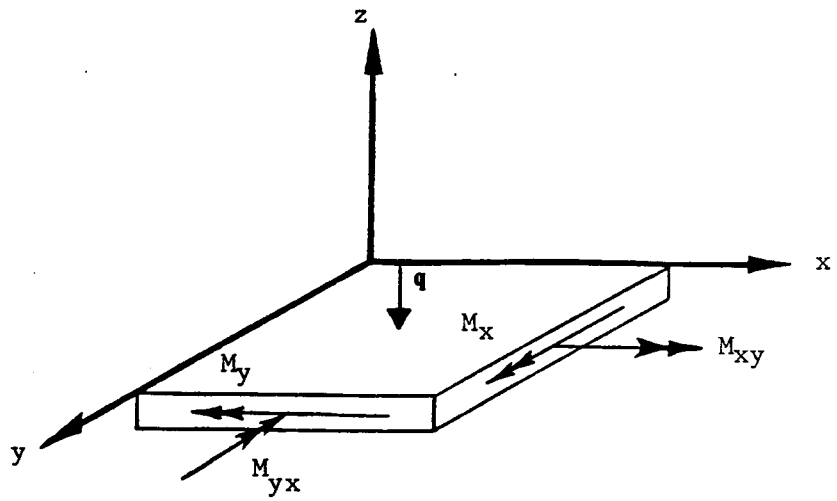

Figure 3.2 Plate bending element

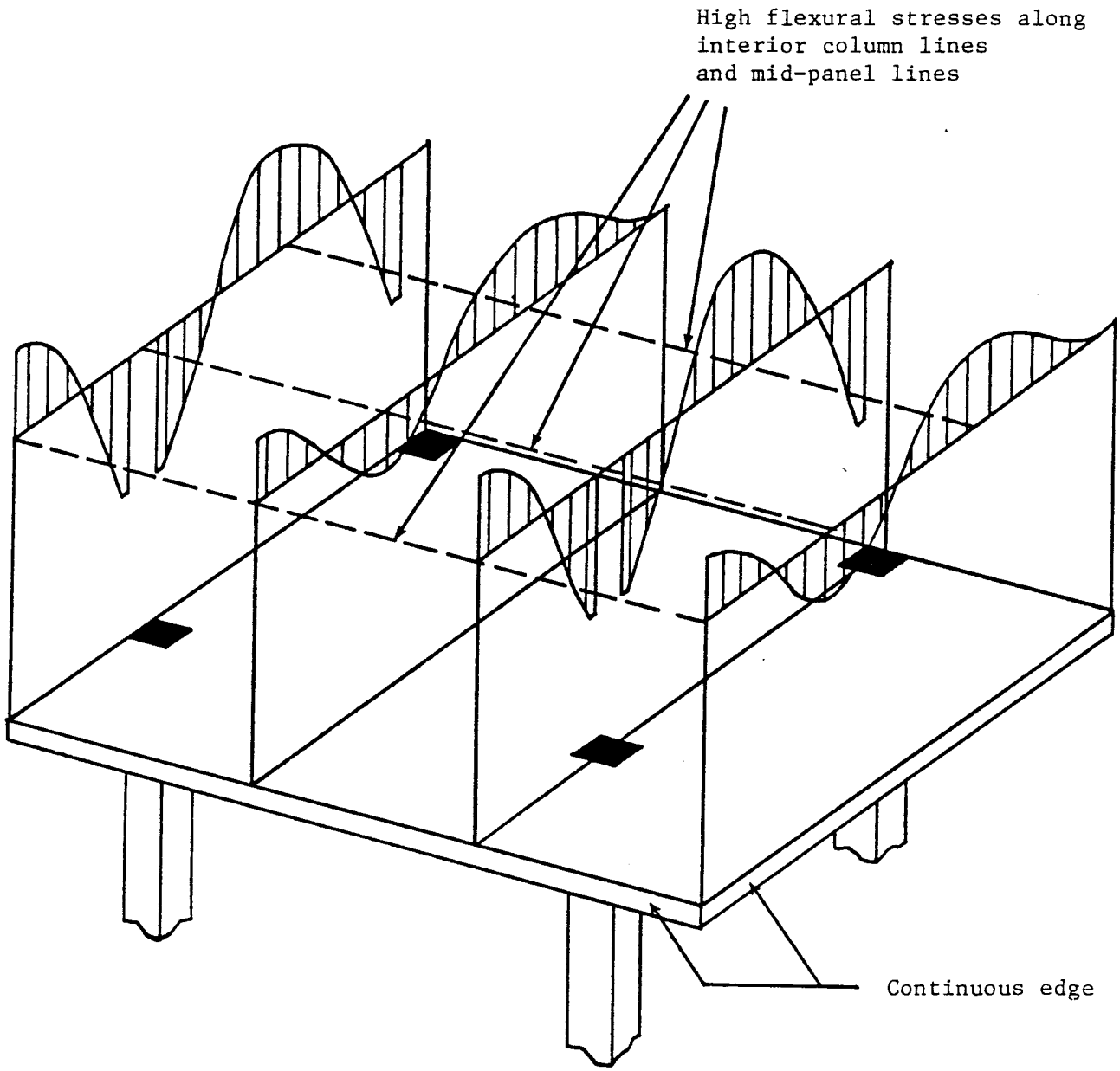

Figure 3.3 Tensile stress distribution in slab along column lines and panel centre lines due to uniform transverse load

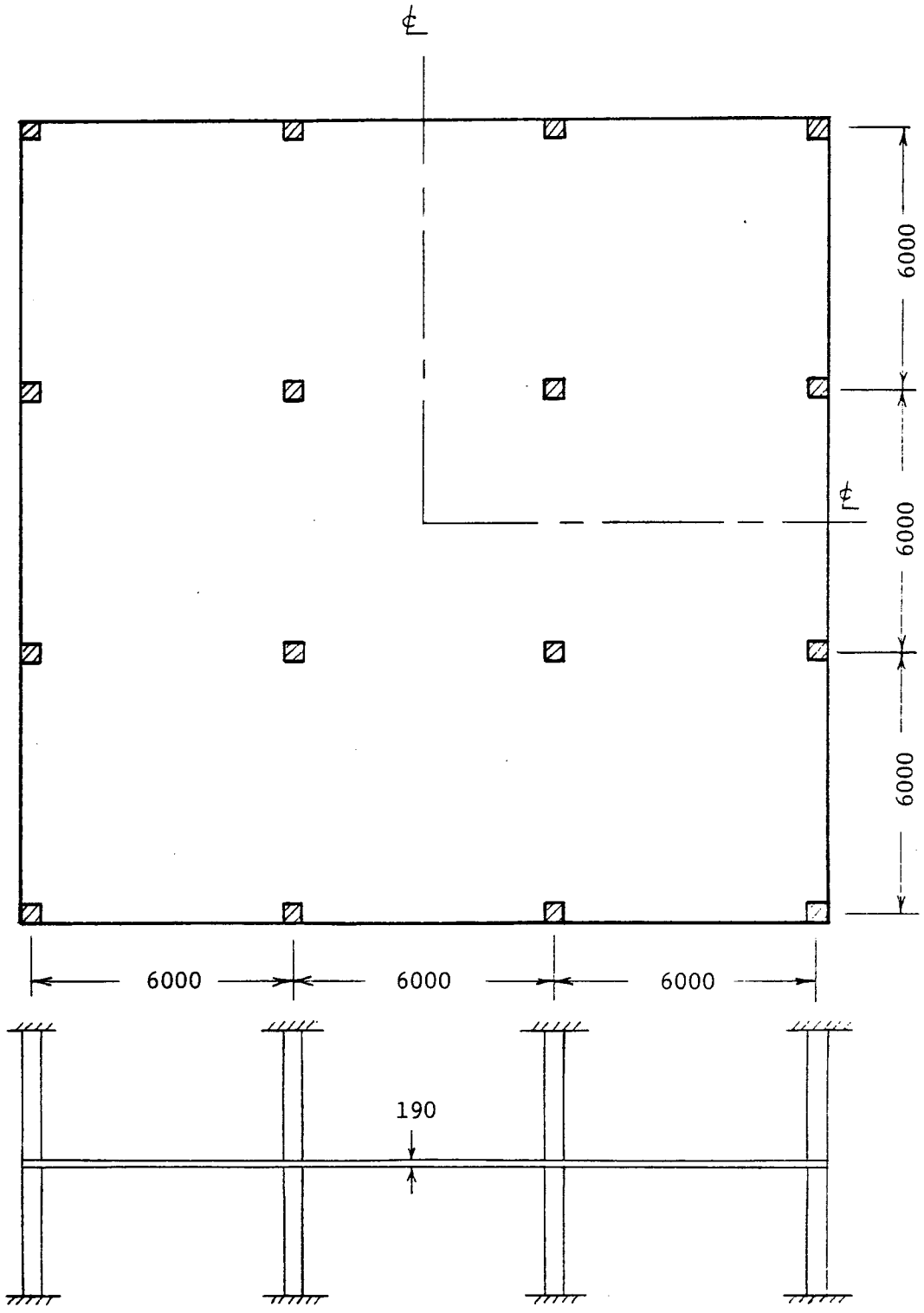

All columns 550mmx550mm

Figure 3.4 Structure layout of slab system

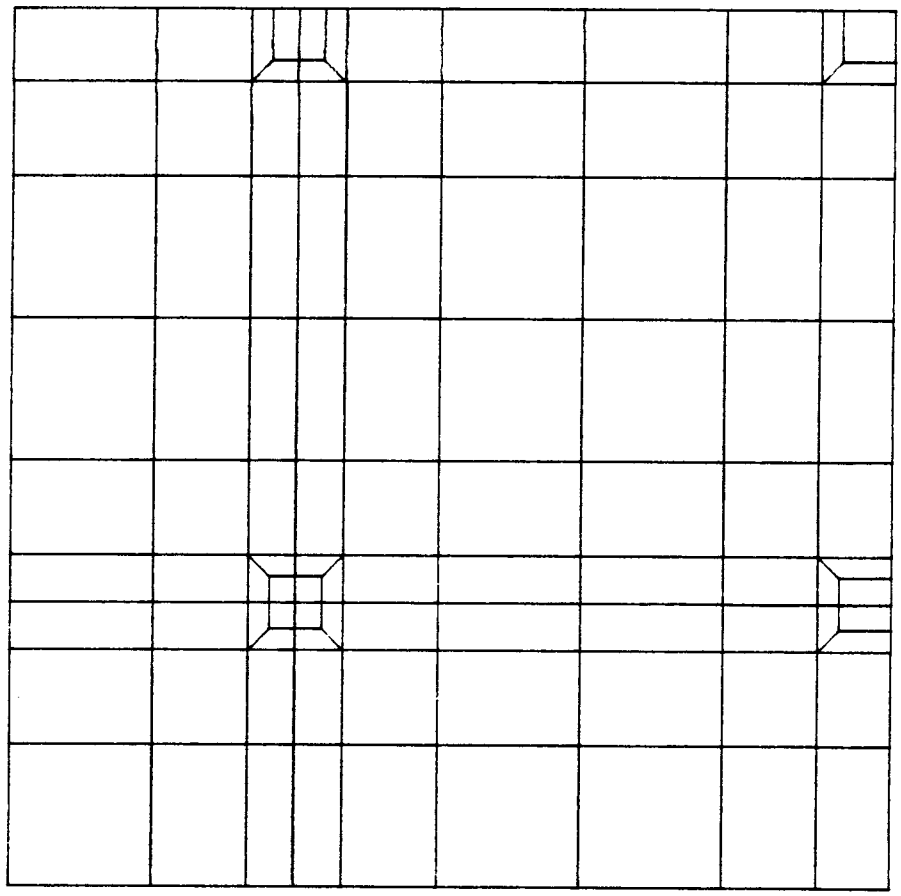

Figure 3.5 Mesh layout for Slab S1

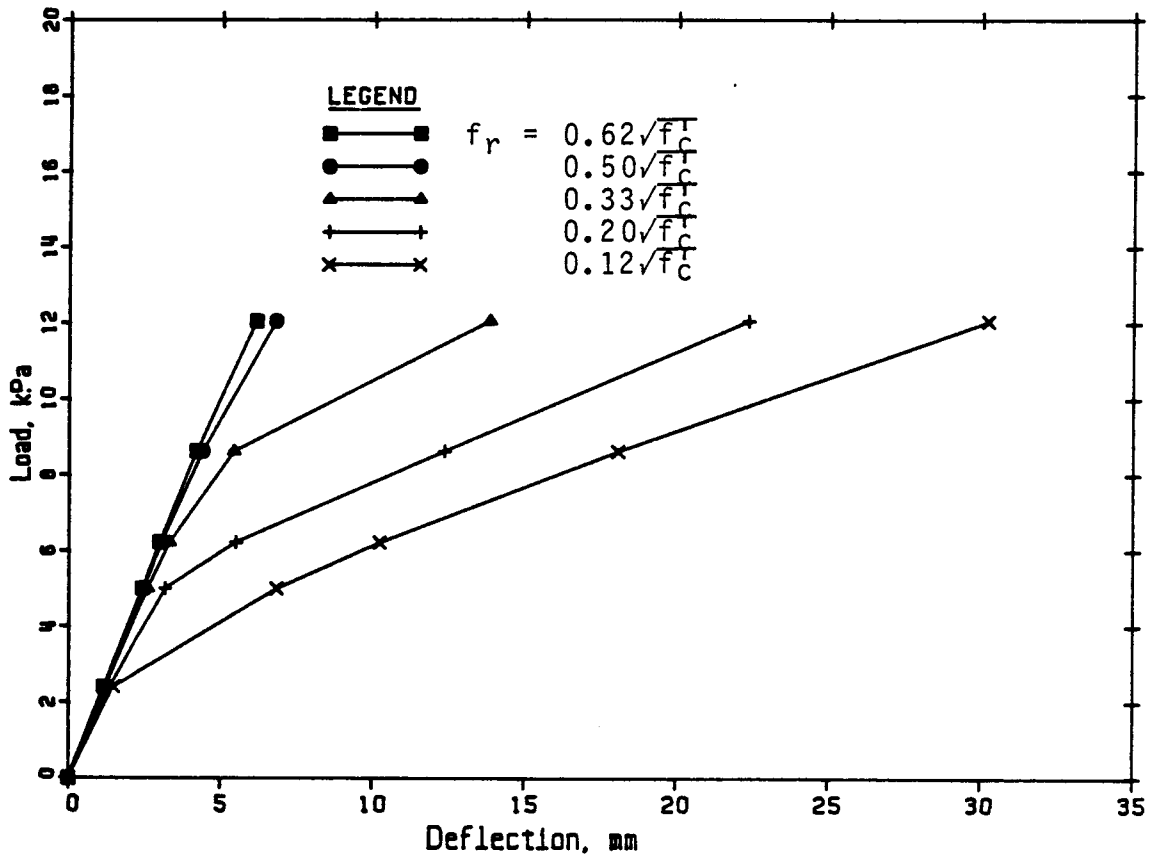

Figure 3.6 Load-deflection curves at center of exterior panel of Slab S1

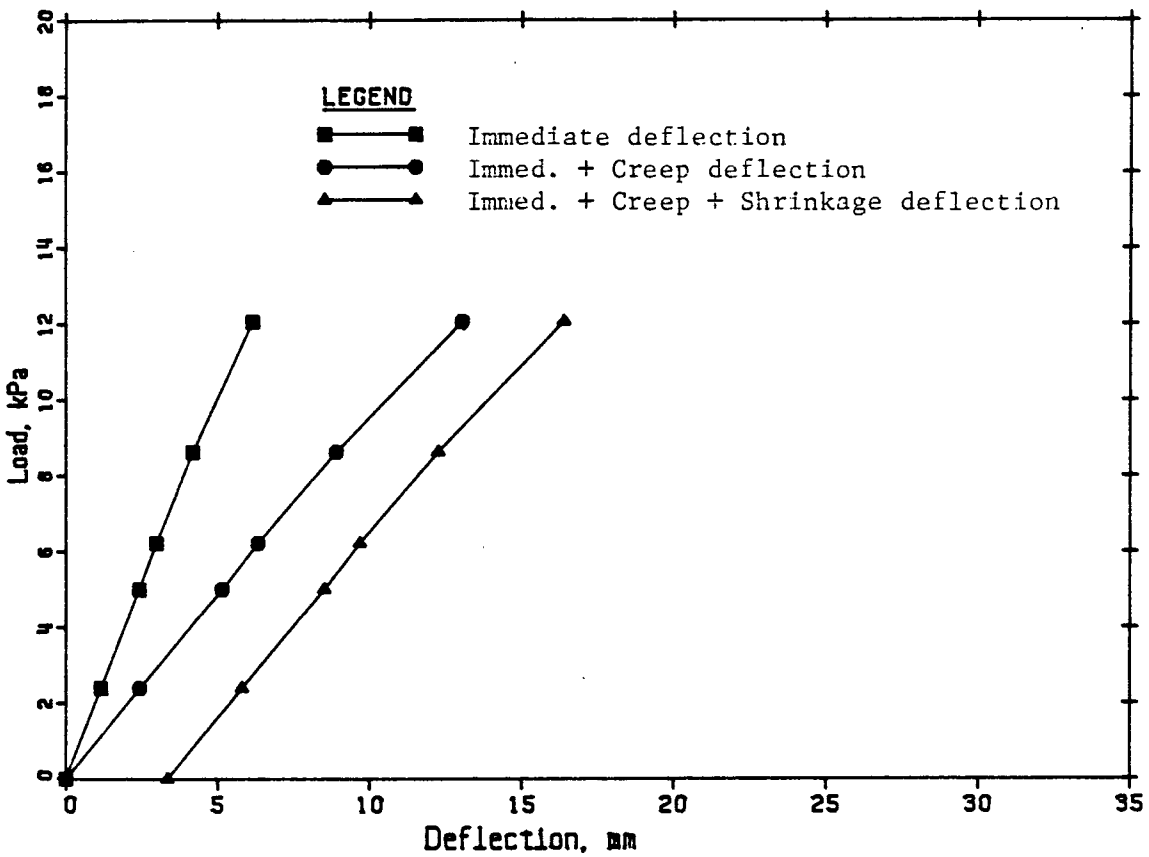

Figure 3.7 Long-term deflection curves at center of exterior panel of Slab S1

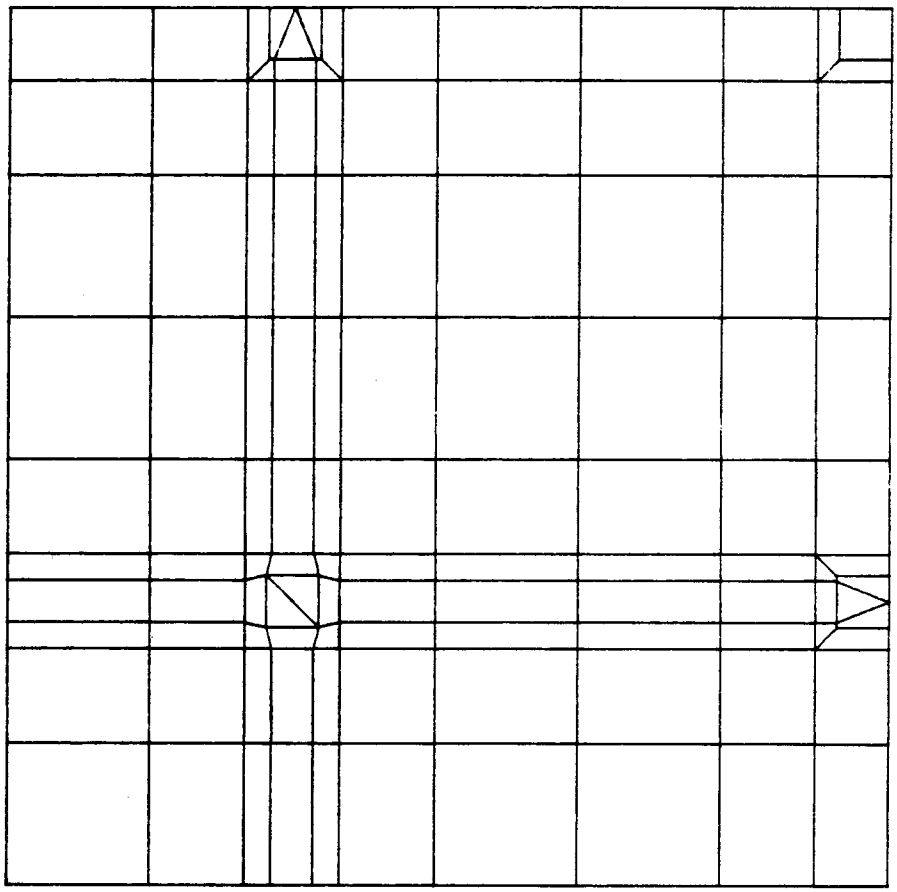

Figure 3.8 Mesh layout for Slab S2

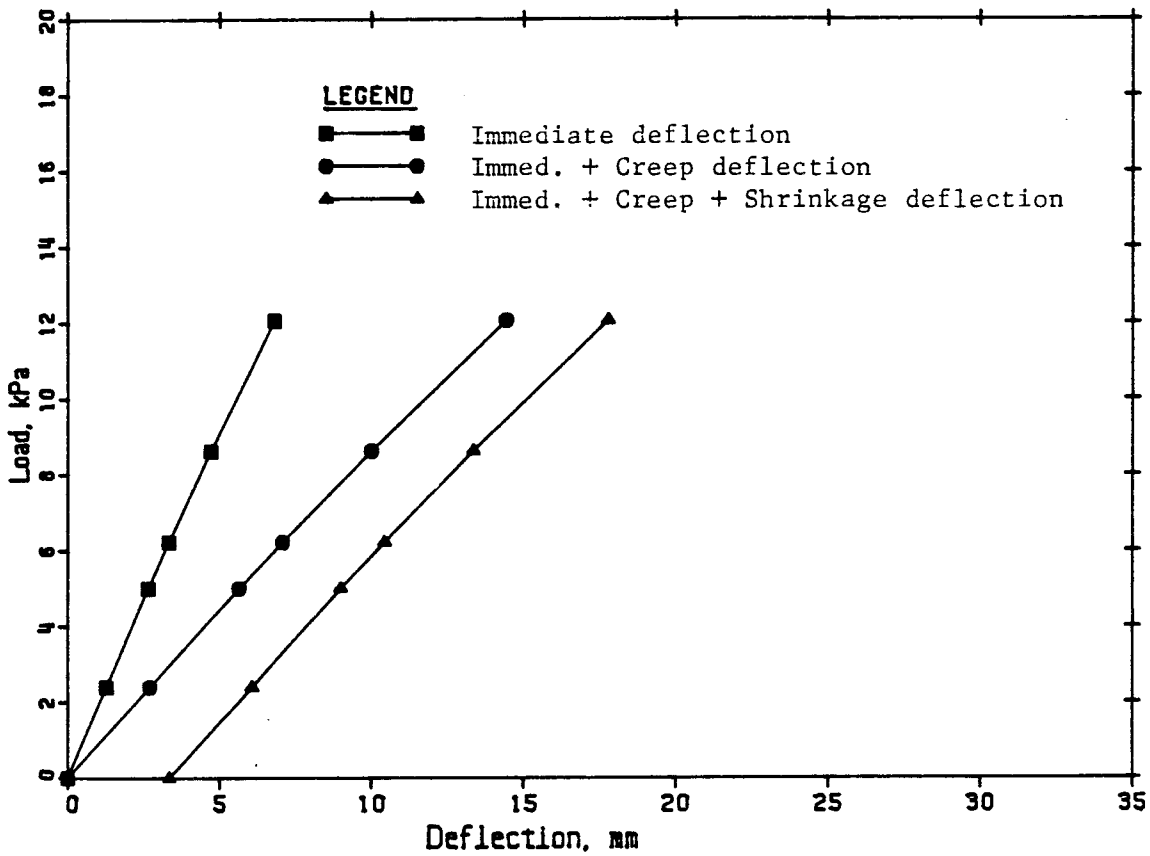

Figure 3.9 Long-term deflection curves at center of exterior panel of Slab S2

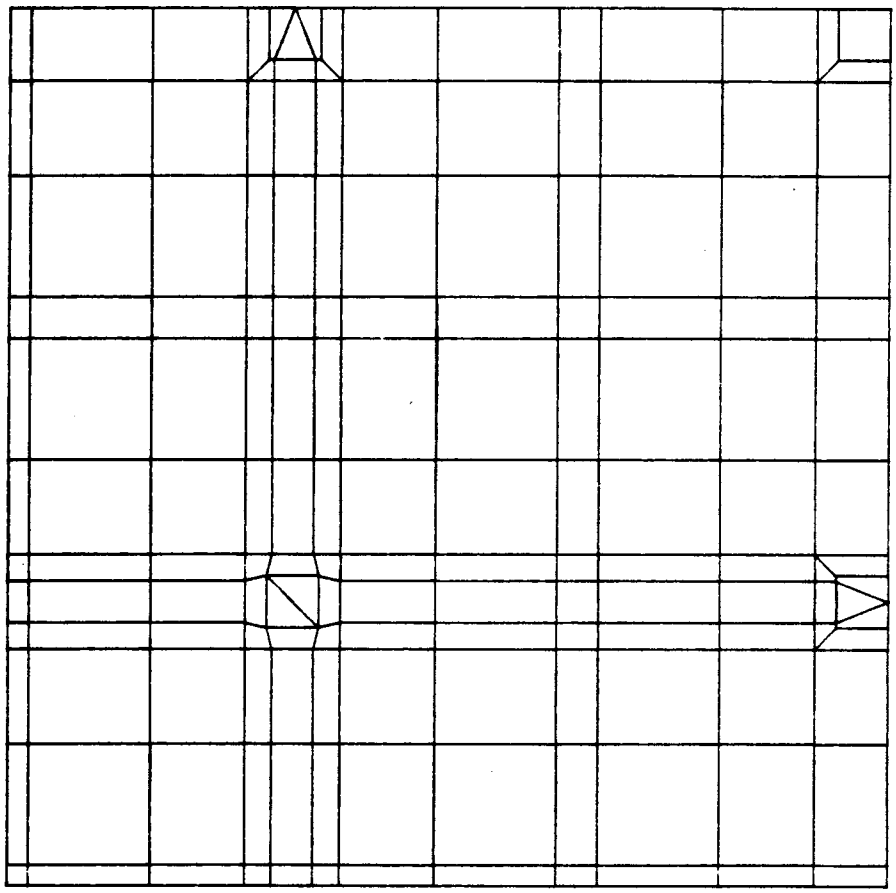

Figure 3.10 Mesh layout for Slab S3

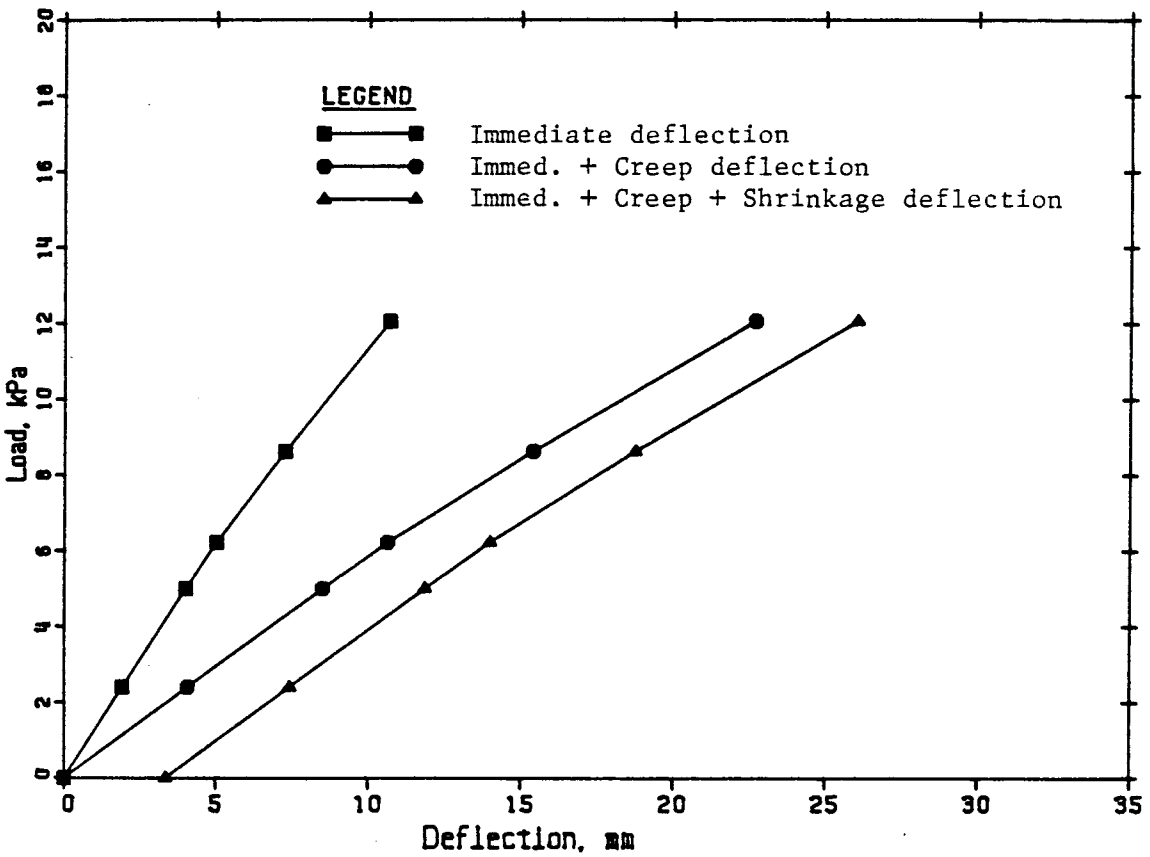

Figure 3.11 Long-term deflection curves at center of exterior panel of Slab S3

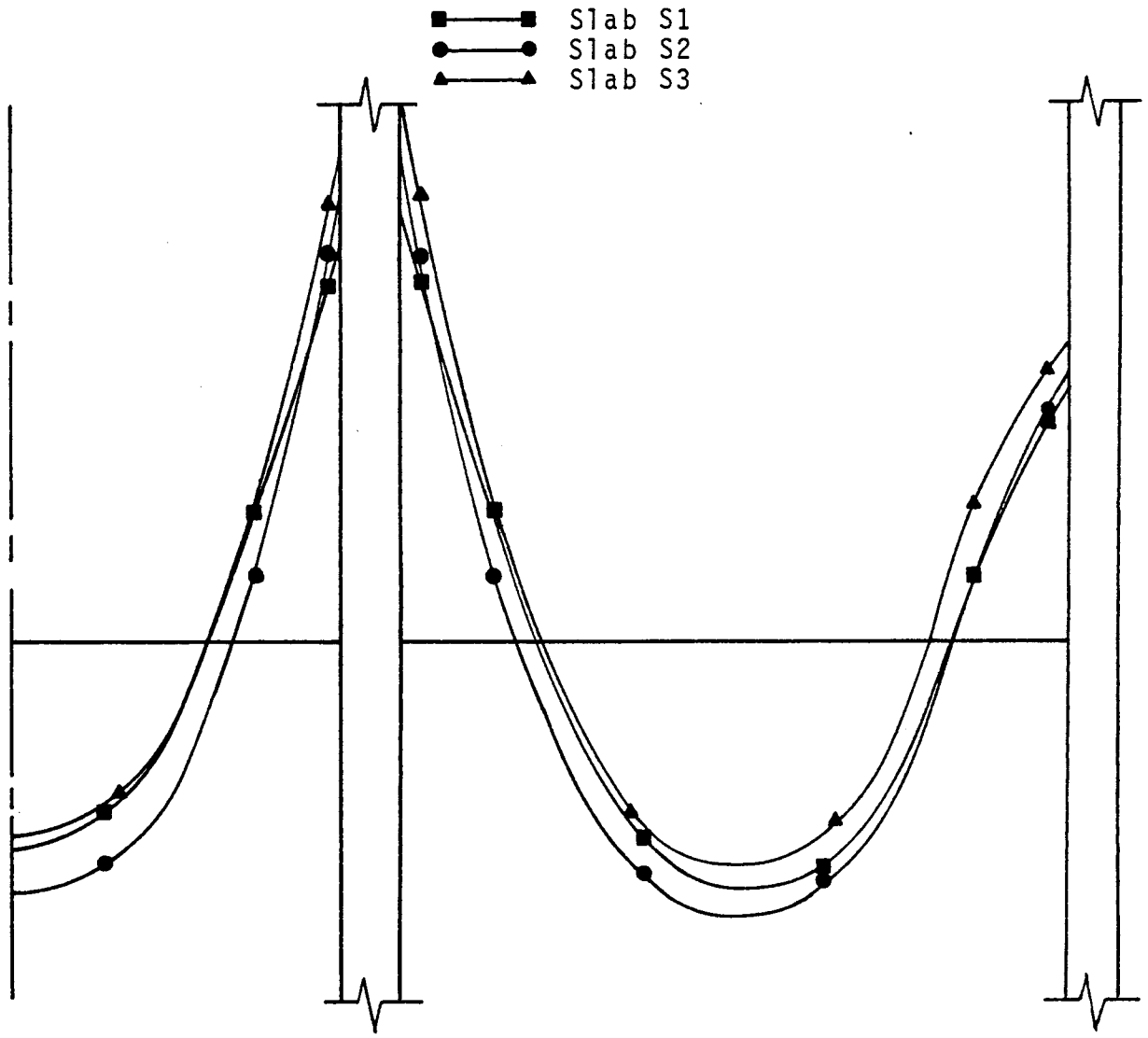

Figure 3.12 Moment distribution along interior column strip

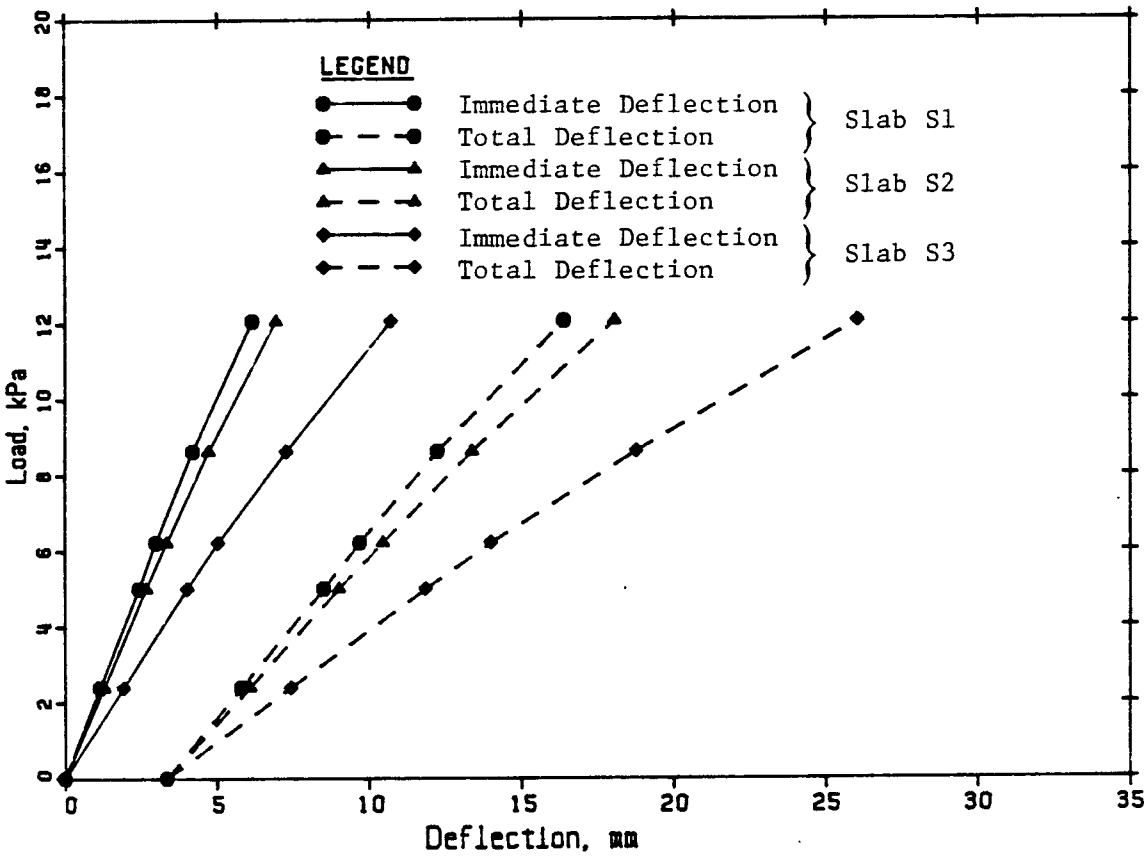

Figure 3.13 Effect of precracking on deflection at centre of exterior panel

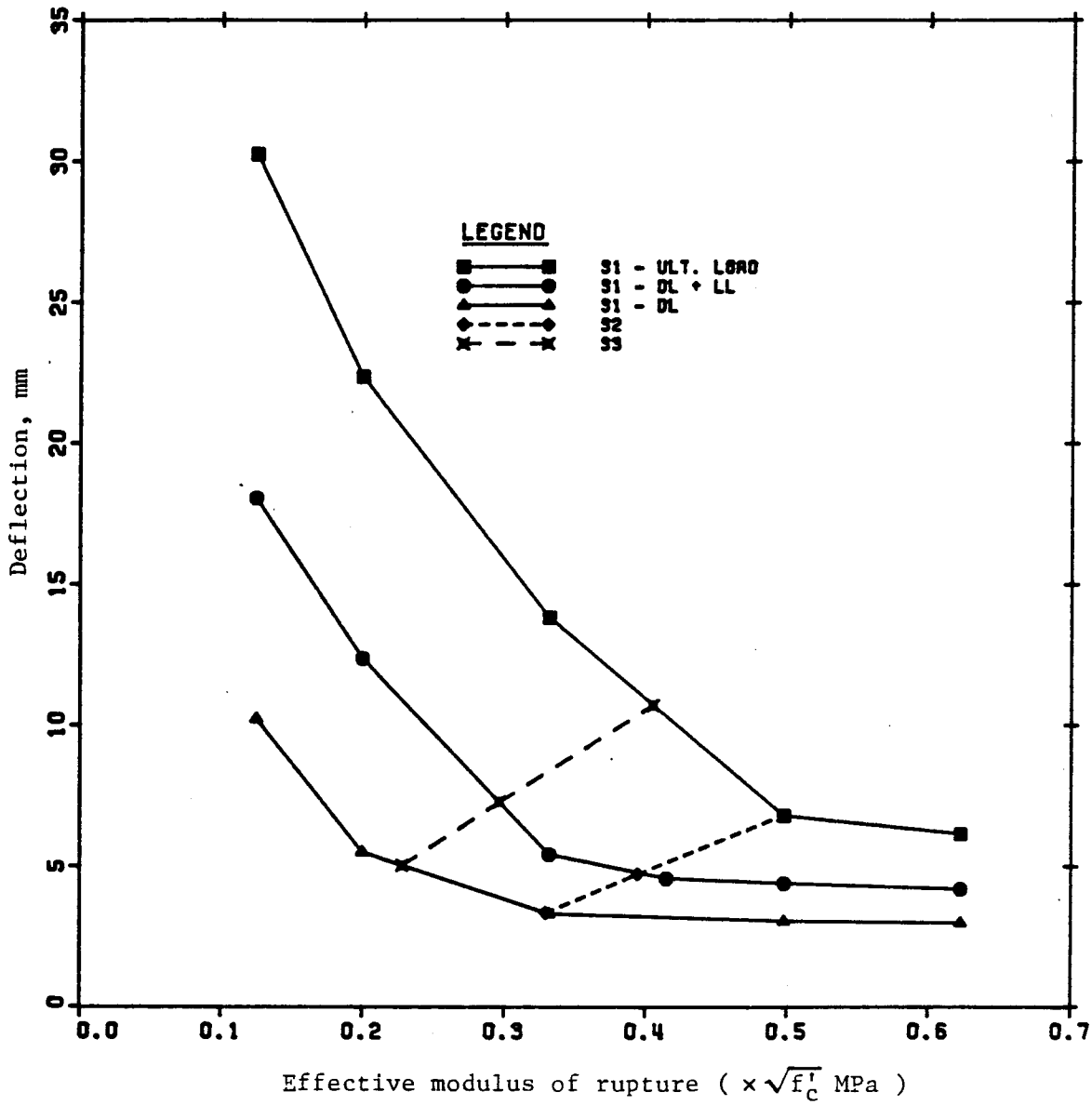

Figure 3.14 Effect of variation in modulus of rupture

4. SUMMARY, CONCLUSIONS AND RECOMMENDATIONS

4.1 Summary

In continuous reinforced concrete slab systems, the effects of shrinkage on slab deflections are often underestimated. The current ACI Building Code considers the additional deflections due to shrinkage as a result of shrinkage warping which arises from nonuniform shrinkage through the section. Reinforcement of different amounts in the two faces of a member, which is usually the case for reinforced concrete slabs, is the main cause of nonuniform shrinkage. The Code however does not explicitely recognize the induced tensile stresses in concrete due to restraint of shrinkage in continuous slab systems. These induced tensile stresses may contribute to cracking of concrete resulting in an increase in deflections. This study presents a procedure using the finite element method to estimate the effects of restrained shrinkage on two-way slab systems.

A new mathematical model is developed in Chapter 2 to analyze the uniaxial shrinkage behaviour of a completely restrained reinforced concrete member. Cracking occurs when the induced tensile stresses in concrete exceed the concrete tensile strength. Reduction in member axial stiffness is made by assuming a linear steel stress distribution within the zone of influence of cracking, or cracked region. The length of the cracked region is based on a crack spacing

formula. The analysis determines the number of cracks for a given length of member and the shrinkage strain at which each crack forms. A parameter study was carried out to study the effects of variations in span length, steel area, reinforcing bar size and tensile strength on the total number of shrinkage cracks forming. Results obtained are used to select the locations of precracked regions in the analysis of a slab system subjected to restrained shrinkage and transverse loads.

Chapter 3 describes the finite element analysis of a two-way reinforced concrete slab system subjected to restrained shrinkage and transverse loads. The effects of restrained shrinkage are modelled by forming shrinkage cracks prior to analyzing the slab for applied loading. Precracking is accomplished by reducing the flexural stiffness of elements at the locations of shrinkage cracks based on a linear curvature variation across the width of the precracked elements. The effects of the number of shrinkage cracks and variations in the modulus of rupture are studied. Results of the study are used to assess a simplified deflection calculation procedure proposed by Scanlon and Murray (1982) for slabs with restrained shrinkage. Scanlon and Murray proposed values for reduced effective modulus of rupture based largely on intuitive grounds. The present study has provided a basis for specifying values for effective modulus of rupture based on numerical studies including explicit consideration of the

presence of shrinkage restraint cracks.

4.2 Conclusions

The following conclusions are drawn from this investigation:

1. Uniaxial shrinkage analysis
   a. Reduced axial stiffness in cracked region is expressed as

$$K_{cr} = \alpha A_e E_c$$

where $$\alpha = \frac{1}{1 + \frac{1}{2n\rho}}$$

   b. The 'no-slip' approach can be used to approximate the length of the cracked region:

$$L_{cr} = 2k_1 c$$

Using a value of $k_1 = 1.4$ in the above expression yields similar results as those using the more complicated 'slip' or general approaches. Having the advantage of simplicity, the stress diffusion expression with value of $k_1 = 1.4$ was also used in the two-way slab analysis.

2. Reinforced concrete two-way slab system
   a. Shrinkage cracks are modelled by precracking

elements at the locations of the cracks. The width of the precracked elements is

$$L_{cr} = 2(1.4)c$$

and the reduced flexural stiffness is

$$(EI)_{cr} = \alpha_p E_c I_g$$

where $$\alpha_p = \frac{2}{1 + I_g/I_{cr}}$$

b. Based on results of a brief parameter study, a reduced effective modulus of rupture in the range of 0.2 to $0.4\sqrt{f'_c}$ can be used to account for effects of restraint stresses on slab deflections.

4.3 Recommendations for Further Research

The uniaxial shrinkage analysis can be extended to include the following features:

1. effects of creep (see Appendix D),
2. unsymmetrical reinforcement placement,
3. varying amounts of steel area along the span,
4. presence of flexural stresses, and
5. supports with partial fixity (see Appendix C).

A complete parameter study for the extended analysis can then be carried out.

The finite element analysis of two-way slab systems may be extended to include the following capabilities:

1. Consideration of post-yield behaviour;
2. Modification of the cracking criterion to consider principal moments that may be at a different orientation than the element coordinate system.

Further research may be directed to a detailed parameter study of factors such as the effects of drop panels, edge beams and depth to span ratio.

REFERENCES

ACI Committee 209, Subcommittee 2, 1971. *Prediction of Creep, Shrinkage and Temperature Effects in Concrete Structures.* Designing for Effects of Creep, Shrinkage, Temperature in Concrete Structures, SP-27, American Concrete Institute, Detroit, pp.51-93.

ACI Committee 318, 1977. *Building Code Requirements for Reinforced Concrete (ACI 318-77).* American Concrete Institute, Detroit, 102pp.

ACI Committee 435, 1966. *Deflections of Reinforced Concrete Flexural Members.* ACI Journal, Proceedings Volumn 63, Number 6, pp.637-674.

Bathe, K.J., Wilson, E.L. and Peterson, F.E. 1974. *SAPIV - A Structural Analysis Program for Static and Dynamic Response of Linear Systems.* Department of Civil Engineering, University of California, Berkeley, 59pp.

Bazant, Z.P. and Oh, Byung H. 1983. *Deformation of Cracked Net-Reinforced Concrete Walls.* Journal of the Structural Division, ASCE Proceedings, Volumn 109, Number ST1, pp.93-108.

Beeby, A.W. 1979. *The Prediction of Crack Widths in Hardened Concrete.* The Structural Engineer, Volume 57A, Number 1, pp.9-17.

Branson, D.E. 1963. *Instantaneous and Time-Dependent Deflections of Simple and Continuous Reinforced Concrete Beams.* Alabama Highway Research Report Number 7, Bureau of Public Roads.

Comite Euro-International du Beton, 1982. *Bond Action and Bond Behaviour of Reinforcement (State-of-the-Art Report).* Bulletin d'information, Number 151, 153pp.

Clark, L.A. and Speirs, D.M. 1978. *Tension Stiffening in Reinforced Concrete Beams and Slabs under Short-Term Load.* Technical Report 42.521, Cement and Concrete Association, London, 19pp.

Ferry-Borges, J. 1966. *Cracking and Deformability of Reinforced Concrete Beams.* Publications, Association Internatinal des Ponts et Charpentes, 26.

Hand, F.R., Pecknold, D.A. and Schnobrich, W.C. 1973. *Nonlinear Layered Analysis of Reinforced Concrete Plates and Shells.* Journal of the Structural Division, ASCE Proceedings, Volumn 99, Number ST7, pp.1491-1505.

Heiman, J.L. 1974. *A Comparison of Measured and Calculated Deflections of Flexural Members in Four Reinforced Concrete Buildings.* Deflections of Concrete Structures, SP-43, American Concrete Institute, Detroit, pp.515-545.

Jofriet, J.C. and McNeice, M. 1971. *Finite Element Analysis of Reinforced Concrete Slab.* Journal of the Structural Division, ASCE Porceedings, Volumn 97, Number ST3, pp.785-806.

Kupfer, Helmut; Hilsdorf, Huber K. and Rusch, Hubert. 1969. *Behavior of Concrete Under Biaxial Stresses.* ACI Journal, Proceedings Volumn 66, Number 8, pp.656-666.

Lenschow R. and Sozen, M.A. 1966. *A Yield Criterion for Reinforced Concrete under Biaxial Moments and Forces.* Civil Engineering Studies, Structural Research Series, Number 311, University of Illinois, Urbana.

Leonhardt, Fritz. 1977. *Crack Control in Concrete Structures.* IABSE Periodica, Number S-4/77, International Association for Bridge and Structural Engineering, 24pp.

Mayer, H. and Rusch, H. 1967. *Building Damage Caused by Deflection of Reinforced Concrete Building Components.* Technical Translation 1412,

National Research Council, Ottawa, from Deutscher Auschuss fur Stahlbeton Heft 193, Berlin.

Rangan, B.V. 1976. *Prediction of Long-Term Deflections of Flat Plates and Slabs.* ACI Journal, Proceedings V.73, Number 4, pp.223-226.

RILEM Committee 42-CEA. 1981. *Properties of Set Concrete at Early Ages – State-of-the-Art report.* Materiaux et Constructions, Volumn 14, Number 84, pp.399-450.

Saliger, R. 1936. *High-grade Steel in Reinforced Concrete.* Proceedings Second Congress of the International Association for Bridge and Structural Engineering. Berlin-Munich.

Scanlon, A. and Murray, D.W. 1982. *Practical Calculation of Two-way Slab Deflections.* Concrete International, Volumn 4, Number 11, pp.43-50.

APPENDIX A

Coefficient k_2 for Development Length

From Equations 2.21 and 2.22, the coefficient k_2 for the development length L_d is given by:

$$k_2 = \frac{1}{4}\frac{f_r}{\tau_{ult}}$$

for pure tension.

The average ultimate unit bond stress capacity τ_{ult} is given in the 1963 ACI Code as:

$$\tau_{ult} = \frac{9.5\sqrt{f'_c}}{\phi} \leq 800 \text{ psi}$$

$$\text{or} \quad \frac{20\sqrt{f'_c}}{\phi} \leq 5.53 \text{ MPa}$$

for #11 and smaller bars, which are usually used in concrete slab design. Using this value of τ_{ult}, k_2 can be computed for different values of modulus of rupture f_r as summarized in Table A.1.

Bar size	f_r (MPa)			
	3.415	2.732	1.821	0.911
10M	0.16	0.12	0.082	0.041
15M	0.16	0.12	0.082	0.041
20M	0.16	0.12	0.082	0.041
25M	0.16	0.12	0.082	0.041

f'_c = 30MPa

Table A.1 Summary of values of k_2 for development length

APPENDIX B

Computer Program for Uniaxial Shrinkage Analysis

```
C
C   This program analyzes the shrinkage response of a symmetrically
C   reinforced member.
C
C
      REAL L,K1,K2,LCR,LSLIP,N,KG,KCR,KNEW,KOLD
      INTEGER*4 TITLE(20)
      COMMON/PROP/ L,LCR,KG,KCR
      EXTERNAL STIFF
C
C***  Input Data
C
C
    5 READ(5,1000,END=997)TITLE,
     *                    AG,AS,EC,ES,FR,
     *                    C,L,K1,K2,DIA,ESHU
C
C*********                  Analysis                        **********
C
C    ********
C    *
C    *  STEP 1 - Calculate the constants for the member.
C    *
C    ********
C
        AC    = AG-AS
        RHO   = AS/AC
        N     = ES/EC
        AE    = (1.0E0 + N*RHO) *AC
        KG    = AE*EC
        KCR   = 1.0E0/(1.0E0+1.0E0/(2*N*RHO)) * KG
        LSLIP = K2*DIA/RHO *2.E0
        LCR   = K1*C *2.E0 + LSLIP
C
        WRITE(6,2000)TITLE,AG,C,L,AC,EC,FR,AS,RHO,ES,DIA,K1,K2,ESHU
        WRITE(6,2001)
C
C    ********
C    *
C    *  STEP 2 - Calculate the shrinkage strain
C    *
C    ********
C
        M     = 1
        RATIO = 1.0
        KOLD  = KG
   10   ESH   = AE*FR/ (KOLD * RATIO)
C
C    ********
C    *
C    *  STEP 3 - Check the shrinkage strain
C    *
C    ********
C
        IF(ESH.GT.ESHU) GOTO 999
C
C    ********
C    *
C    *  STEP 4 - Check the total cracked length
C    *
```

```
C    ********
C
        TLCR = M*LCR
        IF (TLCR.GT.L) GOTO 995
C
C    ********
C    *
C    *  STEP 5 - Calculate the stresses
C    *
C    ********
C
         KNEW  = STIFF(M)
         RATIO = (L-M*LSLIP)/L
         P     = KNEW * ESH * RATIO
         FC    = P/AE
C
C        Calculate the steel stresses
C
         PNET  = P - AS*ES*ESH*RATIO
         FSCR  = PNET/AS
         FSG   = FSCR - FC/RHO
C
C        Output
C
         WRITE(6,2020)M,ESH,FC,FSG,FSCR,TLCR
C
C     ********
C     *
C     *  STEP 6 - Repeat the procedure for subsequent cracks
C     *
C     ********
C
        M=M+1
        KOLD = KNEW

        GOTO 10
C
C*********                TERMINATION                    **********
C
  999 WRITE(6,3000)
      WRITE(6,3010)
      GOTO 5
  995 WRITE(6,3020)
      WRITE(6,3010)
      GOTO 5
  997 STOP
C
C*********                  FORMAT BLOCK                 **********
C
 1000 FORMAT(20A4/5F10.0/6F10.0)
 2000 FORMAT('1',/' ',20A4///' MEMBER''S DETAIL'/
     *       ' ','     Gross Area      Max Cover    Span Length'/
     *       ' ',3F15.4///
     *       ' ','CONCRETE DETAIL'/
     *       ' ','  Concrete Area     Elasticity    Tensile Str'/
     *       ' ',F15.4,2G15.4///
     *       ' ','REINFORCEMENT DETAIL'/
     *       ' ','     Steel Area    Steel ratio     Elasticity',
     *         '       Diameter'/
     *       ' ',F15.4,2G15.4,F15.4///
```

```
     121           *       ' ','CRACKED LENGTH COEF.'/
     122           *       ' ','   K1= ',F6.4,'   K2 = ',F6.4///
     123           *       ' ','Ultimate shrinkage strain = ',E15.4///)
     124       2001 FORMAT(
     125           *' ','U N I A X I A L   S H R I N K A G E   A N A L Y S I S'//
     126           *           ' ',' Crack      Shrinkage     ',
     127           *           '    Conc Stress    Steel(gross)   Steel(crack)',
     128           *           '     Cr. Length'/)
     129       2020 FORMAT(I7,E15.4,5X,3G15.4,F15.2)
     130       3000 FORMAT(/' *** Shrinkage strain exceeds ultimate value ***')
     131       3010 FORMAT(/' *** No further cracks will form ***')
     132       3020 FORMAT(/' *** Total cracked length exceeds member length ***')
     133      C
     134            END
     135      C*****************************************************************
     136      C
     137            REAL FUNCTION STIFF(M)
     138      C
     139      C     ***************
     140      C     *
     141      C     *    This function evaluates the member's average
     142      C     *    stiffness with mth cracks.
     143      C     *
     144      C     ***************
     145      C
     146            REAL L,LCR,KG,KCR
     147            COMMON/PROP/ L,LCR,KG,KCR
     148      C
     149            STIFF = L/((L-M*LCR)/KG + M*LCR/KCR)
     150            RETURN
     151            END
End of file
```

APPENDIX C

Partial Fixity

A simple case of partial fixity may be included in the uniaxial shrinkage analysis as follows.

Consider the simplified slab system with partial fixity in Figure C.1a. The slab is fully fixed at one end and attached to a column at the other end. The slab and the column have stiffnesses K_m and K_c respectively.

If the restraint at B is released as shown in Figure C.1b, then the slab shrinks freely by an amount

$$\Delta = \epsilon_m L \tag{C.1}$$

where ϵ_m is given by Equation 2.16.

When the restraint is reapplied, a tensile force P is induced in the slab and the slab elongates by an amount

$$\Delta_{slab} = PL/K_m \tag{C.2}$$

as shown in Figure C.1c.

The slab thus actually shortens by $(\Delta - \Delta_{slab})$. The column also deflects by the same amount as shown in Figure C.2.

Therefore,

$$P = K_c(\Delta - \Delta_{slab})/L_c \tag{C.3}$$

Substitute Equations C.1 and C.2 into C.3,

$$P = K_c(\epsilon_m L - PL/K_m)/L_c$$

Rearranging,

$$P = \left[\frac{L}{L_c/K_c + L/K_m}\right] \epsilon_m$$

$$P = K_{sys}\epsilon_m$$

where K_{sys} = Stiffness of the system

$$= \frac{L}{L_c/K_c + L/K_m} \qquad (C.4)$$

K_m is given by Equation 2.4 and K_c is given in Figure C.3 for several cases of support conditions. Substituting K_{sys} for all occurrences of K_m in the previous equations in Chapter 2 will include the effects of partial fixity in the uniaxial shrinkage analysis.

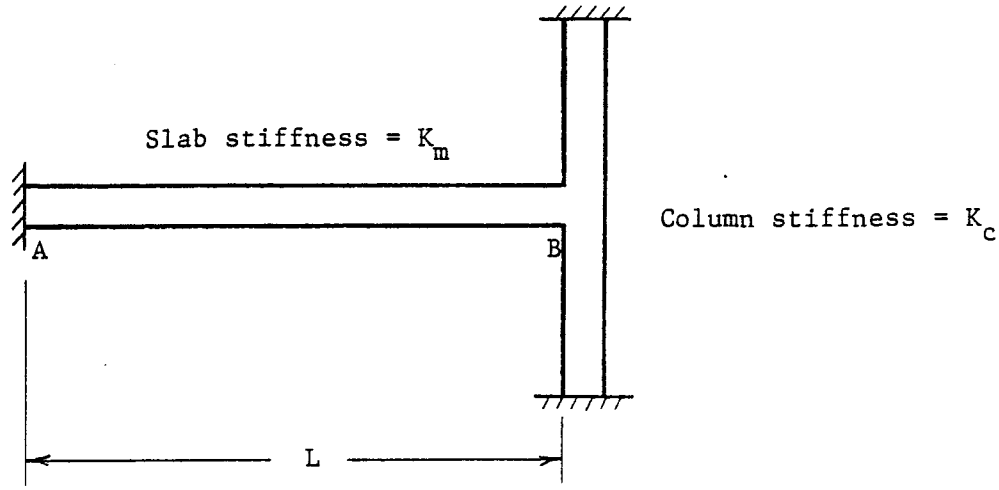

(a) Slab system

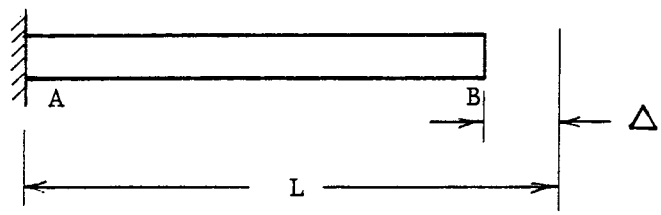

(b) Restraint at B released

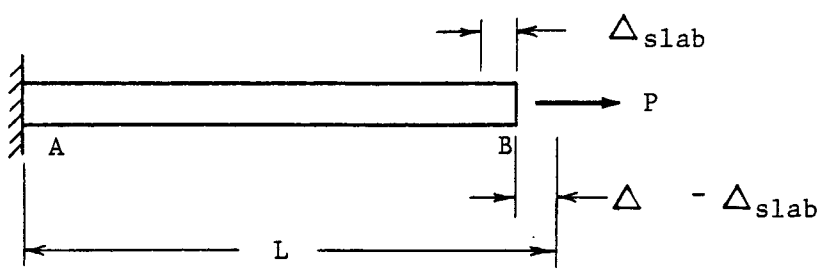

(c) Restraint reapplied

Figure C.1 Slab system with partial fixity

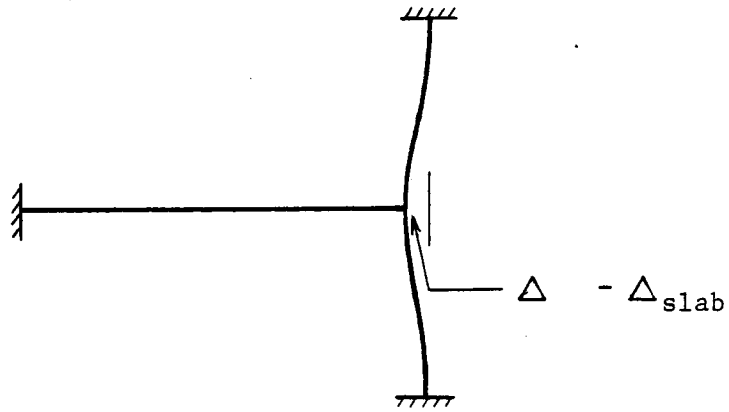

(a) Slab system

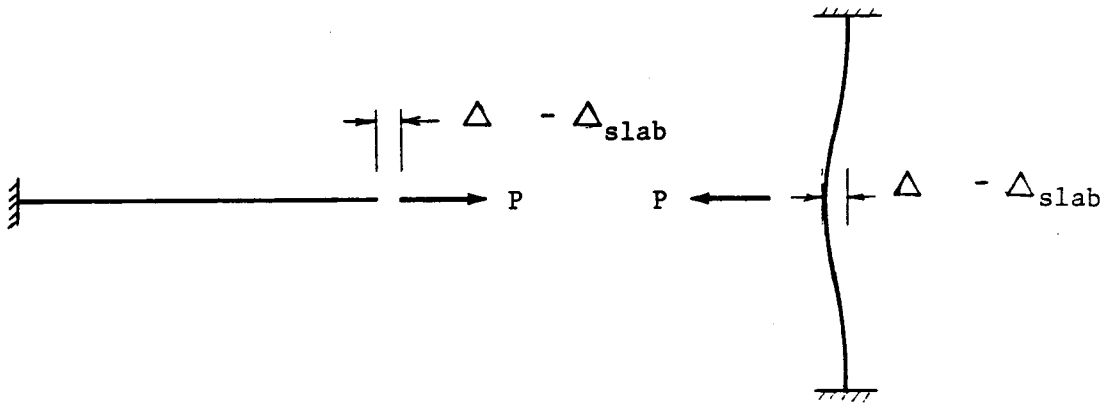

(b) Slab (c) Column

Figure C.2 Free body diagram of the slab and the column

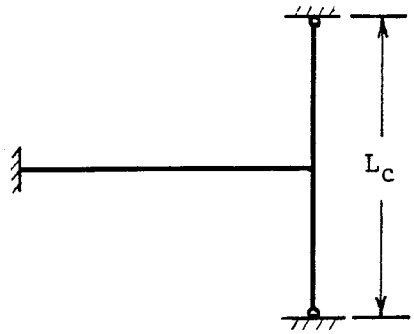

$$K_c = \frac{48\ EI}{L_c^2}$$

(a) Both ends hinged

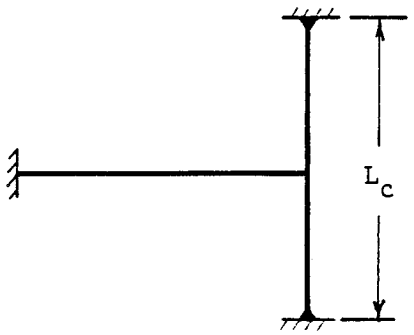

$$K_c = \frac{192\ EI}{L_c^2}$$

(b) Both ends fixed

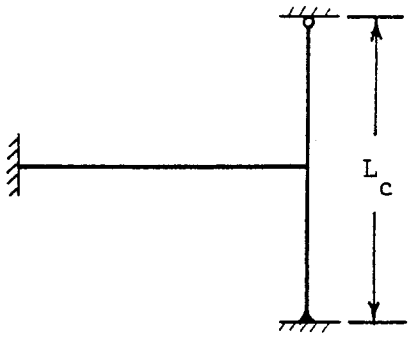

$$K_c = \frac{768\ EI}{7\ L_c^2}$$

(c) One end fixed, one end hinged

Figure C.3 Column stiffness

APPENDIX D

Alternate Solution Algorithm including Creep

A time-incremental analytical procedure may be used to approximate the effects of creep in the uniaxial shrinkage analysis as follows.

The quantities which must be known for the analysis include: A_g, A_s, c, L, f_r, E_s, k_1, k_2 and ϕ. It is assumed that

1. shrinkage and creep start at time t=0,
2. the concrete has attained its design strength before creeping occurs,
3. the slab element is initially uncracked, i.e. m=0, and
4. the concrete is unstressed before shrinkage begins.

The following constants for the member shown in Figure 2.2a are evaluated initially:

Net concrete area, $A_c = A_g - A_s$

Steel ratio, $\rho = A_s/A_c$

Cracked length, $L_{cr} = 2(k_1 c + k_2 \phi/\rho)$

Slipping length, $L_{slip} = 2k_2 \phi/\rho$

During any time step t, the following procedure is used:

Step 1. Compute the modified modulus of elasticity due to creep, E_{ct}, and the unrestrained shrinkage strain, ϵ_{sh}, at time t using the formulae suggested by ACI Committee 209.

Step 2. Compute the following time-dependent quantities:

$$\text{Modular ratio, } n = E_s/E_{ct}$$

Equivalent transformed area,

$$A_e = (1+n\rho)A_c$$

Stiffness at uncracked section,

$$K_g = A_e E_{ct}$$

Stiffness reduction coefficient,

$$\alpha = \frac{1}{1 + \frac{1}{2n\rho}}$$

Stiffness at cracked section,

$$K_{cr} = \alpha K_g$$

Member's average stiffness,

$$K_m = \frac{L}{(L-mL_{cr})/K_g + mL_{cr}/K_{cr}}$$

Member's average shrinkage strain,

$$\epsilon_m = \epsilon_{sh}(L-mL_{slip})/L$$

Step 3. Compute the concrete stress,

$$f_{cm} = K_m \epsilon_m / A_e$$

Step 4. (a) If $f_{cm} < f_r$, the member does not form a new crack. Repeat Steps 1 to 3 using the same m value but a new time-step, $t+\Delta t$.

(b) If $f_{cm} \geq f_r$, then the member cracks. The time at which the member cracks may be obtained by using the bisection method.

The required initial bracket is $[t'_o, t''_o]$ where t'_o is the previous time-step and t''_o is the current time-step

as shown in Figure D.1. An iteration of the bisection method consists of three steps:

1) compute the mid-point

$$t_k = \frac{t'_k + t''_k}{2}$$

2) evaluate the concrete stress $f_c(t_k)$ at time t_k by repeating Steps 1 to 3.

3) determine a new interval $[t'_{k+1}, t''_{k+1}]$ according to the rule

$$[t'_{k+1}, t''_{k+1}] = \begin{cases} [t'_k, t_k] \text{ if } f_c(t_k) > f_r \\ [t_k, t''_k] \text{ otherwise} \end{cases}$$

The iteration continues until one of the stopping criteria is satisfied:

1) $| t''_k - t'_k | \leq TTOL$

2) $| f_r - f_c(t_k) | \leq FTOL$

where TTOL = The acceptable tolerance in time,

FTOL = The acceptable tolerance in concrete stress.

Step 5. After the time at cracking t_{cr} is determined in Step 4(b), increment the number of cracks, m, and repeat Steps 1 to 4 at time t_{cr} for the residual concrete stress after cracking (point B

in Figure D.1) and at subsequent time-steps.

Step 6. The analysis should be continued until the ultimate specified time limit is reached.

A computer program which includes the effects of creep and partial fixity is written in Appendix E.

The thirteen members in the parameter study is reanalyzed to examine the effects of creep. The modified modulus of elasticity and the unrestrained shrinkage strain in the study are determined as follows:

$$E_{ct} = \frac{E_c}{(1 + 0.8C_t)}$$

where

$$C_t = 2.35 \left[\frac{t^{0.6}}{10 + t^{0.6}}\right]$$

$$\epsilon_{sh} = \left[\frac{t}{35 + t}\right] 740 \times 10^{-6}$$

E_{ct} and ϵ_{sh} are plotted in Figures D.2 and D.3 as a function of time. Results are presented in Figures D.4 to D.7 for f_c versus log t, also in Figures D.8 to D.11 for f_c versus ϵ_{sh}. Table D.1 summarizes the total number of cracks formed in each member. The results show that shrinkage cracking occurs at an early age and the total number of cracks formed is close to that obtained from the previous analysis using an ultimate shrinkage strain of 400 millionths.

L_{cr}	M1	M2	M3	M4	M5	M6	M7	M8	M9	M10	M11	M12	M13
2(1.0)c	1	2	3	4	2	4	5	5	5	5	4	8	17
2(1.4)c	1	2	2	3	2	3	4	4	4	4	3	6	12
$2(L_d)$	1	1	1	1	1	1	2	1	1	1	2	3	9

Table D.1 Summary of total number of cracks formed in members (including creep)

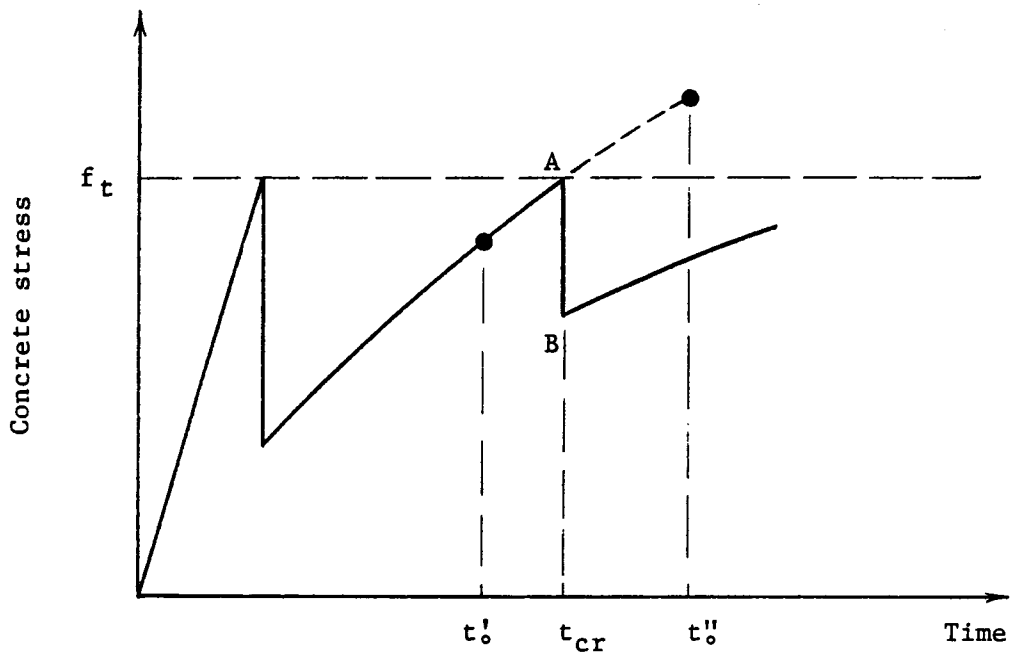

Figure D.1 Concrete stress versus time curve

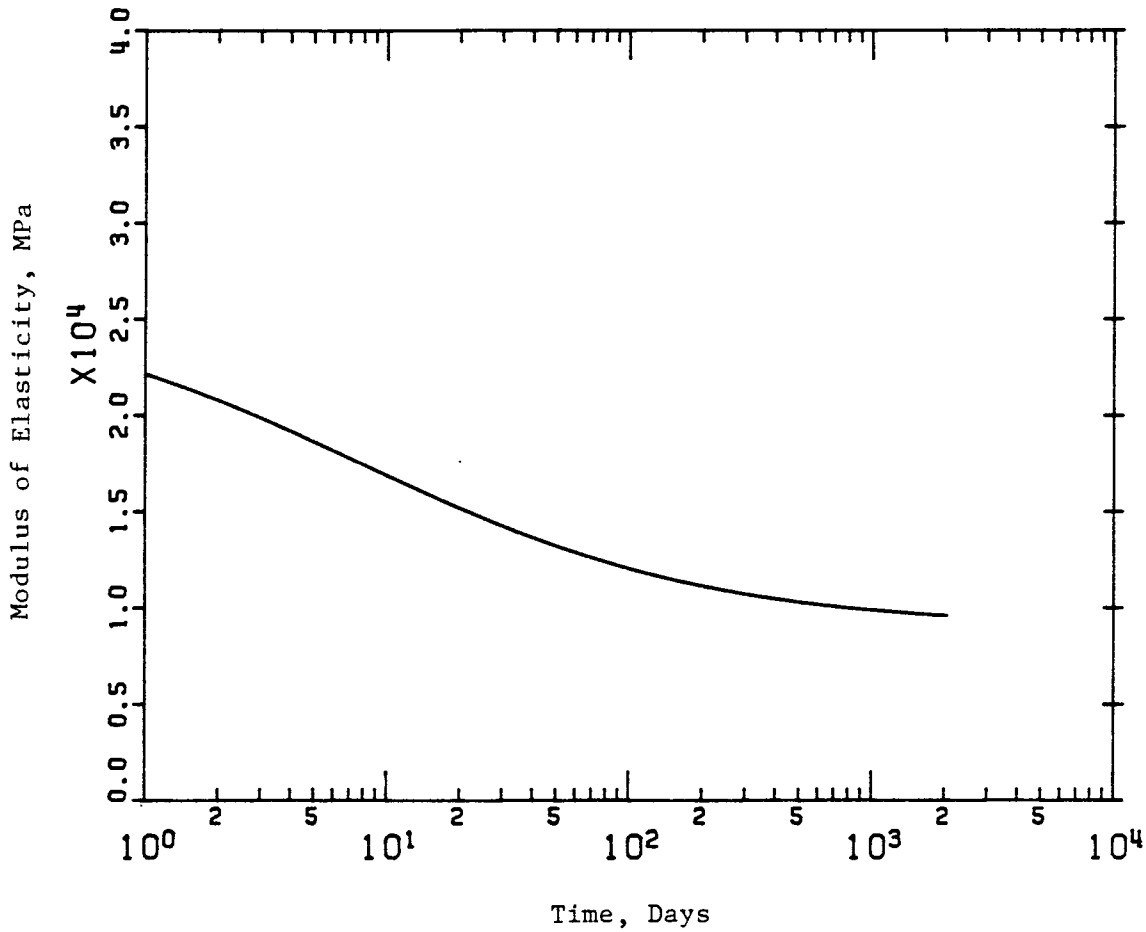

Figure D.2 Modulus of Elasticity versus log time curve

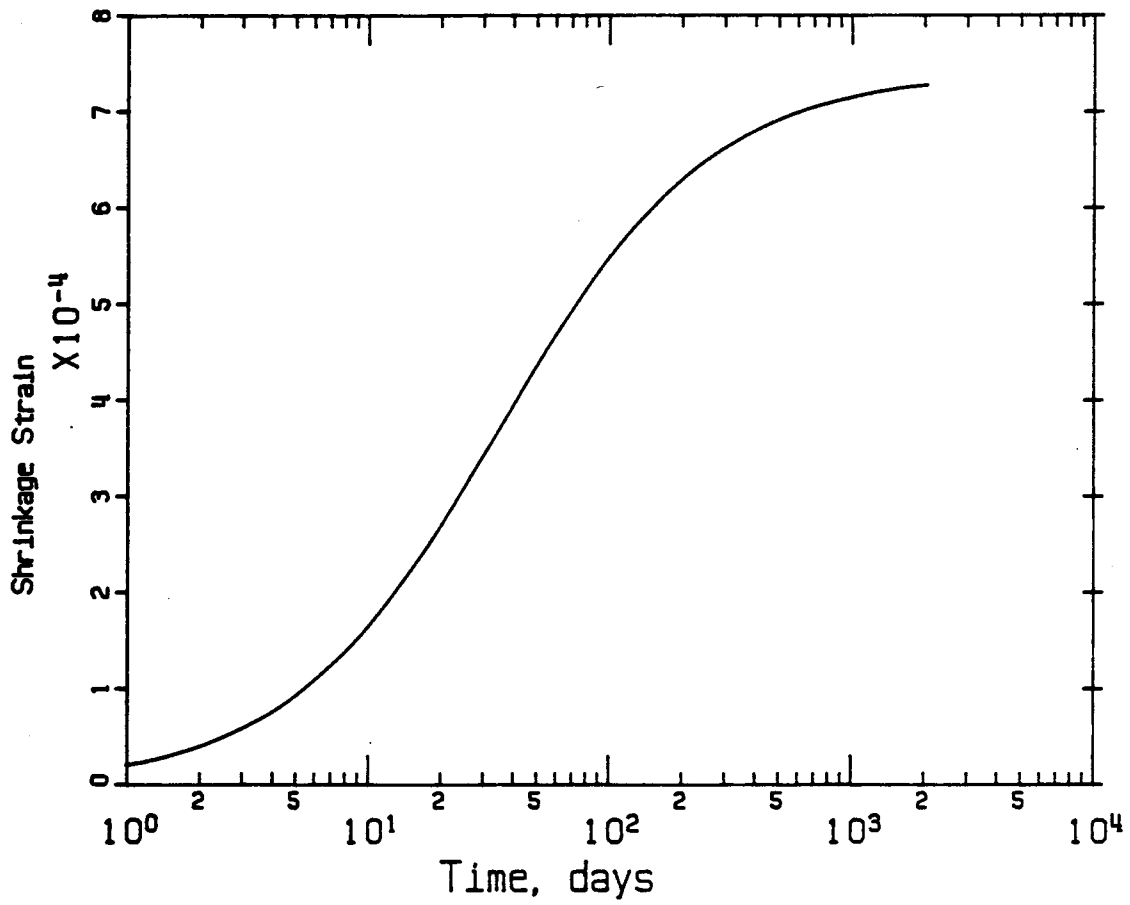

Figure D.3 Shrinkage strain versus log time curve

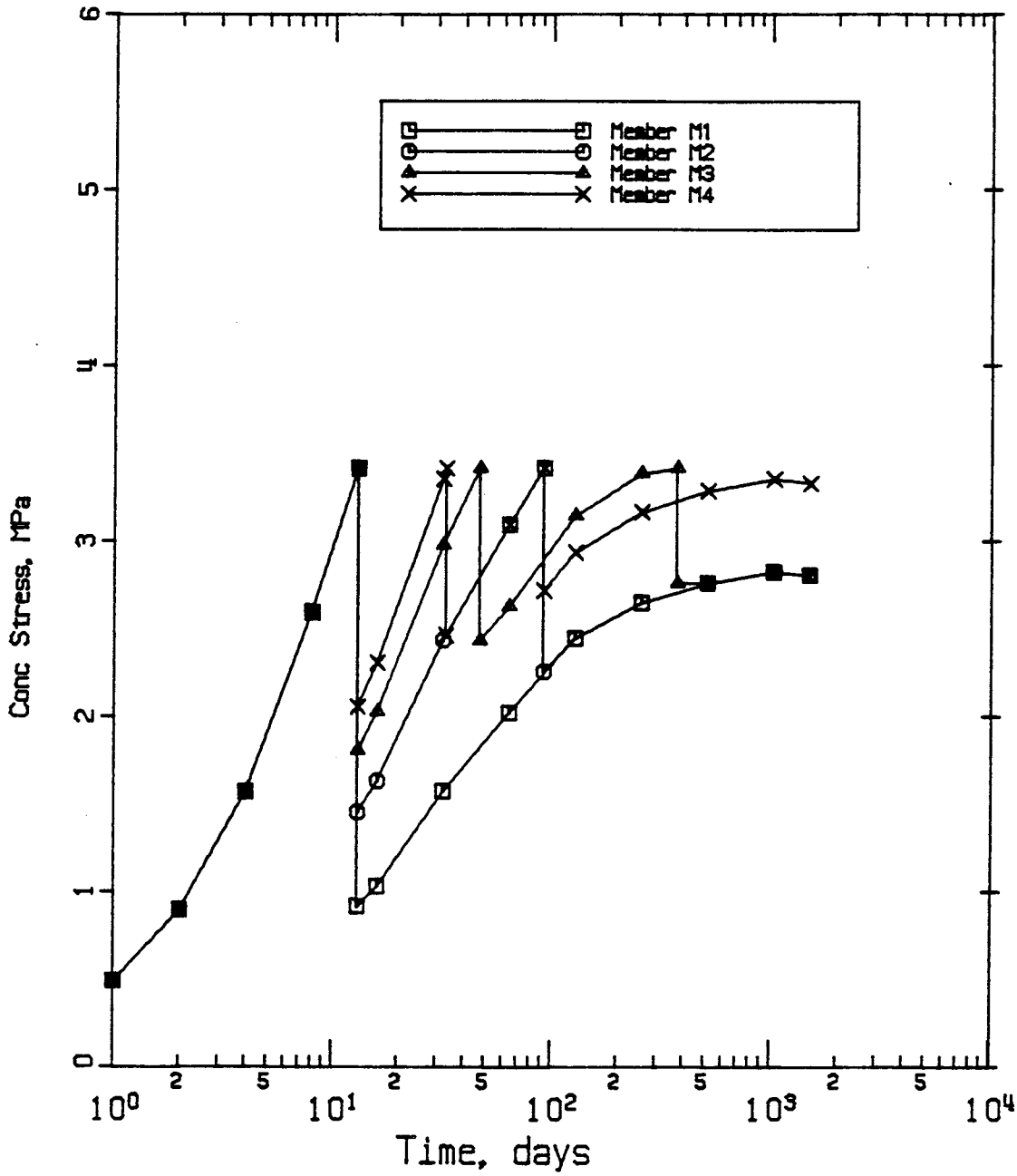

Figure D.4 Concrete stress versus log time curve for effects of variations in span length

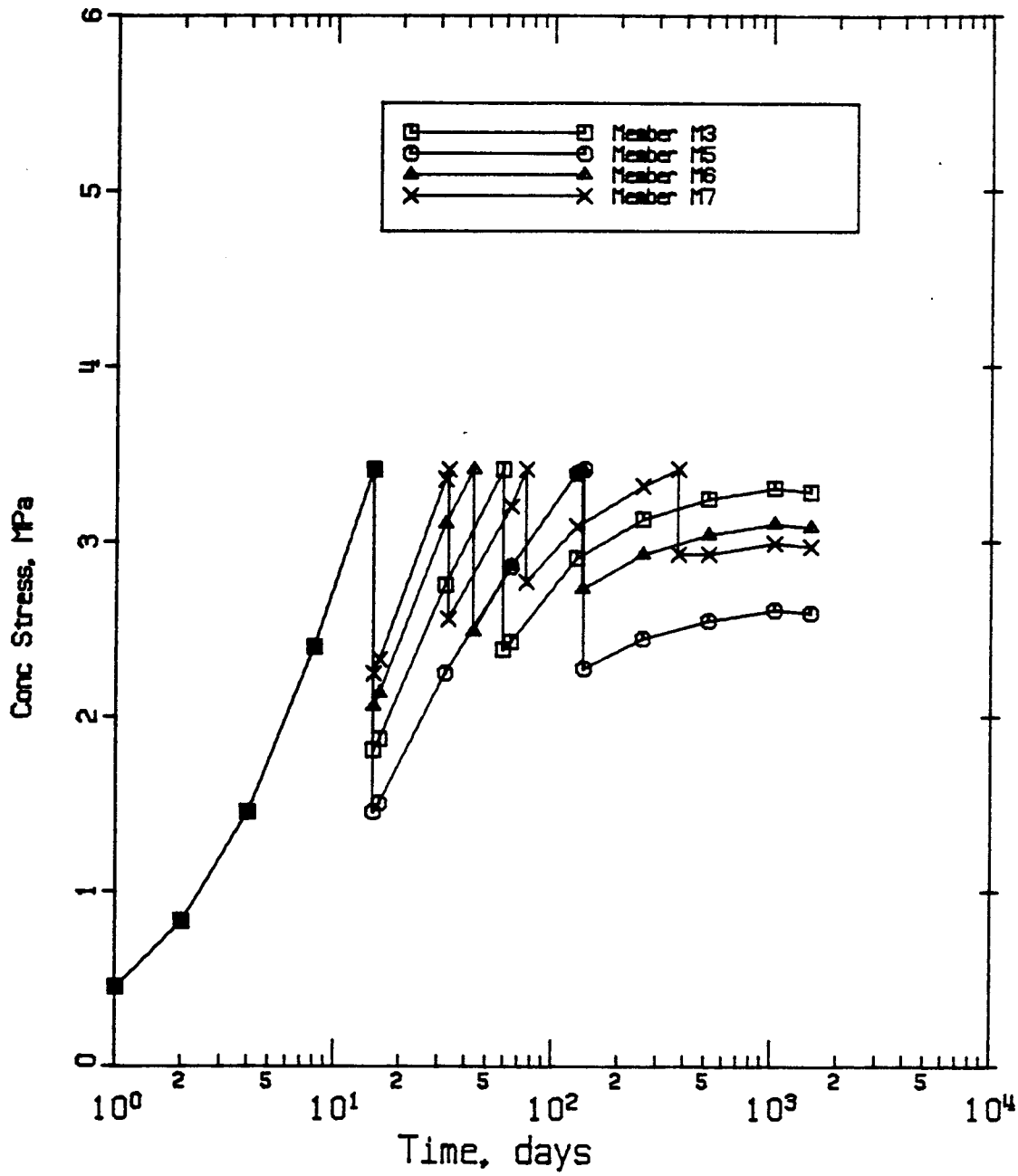

Figure D.5 Concrete stress versus log time curve for effects of variations in steel area

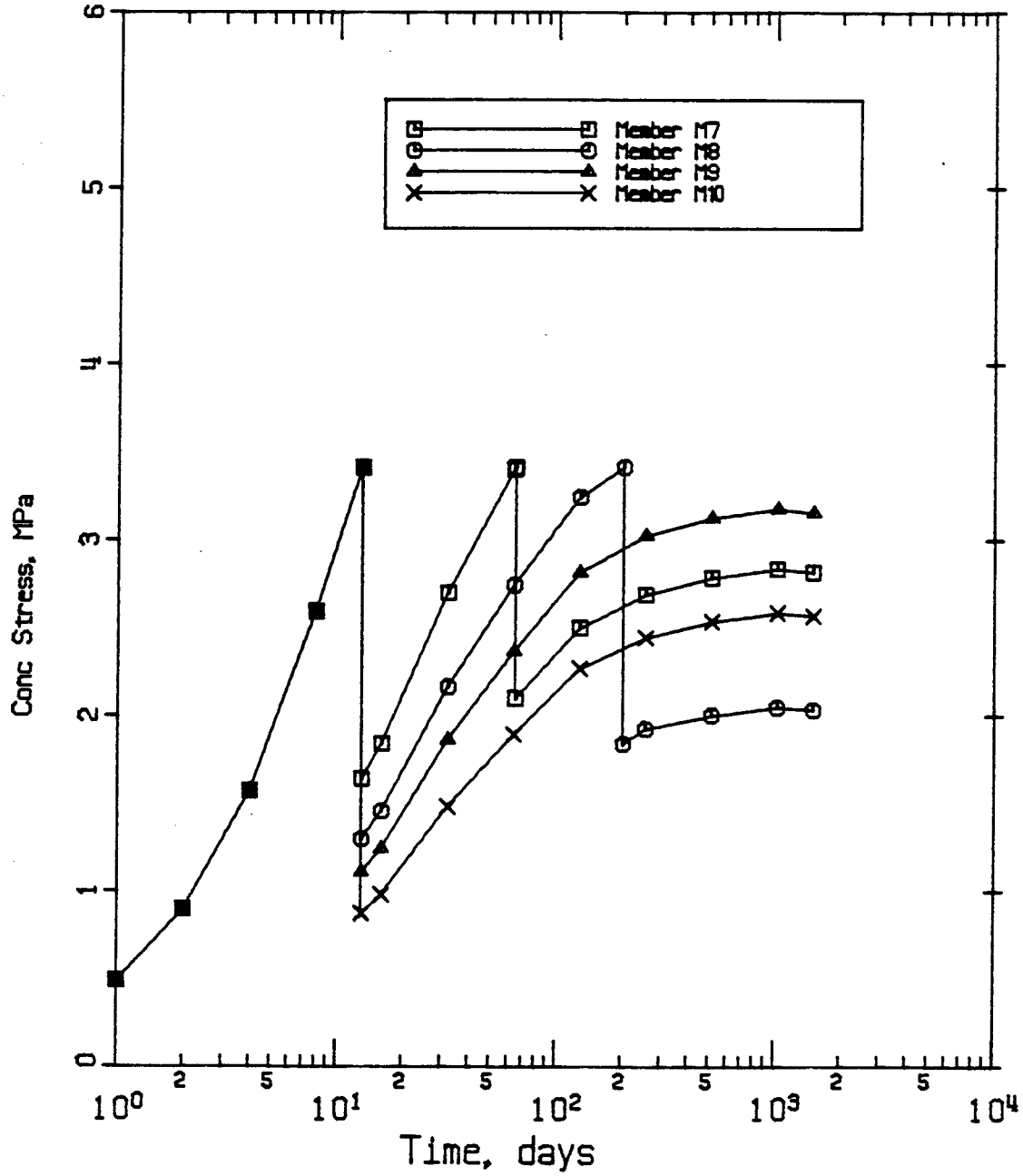

Figure D.6 Concrete stress versus log time curve for effects of variations in bar size

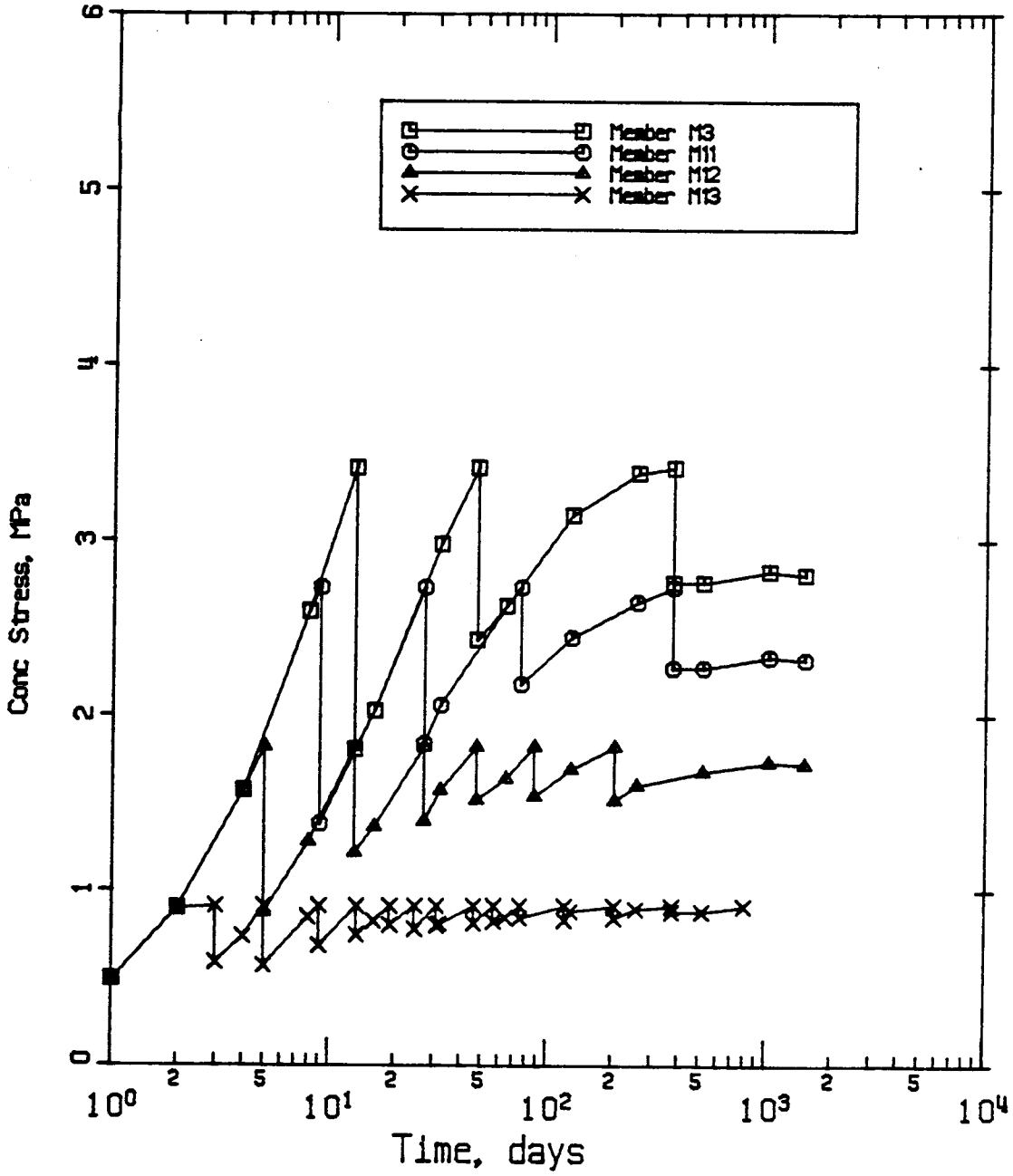

Figure D.7 Concrete stress versus log time curve for effects of variations in tensile strength

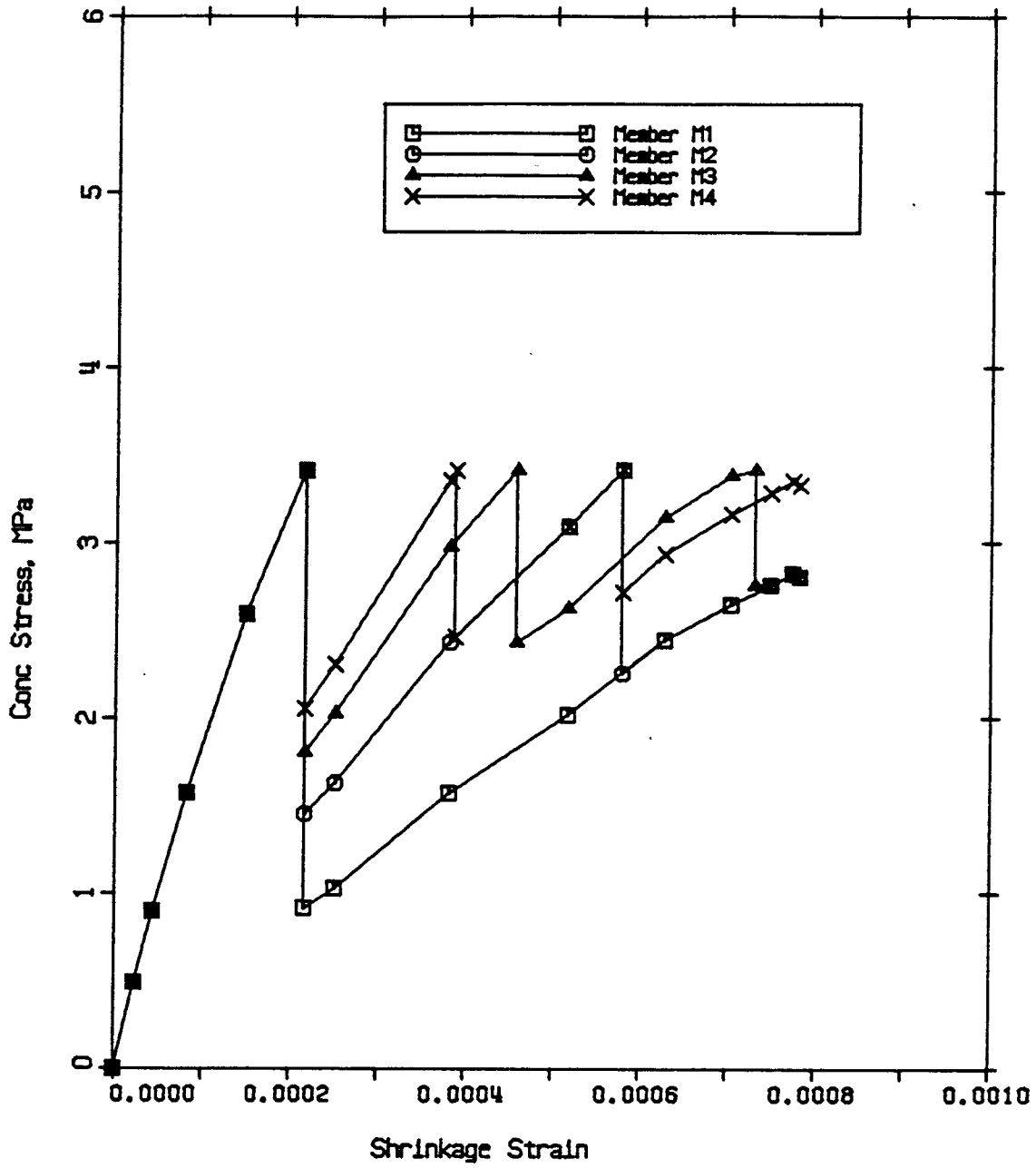

Figure D.8 Effects of variations in span length (including creep)

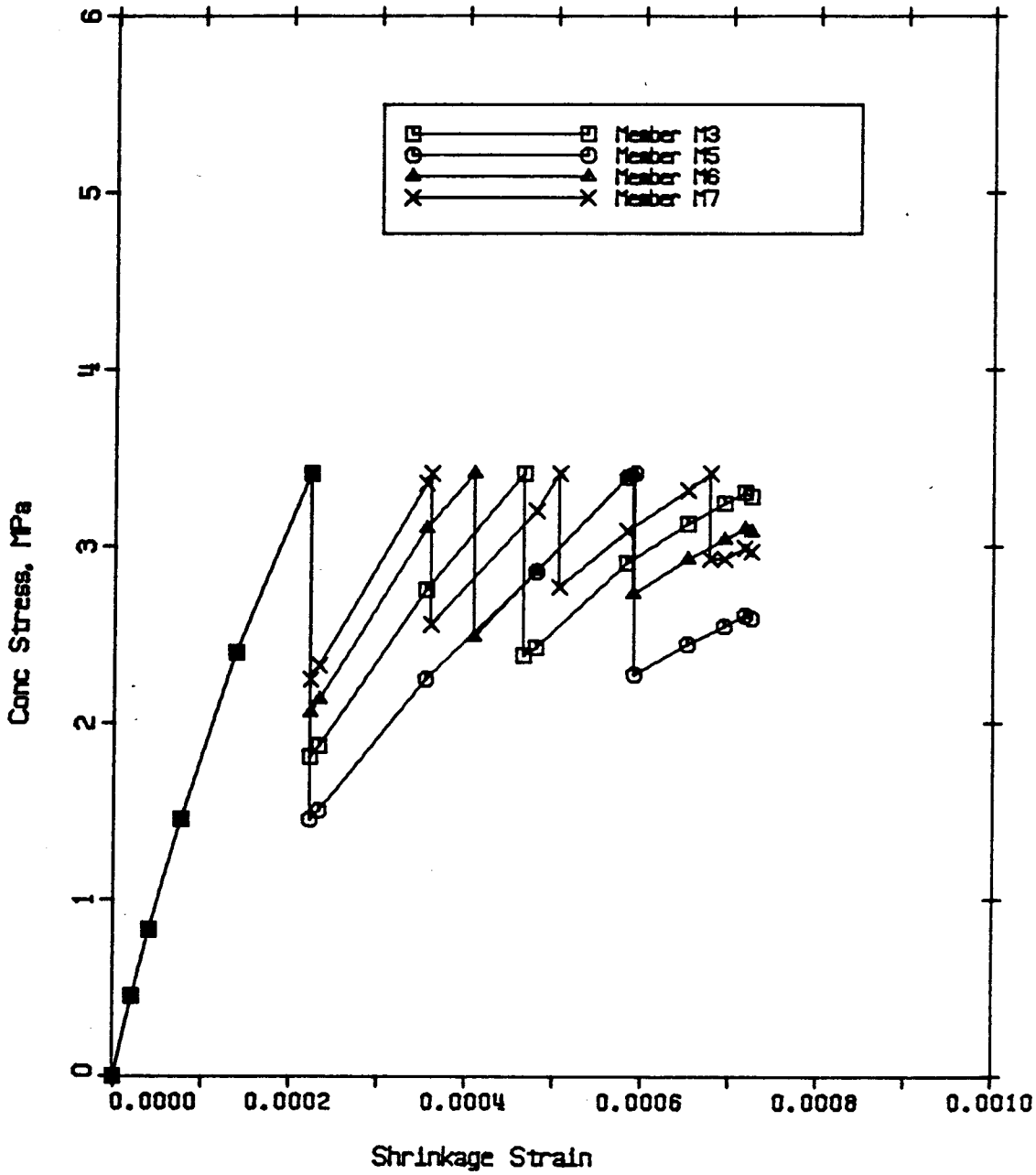

Figure D.9 Effects of variations in steel area

(including creep)

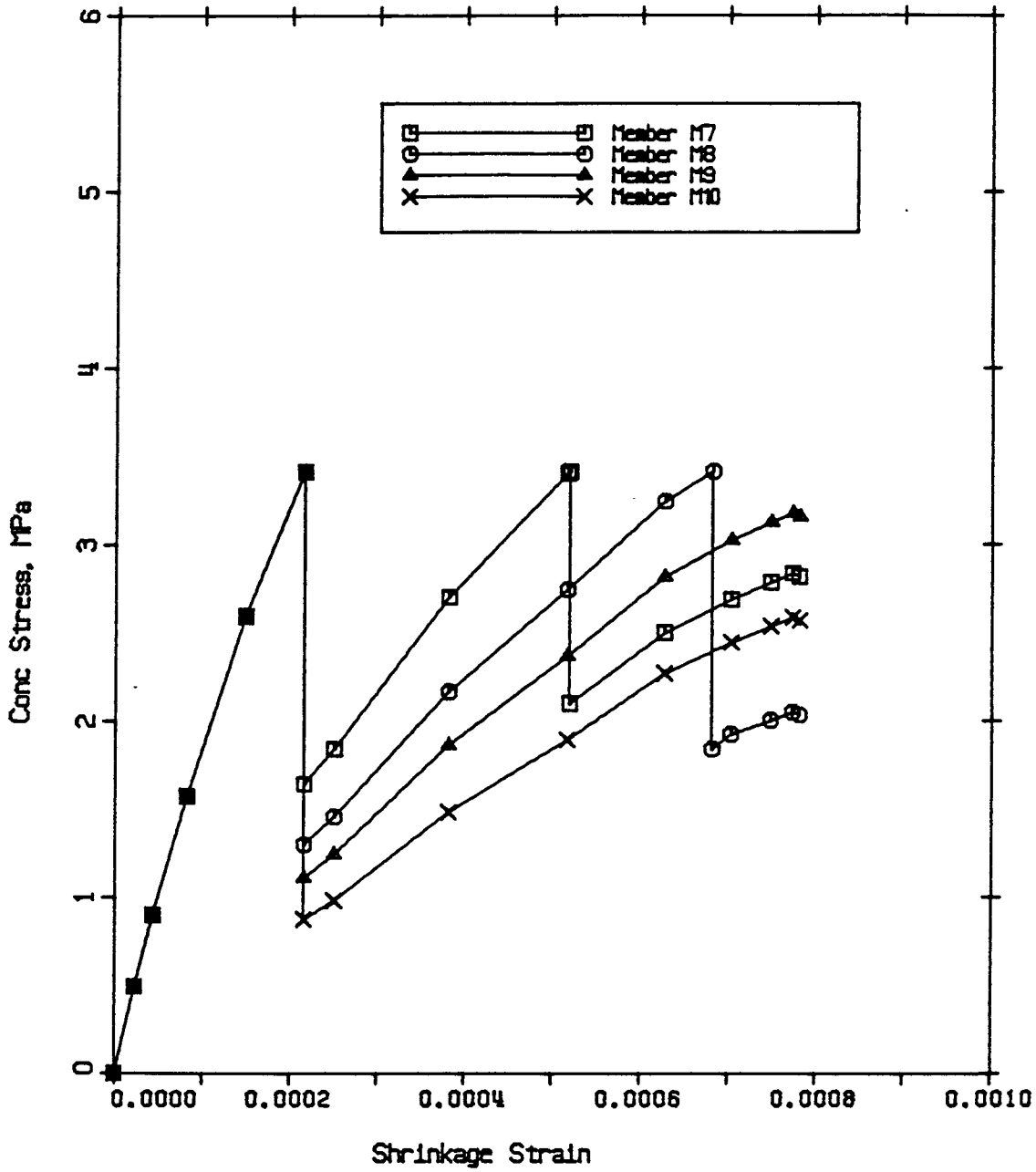

Figure D.10 Effects of variations in bar size (including creep)

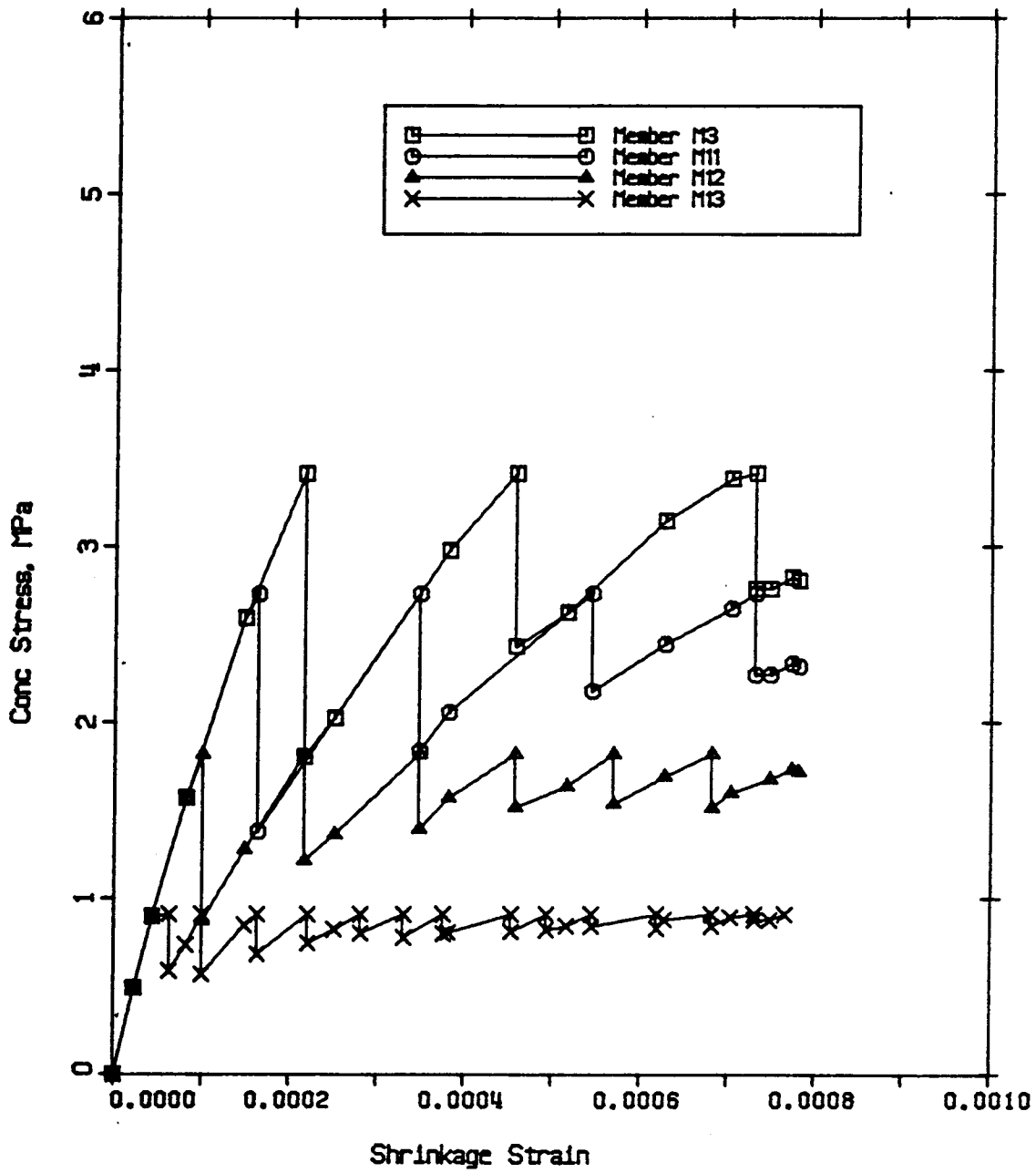

Figure D.11 Effects of variations in tensile strength (including creep)

APPENDIX E

Computer Program including Creep and Partial Fixity

```
C
C   THIS PROGRAM ANALYZE THE SHRINKAGE RESPONSE OF A SYMMETRICALLY
C   REINFORCED MEMBER.
C
C
      REAL L,LC,K1,K2,LCR,LSLIP,KG,KCR,KS,KM,KC
      LOGICAL CHECK
      INTEGER*4 TITLE(20)
      COMMON/PROP/ AS,ES,KM,EM,RHO
      EXTERNAL RITE
C
C***  Input Data and Initialize
C
C
    5 READ(5,1000,END=997)TITLE,
     *                    AG,AS,EC,ES,FR,
     *                    C,L,K1,K2,DIA,ESHU,
     *                    CU,X,TULT,TTOL,FTOL,KC,LC
      CHECK = .FALSE.
      ITER  = 0
      ITIME = 1.5+ALOG(TULT)/ALOG(2.0)
      TLCR  = 0.0
      M     = 0
C
C     ********
C     *
C     *  Evaluate the constants for the member
C     *
C     ********
C
         AC    = AG-AS
         RHO   = AS/AC
         LSLIP = (K2*DIA/RHO)*2.E0
         LCR   = K1*C*2.E0 + LSLIP
C
C        Output of member description
C
         WRITE(6,2000)TITLE,AG,C,L,AC,EC,FR,AS,RHO,ES,DIA,K1,K2,
     *             ESHU,CU,X,TULT
         WRITE(6,1999)KC
         WRITE(6,2001)
C
C     ********
C     *
C     *  STEP 1 - Compute the modified modulus of elasticity
C     *           and the unrestrained shrinkage strain
C     *
C     ********
C
          K   = 0
          T   = 0.0
   10     IF (K.GT.ITIME) GOTO 995
          IF(T.GT.TULT)T=TULT
C
          CT  = CU*(T**0.6/(10.0 + T**0.6))
          ECT = EC/(1.0 + X*CT)
          ESH = (T/(35.0 + T))*ESHU
C
C     ********
C     *
```

```
C     *  STEP 2 - Compute the time-dependent quantities
C     *
C     ********
C
          N     = ES/ECT
          AE    = (1.0 + N*RHO) * AC
          KG    = AE * ECT
          ALFA  = 1.0/(1.0 + 1.0/(2*N*RHO))
          KCR   = ALFA * KG
          KM    = L / ( (L-TLCR)/KG + TLCR/KCR)
C
C         Redefine KM to include partial fixity
C
          KM    = L/(LC/KC + L/KM)
          EM    = ESH*(L-M*LSLIP)/L
C
C     ********
C     *
C     *  STEP 3 - Compute the concrete stress
C     *
C     ********
C
          FC    = KM*EM/AE
C
C     ********
C     *
C     *  STEP 4 - Check the concrete stress
C     *
C     ********
C
          IF(CHECK)GOTO 50
          IF(FC-FR)20,30,40
C
C         (a)  FC.LT.FR
C
   20         CALL RITE(M,T,ESH,ECT,FC,TLCR)
              FCPR = FC
              TPR = T
              T    = 2.0**K
              K    = K+1
              GOTO 10
C
C         (b)  FC.GE.FR - Bisection method to find cracking time
C
C              Compute mid-point and evaluate concrete stress
C
   40         TDPR  = T
   45         T     = (TPR + TDPR)/2.0
              CHECK = .TRUE.
              GOTO 10
C
C             Check stopping criteria
C
   50         IF(ABS(TDPR-T).LE.TTOL.OR.
     *           ABS(FR-FC).LE.FTOL) GOTO 60
C
C             Determine new bracket
C
              IF(FC.GT.FR)GOTO 40
              TPR    = T
```

```
121                 GOTO 45
122        60       CHECK  = .FALSE.
123     C
124     C     ********
125     C     *
126     C     *  STEP 5 - TCR is determined, compute the residual stress
127     C     *
128     C     ********
129     C
130        30    M     = M+1
131              TLCR  = M*LCR
132              IF(TLCR.GT.L)GOTO 996
133              K     = K-1
134              GOTO 10
135     C
136     C*********                TERMINATION                      **********
137     C
138       995    WRITE(6,2100)
139              GOTO 5
140       996    WRITE(6,2110)
141              GOTO 5
142     C
143       997 STOP
144     C
145     C*********                 FORMAT BLOCK                    **********
146     C
147      1000 FORMAT(20A4/5F10.0/6F10.0/7F10.0)
148      2100 FORMAT(///'*** Ultimate time exceeded ***')
149      2110 FORMAT
150          *( ///'*** Total cracked length exceeds member length ***')
151      2000 FORMAT('1',/' ',20A4///' MEMBER''S DETAIL'/
152          *       ' ',','     Gross Area      Max Cover    Span Length'/
153          *       ' ',3F15.4///
154          *       ' ','CONCRETE DETAIL'/
155          *       ' ','  Concrete Area     Elasticity    Tensile Str'/
156          *       ' ',F15.4,2G15.4///
157          *       ' ','REINFORCEMENT DETAIL'/
158          *       ' ','     Steel Area    Steel ratio     Elasticity',
159          *         '     Diameter'/
160          *       ' ',F15.4,2G15.4,F15.4///
161          *       ' ','CRACKED LENGTH COEF.'/
162          *       ' ','   K1= ',F6.4,'   K2 = ',F6.4///
163          *       ' ','TIME DEPENDENT COEF.'/
164          *       ' ',' Ult. Shrinkage    Creep Coef.     Chi-Factor',
165          *         '     Time Limit'/  ' ',E15.4,3F15.2///)
166      1999 FORMAT(' ','COLUMN STIFFNESS = ',G15.4///)
167      2001 FORMAT(
168          *' ','U N I A X I A L   S H R I N K A G E   A N A L Y S I S'//
169          *       ' ',' Crack      Time      Shrinkage     Elasticity',
170          *         '    Conc Stress    Steel(gross)   Steel(crack)',
171          *         '     Cr. Length'/)
172           END
173     C*************************************************************
174     C
175           SUBROUTINE RITE(M,T,ESH,ECT,FC,TLCR)
176     C
177     C     *************
178     C     *
179     C     *   This subroutine computes the steel stresses
180     C     *   and writes the output.
```

```
C     *
C     *************
C
      REAL KM, FSCR/0.0/, FSG/0.0/
      COMMON/PROP/ AS,ES,KM,EM,RHO
C
C     Calculate the steel stresses
C
      IF (M.EQ.0) GOTO 10
      PNET   = (KM - AS*ES)*EM
      FSCR   = PNET/AS
      FSG    = FSCR - FC/RHO
   10 WRITE(6,2020)M,T,ESH,ECT,FC,FSG,FSCR,TLCR
 2020 FORMAT(I7,F10.1,2E15.4,3G15.4,F15.2)
      RETURN
      END
End of file
```

APPENDIX F

Principal Moment Analysis

In the finite element analysis in Chapter 3, cracking was assumed to occur when M_x or M_y exceeds the cracking moment M_{cr}. However, experiments have indicated that cracks are initiated normal to the major principal moments (Lenschow and Sozen, 1966). There may be elements where the major principal moment exceeds M_{cr} but not M_x or M_y. In such cases, cracking in the element is undetected and may result in an underestimation of deflection.

The slab system in Chapter 3 is therefore reanalyzed to check for the principal moment in each elements. The principal moment is computed using the Mohr's circle as shown in Figure F.1. Figure F.2 shows the major principal moments in Slab S1 after three iterations of modified SAPIV analysis. Because of symmetry, the principal moments are shown for only half of the elements.

The results indicate that only four of the elements has undetected cracking; also, all the cracked elements have M_x or M_y close to the major principal moment, presumably because of relatively low twisting moments M_{xy} along the column lines. The deflection is therefore not significantly affected by the assumption of checking M_x and M_y for cracking in the slab system analyzed.

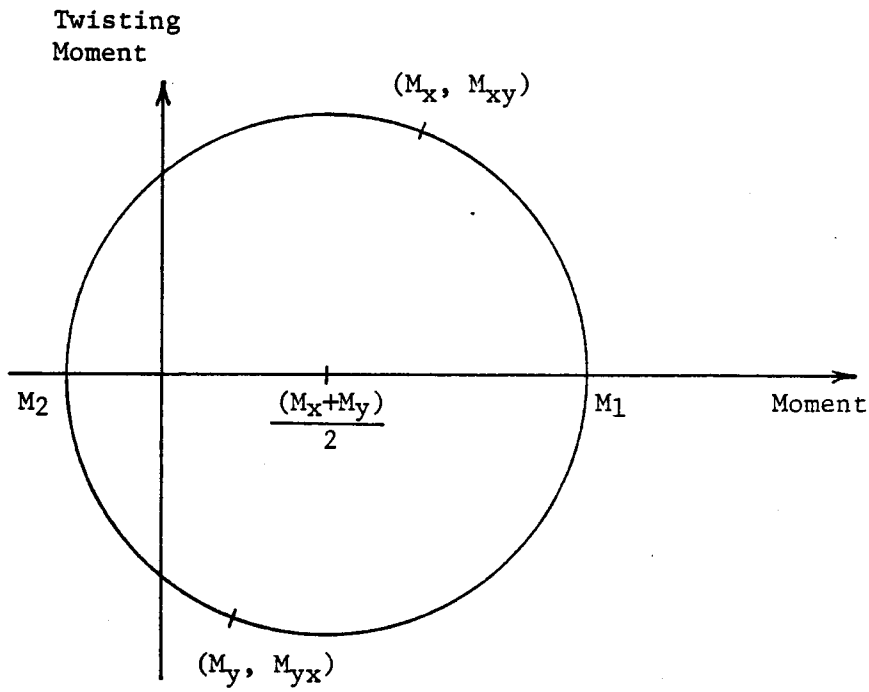

$$\text{Diameter, } d = \sqrt{\left[\frac{(M_x+M_y)}{2} - M_x\right]^2 + M_{xy}^2}$$

$$M_1 = \frac{(M_x+M_y)}{2} + d$$

$$M_2 = \frac{(M_x+M_y)}{2} - d$$

Figure F.1 Determination of principal moment using Mohr's circle

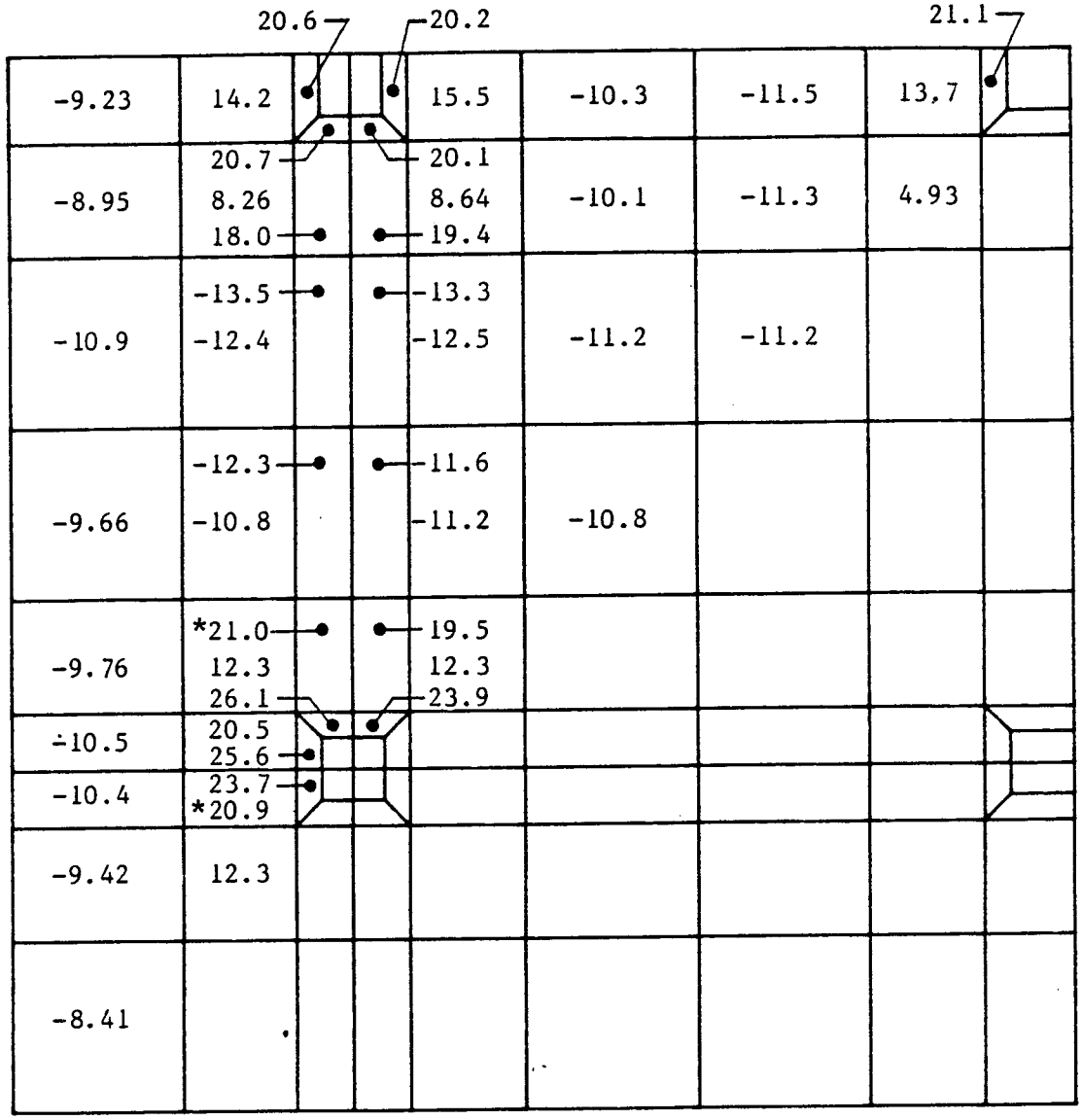

All units in kNmm/mm

M_{cr} = 20.5 kNmm/mm

* Undetected cracking

Figure F.2 Major principal moments in Slab S1

APPENDIX G

Conversion Factors

Imperial – SI	SI – Imperial
1 in = 25.4 mm	1 mm = 0.0394 in
1 in^2 = 645.16 mm^2	1 mm^2 = 1.55x10^{-3} in^2
1 lb(mass) = 0.45359237 kg	1 kg = 2.20 lb(mass)
1 lb(force) = 4.448222 N	1 N = 0.225 lb(force)
1 kip = 4.448222 kN	1 kN = 0.225 kip
1 psi = 6.894757 kPa	1 kPa = 0.145 psi
1 ksi = 6.894757 MPa	1 MPa = 0.145 ksi
1 in-kip = 0.1129848 N.m	1 N.m = 8.85 in-kip
1 ft-kip = 1.355818 N.m	1 kN.m = 0.738 ft-kip

RECENT STRUCTURAL ENGINEERING REPORTS

Department of Civil Engineering

University of Alberta

90. *Analysis and Design of Stub-Girders* by T.J.E. Zimmerman and R. Bjorhovde, August 1980.

91. *An Investigation of Reinforced Concrete Block Masonry Columns* by G.R. Sturgeon, J. Longworth and J. Warwaruk, September 1980.

92. *An Investigation of Concrete Masonry Wall and Concrete Slab Interaction* by R.M. Pacholok, J. Warwaruk and J. Longworth, October 1980.

93. *FEPARCS5 - A Finite Element Program for the Analysis of Axisymmetric Reinforced Concrete Structures - Users Manual* by A. Elwi and D.W. Murray, November 1980.

94. *Plastic Design of Reinforced Concrete Slabs* by D.M. Rogowsky and S.H. Simmonds, November 1980.

95. *Local Buckling of W Shapes Used as Columns, Beams, and Beam-Columns* by J.L. Dawe and G.L. Kulak, March 1981.

96. *Dynamic Response of Bridge Piers to Ice Forces* by E.W. Gordon and C.J. Montgomery, May 1981.

97. *Full-Scale Test of a Composite Truss* by R. Bjorhovde, June 1981.

98. *Design Methods for Steel Box-Girder Support Diaphragms* by R.J. Ramsay and R. Bjorhovde, July 1981.

99. *Behavior of Restrained Masonry Beams* by R. Lee, J. Longworth and J. Warwaruk, October 1981.

100. *Stiffened Plate Analysis by the Hybrid Stress Finite Element Method* by M.M. Hrabok and T.M. Hrudey, October 1981.

101. *Hybslab - A Finite Element Program for Stiffened Plate Analysis* by M.M. Hrabok and T.M. Hrudey, November 1981.

102. *Fatigue Strength of Trusses Made From Rectangular Hollow Sections* by R.B. Ogle and G.L. Kulak, November 1981.

103. *Local Buckling of Thin-Walled Tubular Steel Members* by M.J. Stephens, G.L. Kulak and C.J. Montgomery, February 1982.

104. *Test Methods for Evaluating Mechanical Properties of Waferboard: A Preliminary Study* by M. MacIntosh and J. Longworth, May 1982.

105. *Fatigue Strength of Two Steel Details* by K.A. Baker and G.L. Kulak, October 1982.

106. *Designing Floor Systems for Dynamic Response* by C.M. Matthews, C.J. Montgomery and D.W. Murray, October 1982.

107. *Analysis of Steel Plate Shear Walls* by L. Jane Thorburn, G.L. Kulak, and C.J. Montgomery, May 1983.

108. *Analysis of Shells of Revolution* by N. Hernandez and S.H. Simmonds, August 1983.

109. *Tests of Reinforced Concrete Deep Beams* by D.M. Rogowsky, J.G. MacGregor and S.Y. Ong, September 1983.

110. *Shear Strength of Deep Reinforced Concrete Continuous Beams* by D.M. Rogowsky and J.G. MacGregor, September 1983.

111. *Drilled-In Inserts in Masonry Construction* by M.A. Hatzinikolas, R. Lee, J. Longworth and J. Warwaruk, October 1983.

112. *Ultimate Strength of Timber Beam Columns* by T.M. Olatunji and J. Longworth, November 1983.

113. *Lateral Coal Pressures in a Mass Flow Silo* by A.B.B. Smith and S.H. Simmonds, November 1983.

114. *Experimental Study of Steel Plate Shear Walls* by P.A. Timler and G.L. Kulak, November 1983.

115. *End Connection Effects on the Strength of Concrete Filled HSS Columns* by S.J. Kennedy and J.G. MacGregor, April 1984.

116. *Reinforced Concrete Column Design Program* by C-K. Leung and S.H. Simmonds, April 1984.

117. *Deflections of Two-way Slabs under Construction Loading* by C. Graham and A. Scanlon, August 1984.

118. *Effective Lengths of Laterally Unsupported Steel Beams* by C.D. Schmitke and D.J.L. Kennedy, October 1984.

119. *Flexural and Shear Behaviour of Large Diameter Steel Tubes* by R.W. Bailey and G.L. Kulak, November 1984.

120. *Concrete Masonry Prism Response due to Loads Parallel and Perpendicular to Bed Joints* by R. Lee, J. Longworth and J. Warwaruk.

121. *Standardized Flexible End Plate Connections for Steel Beams* by G.J. Kriviak and D.J.L. Kennedy, December 1984.

122. *The Effects of Restrained Shrinkage on Concrete Slabs* by K.S.S. Tam and A. Scanlon, December 1984.